



# **AC/DC hybrid grid modelling enabling a high share of Renewables**

Final report

# **AC/DC hybrid grid modelling enabling a high share of Renewables**

Final Report

Prepared for the European Commission, DG ENER,  
under service contract N° ENER/2021/OP/0008-B5/SER/2020-563/SI2.864123

## EUROPEAN COMMISSION

Directorate-General for Energy  
Directorate B - Just Transition, Consumers, Energy Efficiency and Innovation  
Unit ENER.B5 - Innovation, Research, Digitalisation, Competitiveness

Contact: Eric Lecomte

E-mail: eric.lecomte@ec.europa.eu

European Commission  
B-1049 Brussels

### Authors:

O. Antoine, L. Papangelis, P. Tielens, K. Karoui (Engie Impact)

H. Ergun, G. Bastianel, A. Agbemuko, J. Beerten, W. Leterme, D. Van Hertem (KU Leuven/EnergyVille)

Manuscript completed: November 2022

First edition: February 2023

### LEGAL NOTICE

This document has been prepared for the European Commission however it reflects the views only of the authors, and do not necessarily reflect the official opinion of the Commission. The Commission does not guarantee the accuracy of the data included in this assessment. Neither the Commission nor any person acting on the Commission's behalf may be held responsible for the use which may be made of the information contained therein. More information on the European Union is available on the Internet (<http://www.europa.eu>).

---

EN PDF

ISBN 978-92-76-60277-4

doi:10.2833/627100

MJ-05-22-426-EN-N

---

Luxembourg: Publications Office of the European Union, 2023

© European Union, 2023



The reuse policy of European Commission documents is implemented by the Commission Decision 2011/833/EU of 12 December 2011 on the reuse of Commission documents (OJ L 330, 14.12.2011, p. 39). Except otherwise noted, the reuse of this document is authorised under a Creative Commons Attribution 4.0 International (CC-BY 4.0) licence (<https://creativecommons.org/licenses/by/4.0/>). This means that reuse is allowed provided appropriate credit is given and any changes are indicated.

For any use or reproduction of elements that are not owned by the European Union, permission may need to be sought directly from the respective rightsholders.



# 1. Executive summary (English)

## Disclaimer

*The information and views set out in this report are those of the authors and do not necessarily reflect the official opinion of the Commission. The Commission does not guarantee the accuracy of the data included in this study. Neither the Commission nor any person acting on the Commission's behalf may be held responsible for the use which may be made of the information contained therein.*

## Context

The following years will see a massive increase in the penetration of renewable energy sources (RES) in Europe. This is valid for wind (onshore and offshore), solar photovoltaics but also other types of renewable resources (e.g. tidal). Most of these renewable energy sources are interfaced via power electronic devices called inverters to the electrical grid and are generally named Inverter Based Resources (IBRs).

The first main impact of the increasing penetration of renewable energy is that the electrical power is transmitted over longer distance (i.e. from RES locations to the load centres) and with a higher variability compared to the existing system with large (thermal) power plants close to load centres.

The second main impact is that the increased penetration of Inverter Based Resources replaces synchronous machines connected to the network. Firstly, this implies a reduction of the directly coupled energy stored in the rotating masses and in the windings of the synchronous generators. The fact to have less mechanical and electromagnetic energy temporarily stored in the grid makes the power system more sensitive to disturbances and therefore potentially more unstable. The second consequence is that the operation of the power system is now governed by the controls of the power electronic inverters, rather than by the natural response of traditional generators. This causes a new paradigm in power system operations and at this moment, there is still no consensus on how to plan and operate a large power system with almost 100% penetration of Inverter Based Resources. There are indeed some mitigation options that could help to improve stability of such systems, such as advanced controls of inverters or HVDC<sup>1</sup> converters (i.e. "Grid Forming"), or installation of additional assets (e.g. synchronous condensers, e-STATCOM, Battery Energy Storage System (BESS), etc.). However, there is still ongoing research and development on the implementation of advanced control loops and on the technology itself, and as such there is to date no universal solution to improve this issue.

These two main impacts reinforce the link between generation and transmission expansion planning, and also outline the necessity to consider transmission grid constraints when integrating more renewable energy sources into the energy mix. For the above-mentioned reasons, it is expected that HVDC technology will be increasingly installed in the European electrical grid and **the network will evolve to a hybrid AC/DC grid**.

## Scope of work

Considering that traditional cost-benefit analyses at the European level are mainly focused on energy needs rather than on power grid needs, this work analyses HVDC technology and its potential to provide additional benefits for integrating more Renewable

---

<sup>1</sup> The study considers exclusively Voltage Source Converter (VSC) HVDC. Therefore, the wording HVDC always refers to VSC-HVDC.

Energy Sources in the network. These additional benefits could be provided by the following range of functionalities:

- Power flow control capability
- Voltage support
- Frequency and inertia support
- Grid forming
- Blackstart capability

This work aims at providing modelling requirements of AC/DC grids and in particular to propose clear guidelines to evaluate, at the planning stage, all benefits that can be provided by the HVDC technology in a system with high share of RES. **The ultimate goal is to allow decision makers to make better informed decisions.**

Therefore, we focus on the long-term planning stage when the evaluation of the costs and benefits of a project candidate takes place. Commonly used CBA methods do not capture all the technical risks related to operation of a system with high penetration of Inverter Based Resources. Therefore, operating conditions might not be stable and would require system services, additional investment or redispatch to be viable. For the sake of illustration, an overview of the HVDC functionalities and their contribution to mitigate technical challenges can be found in Figure 1.

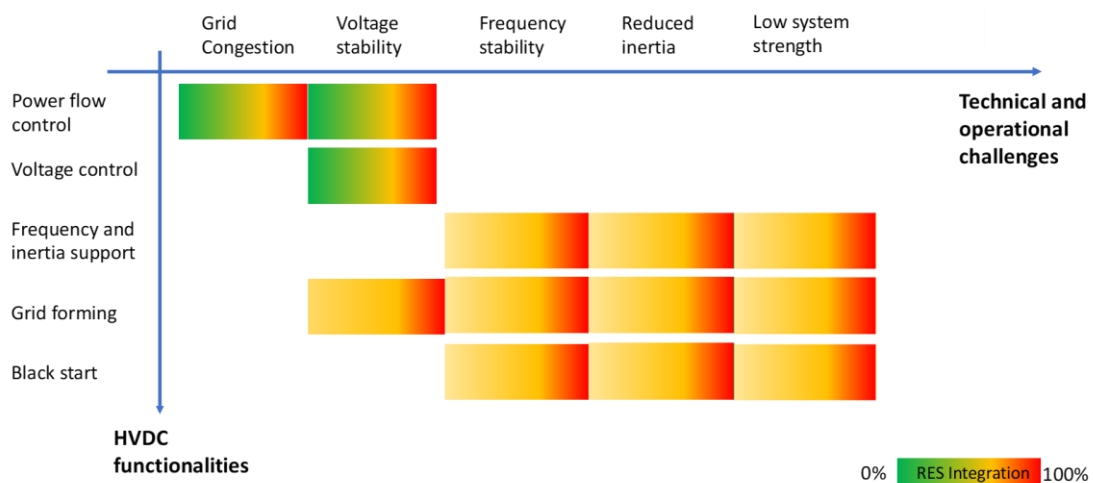


Figure 1 - HVDC functionalities vs technical challenges in grid with high penetration of renewable energy sources.

### Summary of the work

This study identifies limitations of the classical CBA methodologies and proposes improvements that can be summarized by the three following priorities:

- More detailed power system representation, towards a nodal network model
- Integration of power flow control and stability constraints in the optimization problem
- Addition of qualitative KPIs regarding system stability (in particular for frequency and converter-driven stability)

These improvements are to be added to the existing ENTSO-E CBA approach which forms the basis of the proposed incremental approach (illustrated in Figure 2). These incremental levels of complexity are proposed to better quantify some KPIs and also risks in systems with high penetration of Inverter Based Resources. The main point is that the zonal approach may provide optimistic benefits, in the sense that some costs can be “hidden” because of security and operational challenges. Therefore, it is highly recommended to perform a CBA using the nodal network model and considering stability metrics. Both inertia and converter-driven stability metrics can be translated into KPIs by assessing how many operating conditions per year are at risk of frequency or converter-

driven instability. These quantitative KPIs should be used as an indicator of the need for future investment or for operational measures. Regarding frequency stability, a cost is also evaluated based on redispatch methodology (similar to current B.10 KPI of ENTSO-E). Regarding the converter-driven stability KPI, it must be seen as a risk indicator, which can lead to more detailed simulations in the next stage of the project or even to additional investments.

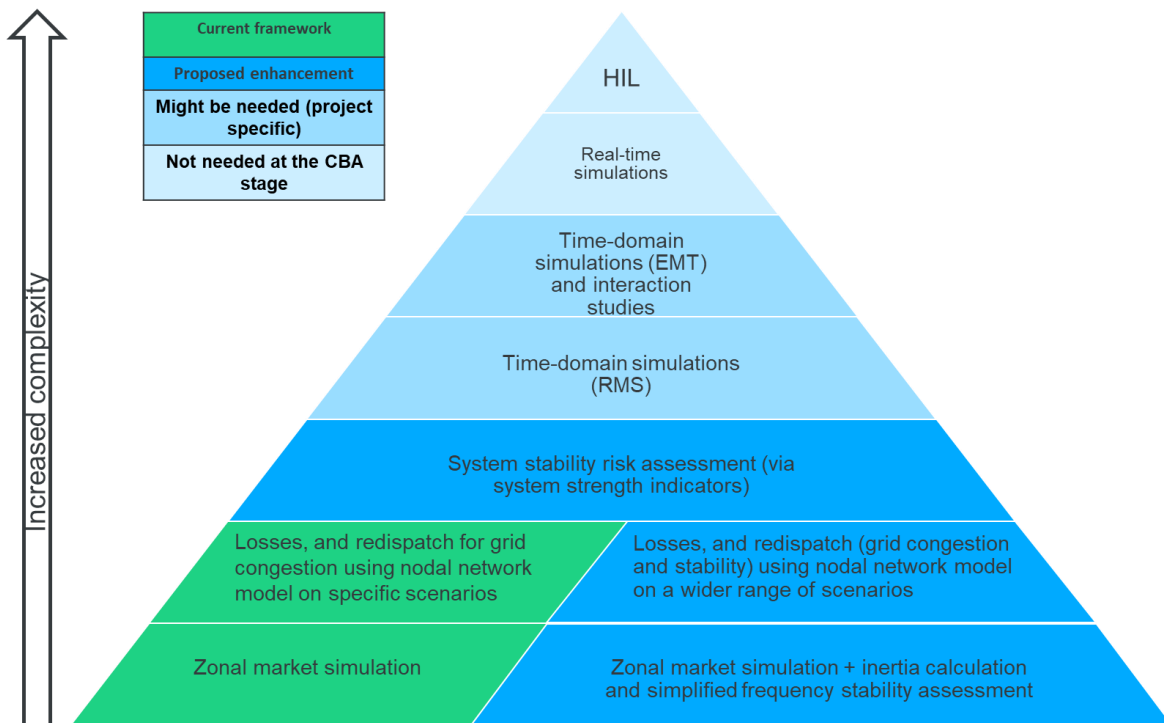


Figure 2 – Overview of proposed CBA approach

The work performed can be summarized into the three following parts (which are more detailed in sections 5, 6 and 7).

### 1. “Enhanced” CBA methodology

The proposed CBA approach quantifies **additional benefits** and **identifies potential risks** for system stability. It is important to note that some of these additional benefits such as through power flow control can only be seen when performing the CBA on a detailed nodal grid model (instead of a zonal model often used) and/or by including stability (inertia) constraints in the analysis.

Firstly, an existing open-source AC/DC grid optimal power flow (OPF) model has been used in order to determine the **social welfare benefits considering internal congestion** in the network, as opposed to using zonal models neglecting intrazonal constraints. Further, the OPF model has been modified to determine the additional benefits provided by the power flow control provided by HVDC links during contingency situations. Using the modified OPF formulation, the **redispatch costs are minimized for a number of selected critical contingencies**. The modified OPF tool has been made available as an open-source tool as well<sup>2</sup>. By performing two separate calculations with disabled and enabled power flow control, the additional benefits through power flow control are determined. The results show that security related redispatch costs can be significantly decreased by making use of such controllability.

<sup>2</sup> The tool can be accessed via <https://github.com/Electa-Git/CBAOPF.jl>

Moreover, the developed OPF implementation allows to include additional constraints. An inertia constraint has been tested for two study cases and it was clearly observed that the **HVDC technology could considerably reduce the minimum inertia constraint**, which by consequence increases the number of stable operating conditions. This effect is also quantified by means of redispatch cost reduction as a proxy of required reserves to ensure frequency stability.

An extremely important aspect is power system stability in a system with high penetration of inverter-based RES. While it is generally agreed that detailed time-domain simulations are needed in order to assess stability in a weak grid, models with the required level of detail and accuracy of the control parameters are typically not available for the considered planning horizon. For this reason, it is **recommended to evaluate risk of instabilities (at specific locations of the grid and/or at specific operating conditions) via calculation of simplified indicators**.

## 2. Modelling and implementation guidelines

One part of the work (summarized in section 6.1) specifically focuses on the modelling requirements for the HVDC technology. A comprehensive review of the type of models and the adequate level of detail for all observed phenomena in presence of inverter based resources was presented. For each functionality/technical aspects of HVDC systems, the modelling requirements have been specified.

Section 6.2 and section 6.3 detail the modelling requirements for implementing the proposed CBA approach. These sections provide to the interested reader all the required information for implementing the proposed approach.

## 3. Illustration on realistic use cases

The use cases provided us not only with quantitative results but also with a return of experience on the proposed implementation. The zonal approach has been easily implemented, however it is clear that the nodal approach has led to significant challenges, mainly attributed to available data. It has been shown that our approach could be implemented on multi-country systems with several thousands of generators.

### *Main findings and recommendations for future improvements*

#### (i) Main Findings

- (1) **Use of nodal network is necessary:** Although zonal models can determine the socio-economic benefits of new interconnectors in a computationally efficient manner, they tend to underestimate these benefits as the internal congestion in the network is not considered. The reason therefore is the zonal approach underestimates the curtailment of renewable energy due to internal network congestion in high RES scenarios, where the added value of interconnection is even more significant. **Our study shows that more complex nodal models can be feasibly used within of CBA methodologies** despite higher computational complexity (24 hours vs. 30 min for yearlong calculations) and higher data requirements.
- (2) **Power flow control provides significant benefits:** The study shows that HVDC technology provides significant benefits through power flow control in case of contingencies by reducing the required redispatch cost. Especially embedded HVDC links can reduce redispatch costs in the order of several tens of millions of Euros per year in case of severe contingencies in the system. To analyse such benefits, the use of nodal models is unavoidable.
- (3) **Stability constraints are necessary:** It is essential to consider stability / inertia constraints in long term planning models to estimate the additional risk of

deteriorating system inertia for determining the best mitigation options. Further, our study shows that **inertia provision through HVDC decreases the necessary cost for ensuring system stability** in the order of several ten million Euros per year.

- (4) **Stability indicator can be used to identify operational risks:** Our study shows that simplified models with stability and inertia constraints can provide acceptable high-level results for CBA analysis. In terms of dynamic data and control parameters, it is clear that the most accurate data allow to be more confident in the results of advanced tools. However, with currently available models and datasets, it is not always adequate to perform intensive detailed simulations for long-term planning studies. We conclude that detailed dynamic simulations should only be used in cases where detailed network and equipment models are available. As such, potential risks and de-risking actions have to be identified but can be done later in the planning process when detailed models are available.
- (5) **Harmonized models are needed:** Our study shows the need to harmonize the network models used in the context of CBAs. Especially, to quantify the effects of congestion and benefits through power flow control as well as to better approximate dynamic stability constraints, harmonized models are essential.

## **(ii) Recommendations for future improvements**

- (1) **Dataset Improvement:** As the network data are mandatory in our proposed approach, it is extremely important to have a reliable European network model (static). To that end, different datasets used for long term generation and transmission expansion planning versus detailed grid models used to perform power flow studies should be harmonized in order to obtain accurate results capturing all benefits. The modelling section provides clear requirements in terms of the tools and model details for studying each phenomenon. It has been shown in this study (and also in the literature) that control parameters have a huge influence on IBR stability. Therefore, in the near future it is extremely important to have a European grid model with representative control parameters for existing IBRs. This will allow to perform a better screening of the instabilities that might occur
- (2) **Need for high-performance computer infrastructure:** Although detailed nodal models are computationally more expensive, parallelization of calculations, application of artificial intelligence methods for contingency filtering, improved clustering techniques for selecting a subset of representative operating points (both for steady state and dynamic analysis) and the use of dedicated high-performance computer infrastructure can allow the implementation of the demonstrated mathematical models within state-of-the art tools. Further, the development of dedicated open-source tools can help to provide transparent results in the context of the CBA.
- (3) **Defining power system stability in the future grid:** Our study shows a particular approach for including stability indicators within CBA methodologies. However, there are a variety of stability indicators, which all can be quantified using different types of optimisation / simulation models. As such, in the long run it will be important to define stability indicators in a harmonized way. Especially, in the context of grid forming and black start capabilities, clear definitions are needed, based on which indicators can be defined, and subsequently models can be developed to quantify these indicators. We believe that fundamental research and a broad stakeholder involvement are necessary to achieve this goal.

## 2. Résumé exécutif (Français)

### Disclaimer

*Les informations et points de vue exposés dans ce rapport sont ceux des auteurs et ne reflètent pas nécessairement l'opinion officielle de la Commission. La Commission ne garantit pas l'exactitude des données incluses dans cette étude. Ni la Commission, ni aucune personne agissant au nom de la Commission ne peuvent être tenues responsables de l'utilisation qui pourrait être faite des informations qui y sont contenues.*

### Contexte

Les années futures verront une intégration massive d'énergie renouvelable en Europe. Cette énergie renouvelable proviendra de l'éolien (onshore et offshore); du solaire photovoltaïque mais également d'autres sources d'énergies (p.ex. via les marées). Ces sources d'énergie sont interfacées via de l'électronique de puissance vers le réseau électrique et sont communément appelées dans la littérature Inverter Based Resources (IBRs).

Un des impacts majeurs de cette pénétration croissante d'énergie renouvelable est que l'électricité doit être transmise sur de grandes distances (depuis la source d'énergie vers les centres de consommation) et avec plus de variabilités qu'avec des sources d'énergie conventionnelles (comme des centrales thermiques).

Le second impact est que les sources d'énergie renouvelables (machines non tournantes et sans inertie) remplacent les machines synchrones connectées au réseau électrique. Cela implique une réduction de l'énergie stockée dans les masses tournantes des turbines et dans les enroulements des générateurs synchrones. Le fait d'avoir moins d'énergie mécanique et électromagnétique disponible temporairement rend le système plus sensible aux perturbations et par conséquent potentiellement plus instable. De plus, la stabilité du réseau est alors gouvernée par les lois de régulation des onduleurs d'électronique de puissance, plutôt que par la réponse naturelle des machines tournantes. Cela cause un nouveau paradigme dans l'exploitation des réseaux électriques et, au jour d'aujourd'hui, il n'y a pas de consensus sur la manière de planifier et exploiter un grand réseau électrique avec presque 100% d'Inverter Based Resources. Il y a bien évidemment des solutions qui existent pour améliorer la stabilité du système, comme l'utilisation de régulation avancée sur les onduleurs des HVDC (p.ex. « Grid Forming »), ou l'installation d'assets supplémentaires (p.ex. compensateur synchrone, e-STATCOM, batteries, etc.). Cependant, l'implémentation de boucles de régulation avancées ainsi que la technologie même ne sont pas encore totalement matures et il n'y a à ce jour pas de solution universelle pour améliorer cela.

Ces deux impacts renforcent le lien nécessaire entre la planification de la génération et du réseau de transport, et soulignent également le besoin de considérer les contraintes du réseau électrique lorsqu'on veut intégrer plus d'énergie renouvelable dans le mix énergétique. Pour ces réseaux, il est attendu que la technologie HVDC soit installée de manière croissante dans le réseau européen qui va **évoluer vers un réseau hybride AC/DC**.

### Cadre du projet

En considérant que les analyses couts-bénéfices traditionnelles, au niveau européen, se concentrent essentiellement sur les besoins énergétiques plutôt que sur les besoins du réseau électrique, ce travail analyse en particulier la technologie HVDC et son potentiel pour fournir de services réseaux additionnelles et ainsi intégrer plus d'énergie renouvelable. Ces bénéfices additionnels peuvent être fournis par les fonctionnalités suivantes:

- Contrôle de l'écoulement de puissance
- Support en tension
- Support en fréquence et inertiel
- Grid forming
- Capacité blackstart

Ce projet vise à fournir des exigences de modélisation pour les réseaux AC/DC et en particulier à proposer des lignes directrices claires pour évaluer, lors de la planification, les bénéfices qui peuvent être fournis par la technologie HVDC dans un système à forte pénétration de renouvelable. L'objectif final étant d'avoir des informations claires pour **faciliter la prise de décisions d'investissements**.

Par conséquent, nous nous sommes concentrés sur la planification long-terme, quand est effectuée l'évaluation des coûts et bénéfices d'un projet candidat. Généralement, les études coûts-bénéfices ne capturent pas tous les aspects techniques liées à l'exploitation d'un système à haute pénétration de renouvelable. Par conséquent, certaines conditions d'exploitation pourraient être instables et ainsi nécessiter des coûts supplémentaires pour être viable (p.ex. via services réseaux, investissements additionnels ou redispatch). La Figure 3 illustre les challenges opérationnels ainsi que les services qui peuvent être fournis par la technologie HVDC.

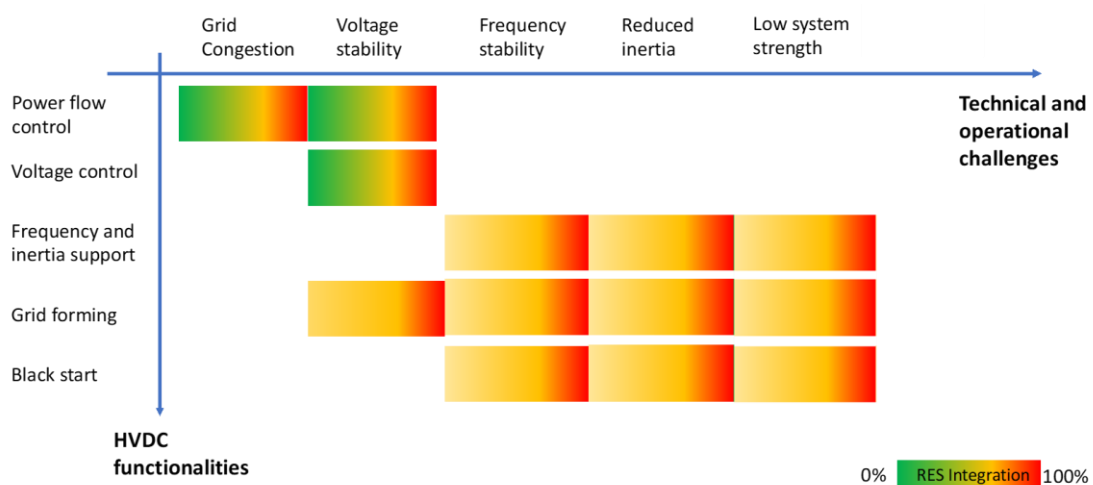


Figure 3 - challenges opérationnels ainsi que les services qui peuvent être fournis par la technologie HVDC.

### Résumé du travail effectué

L'étude a permis d'identifier les limitations des études coûts-bénéfices classiques et propose des améliorations qui peuvent être résumées par les trois points suivants :

- Représentation plus détaillée du réseau électrique, jusqu'à un modèle nodal
- Intégration des régulations d'écoulement de puissance et des contraintes de stabilité dans le problème d'optimisation
- Ajout d'indicateurs évaluant le risque de problèmes de stabilité (notamment pour la stabilité en fréquence et stabilité des onduleurs).

Ces améliorations doivent être ajoutées à l'approche existante utilisée par ENTSO-E, qui forme la base de l'approche incrémentale proposée (illustrée à la Figure 6). Ces niveaux de complexité croissants sont proposés pour mieux quantifier certains indicateurs mais également les risques liés aux systèmes à forte pénétration de renouvelable. Un point important à souligner est que l'approche zonale pourrait montrer des bénéfices optimistes, dans le sens où certains coûts peuvent être « cachés » à cause de contraintes de sécurité ou de challenges opérationnels. Par conséquent, il est hautement recommandé d'exécuter l'étude coûts-bénéfices en utilisant un modèle nodal du réseau et en considérant des indicateurs de stabilité. Les métriques liées à l'inertie et à la stabilité des onduleurs peuvent être traduites en indicateurs de performance en évaluant le nombre de

points de fonctionnement par an qui sont à risque. Cela mène donc à des indicateurs quantitatifs qui peuvent être utilisés pour évaluer la nécessité d'investissements supplémentaires ou de mesures opérationnelles. Concernant la stabilité en fréquence, un cout est également évalué, basé sur la méthodologie de redispatch (similaire à l'indicateur B.10 actuellement utilisé par ENTSO-E). Pour la stabilité liée aux onduleurs, l'indicateur doit être vu comme une quantification de risque et des simulations supplémentaires devront être effectuées à un stade ultérieur d'avancement du projet pour déterminer les potentiels couts additionnels.

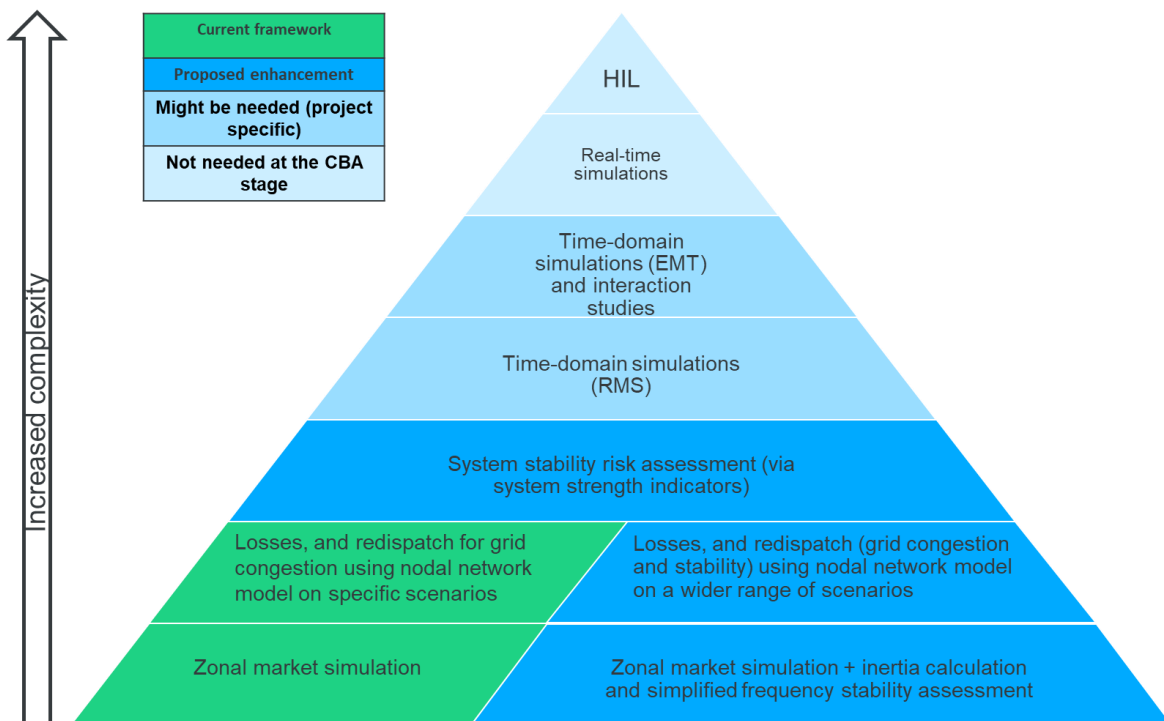


Figure 4 – Overview de l'approche proposée

Le travail effectué peut être résumé en trois parties distinctes, comme suit :

### 1. Méthodologie couts-bénéfices “améliorée”

L'approche couts-bénéfices proposée quantifie les bénéfices additionnels et identifie les risques potentiels pour la stabilité du système. Il est important de noter que certains de ces bénéfices (comme le contrôle de l'écoulement de puissance) ne peuvent être évalués qu'en utilisant un modèle réseau détaillé (plutôt qu'un modèle zonal) et/ou en incluant des contraintes de stabilité (p.ex. inertie).

Premièrement, un modèle open-source existant d'écoulement de charge optimal d'un réseau AC/DC a été utilisé. Ce modèle permet de déterminer les bénéfices pour le bien-être social, en considérant les congestions internes dans le réseau électrique, contrairement au modèle zonal qui néglige les contraintes internes. De plus, le modèle d'optimisation d'écoulement de charge a été modifié de manière à déterminer les bénéfices additionnels fournis par la capacité de contrôle d'écoulement de charge des liens HVDC.

En utilisant cette formulation modifiée<sup>3</sup>, les couts de redispatch sont minimisés pour un nombre de contingences sélectionnées. En exécutant deux calculs séparés, avec et sans la fonctionnalité de contrôle d'écoulement de charge, les bénéfices de cette fonctionnalité

<sup>3</sup> L'outil est accessible via <https://github.com/Electa-Git/CBAOPF.jl>

peuvent être déterminés. Les résultats confirment que les couts de redispatch peuvent effectivement être grandement diminués en utilisant cette fonctionnalité.

De plus, l'implémentation de l'outil d'optimisation permet d'inclure des contraintes additionnelles. L'ajout d'une contrainte d'inertie a été testée pour deux cas d'étude et il a été clairement démontré que la technologie HVDC permettait de réduire l'inertie minimum pour garantir la stabilité du système. Ce qui par conséquent, augmente le nombre de conditions d'exploitations satisfaisant la stabilité en fréquence. Ceci a également été quantifié via un calcul de redispatch.

Un dernier important aspect est la stabilité des réseaux électriques à haute pénétration d'énergie renouvelable (interfacée via de l'électronique de puissance). Il est généralement recommandé de faire des études très détaillées et des simulations temporelles pour vérifier la stabilité de ce type de réseaux. Cependant, les modèles adéquats, et avec le niveau suffisant de détails, ne sont pas disponibles actuellement pour des études de planification. Pour cette raison, il est recommandé d'évaluer le risque d'instabilité via l'utilisation d'indicateurs dédiés.

## **2. Modélisation et lignes directrices pour l'implémentation**

Une partie du travail (décrise en section 6.1), s'est spécifiquement concentrée sur les exigences de modélisation pour la technologie HVDC. Une revue complète des types de modèles ainsi que du niveau de détail adéquat, en fonction du phénomène étudié, a été présenté. Pour chaque fonctionnalité de la technologie HVDC, les exigences de modélisation sont spécifiées.

Les sections 6.2 et 6.3 détaillent les exigences de modélisation pour implémenter la méthode couts-bénéfices proposée. Ces sections contiennent toutes les informations nécessaires pour implémenter cette approche.

## **3. Illustration sur des cas d'études réalistes**

Les cas d'études fournissent non seulement des résultats quantitatifs mais aussi un retour d'expérience sur l'implémentation proposée. L'approche zonale a été implémentée sans problème alors que l'approche utilisant les modèles réseaux plus détaillés (nodal) nous a mené à de nombreux challenges (notamment au niveau des données disponibles). Il a été démontré que notre approche pouvait être utilisée dans un large système comptant plusieurs milliers de générateurs.

## ***Enseignements principaux et recommandations pour le futur***

### **(i) Enseignements principaux**

- (1) **L'utilisation d'un modèle nodal du réseau est nécessaire:** Bien que le modèle zonal permette de déterminer les bénéfices socio-économiques des projets de transmission, les résultats peuvent être optimistes en sous-estimant l'impact des congestions internes. Cela a pour effet de sous-estimer les bénéfices d'assets permettant de contrôler l'écoulement de puissance et il est dès lors important d'utiliser un modèle nodal du réseau. Notre étude a montré qu'il était faisable d'utiliser les modèles nodaux dans une étude couts-bénéfices européenne, malgré un temps de calcul largement supérieur (24 heures vs. 30 min pour le calcul d'une année cible) et des exigences plus élevées sur les données.
- (2) **Le contrôle de l'écoulement de puissance fournit des bénéfices importants:** **L'étude a montré que la technologie HVDC fournit des bénéfices importants via sa capacité à contrôler l'écoulement de puissance, notamment en cas de contingence.** En particulier, les liaisons HVDC

intégrées dans le réseau AC permettent de réduire les couts de redispatch de plusieurs dizaines de millions par an.

- (3) **Les contraintes de stabilité sont nécessaires:** Il est nécessaire de considérer des contraintes de stabilité (p.ex. inertie) dans les modèles de planification long-terme. Cela permet d'estimer le risque lié à la diminution de l'inertie du système et ainsi de déterminer quelles sont les meilleures solutions pour y faire face. De plus, **notre étude a montré que la provision d'inertie via la liaison HVDC réduit le coût de redispatch pour garantir la stabilité du système de plusieurs dizaines de millions par an.**
- (4) **Des indicateurs de stabilité sont recommandés pour identifier les risques opérationnels:** L'étude a montré que l'utilisation d'indicateurs de stabilité donne des résultats acceptables pour des études couts-bénéfices. **Il est bien évidemment plus précis d'utiliser des modèles détaillés, mais lorsque ceux-ci ne sont pas disponibles, l'utilisation des indicateurs proposés est pertinente, de manière à identifier les risques de potentiels coûts supplémentaires.** Il est dès lors recommandé de faire des simulations avancées uniquement lorsque les modèles nécessaires sont disponibles. Par exemple, dans un stade ultérieur de développement du projet.
- (5) **Des modèles harmonisés sont nécessaires:** En particulier, **l'harmonisation des modèles réseaux est importante** pour quantifier l'impact des congestions internes et les bénéfices via contrôle de l'écoulement de puissance. De plus, des modèles harmonisés sont nécessaires pour mieux approximer les limites de stabilité.

## **(ii) Recommandations pour améliorations futures**

- (1) **Amélioration de la base de donnée:** Les données réseaux étant indispensables dans notre approche, il est extrêmement important d'avoir un **modèle fiable du réseau européen**. Pour cela, les bases de données utilisées pour la planification de la génération, de la transmission et pour les études d'écoulement de charge doivent être harmonisées. Par ailleurs, un travail important est nécessaire pour **modéliser de manière adéquate les assets interfacés via de l'électronique de puissance**. Cela permettra une meilleure évaluation des risques d'instabilité.
- (2) **Besoin d'infrastructures de calcul performantes:** Bien que les calculs utilisant des modèles détaillés du réseau électriques sont plus gourmands en puissance de calcul, des techniques existent pour améliorer le temps de calcul. Il est possible de paralléliser les simulations, d'utiliser des algorithmes d'intelligence artificielle, de filtrer les contingences et les points de fonctionnement. De plus, **l'utilisation d'infrastructures hautement performantes permettraient d'implémenter la méthode proposée dans des outils de pointe**. D'autre part, l'utilisation d'outils open-source permet de garantir la transparence envers les parties prenantes.
- (3) **Définition d'un indicateur de stabilité pour le réseau électrique du futur:** Deux indicateurs de stabilité ont été utilisés dans cette étude. D'autres indicateurs existent dans la littérature et certains sont assez prometteurs pour déterminer notamment l'impact de boucles de contrôle avancées sur la stabilité du réseau. Il est dès lors important **de définir un indicateur de stabilité de manière harmonisée** et qui puisse être utilisé dans des études couts-bénéfices. Il est cependant attendu que cela nécessite l'implication des parties prenantes ainsi qu'un effort de recherche fondamentale.

## Table of Contents

1.	Executive summary (English) .....	5
2.	Résumé exécutif (Français) .....	10
3.	Glossary .....	16
4.	Introduction .....	18
5.	“Enhanced” CBA methodology .....	21
5.1.	Description of the existing ENTSO-E CBA approach .....	21
5.2.	Drivers for an “enhanced” CBA approach .....	26
5.3.	Overview of “enhanced” CBA approach .....	30
5.4.	Data for determining CBA-KPIs of the selected use cases .....	34
5.5.	Interface between steady-state optimization and power system simulations .....	35
6.	Modelling and implementation guidelines .....	39
6.1.	Technical Aspects of HVDC and Modelling Requirements .....	39
6.2.	Steady-state Optimization: Modelling Requirements to determine Techno-economic KPIs .....	60
6.3.	Modelling Requirements to determine proposed stability KPIs .....	75
7.	Illustration on use cases .....	80
7.1.	Use case selection .....	80
7.2.	Navarra Landes .....	92
7.3.	Celtic interconnector .....	95
7.4.	Ultranet + A-North .....	107
7.5.	EuroAsia .....	112
7.6.	2050 MTDC .....	117
7.7.	Main challenges encountered during analysis of the use cases .....	118
8.	Main findings and recommendations .....	119
9.	Appendix I: stakeholder interaction .....	123
9.1.	Stakeholder feedback on use case selection .....	123
9.2.	Modelling requirements and cost-benefit analysis .....	123
10.	Appendix II: use case selection .....	126
11.	Appendix III: Data sources for the zonal economic dispatch model .....	127
12.	References .....	129

### 3. Glossary

AVM	Average Value Model
BESS	Battery Energy Storage System
BW	Bandwidth
CBA	Cost-Benefits Analysis
CCS	Carbon capture and storage
CCT	Critical Clearing Time
CCGT	Combined-cycle gas turbine
DSR	Demand side response
ED	Economic dispatch
EMT	Electromagnetic transient
ENS	Energy Not Served
FRR	Frequency Restoration Reserve
IBR	Inverter-Based Resource
IGBT	Insulated Gate Bipolar Transistors
KPI	Key Performance Indicator
LCC	Line Commutated Converter
MMC	Modular Multilevel Converters
MTDC	Multi-terminal HVDC
MS	Member state
OCGT	Open-cycle gas turbine
P2G	Power to grid
PE	Power Electronic
PLL	Phase-locked loop
PTDF	Power Transfer Distribution Factor
PtP	Point-to-Point
POC	Point-Of-Connection

RES	Renewable Energy Source
RMS	Root-Mean Square
RR	Replacement Reserve
SCR	Short-circuit ratio
SPWM	Sinusoidal Pulse Width Modulation
TNEP	Transmission Network Expansion Plan
TYNDP	Ten Year Network Development Plan
VOLL	Value of Lost Load
VSC	Voltage Source converter
Z/Y	Impedance /admittance

## 4. Introduction

The transition towards a carbon neutral economy by 2050 will require a large-scale electrification of the energy system, with an almost fully decarbonized power system. To this end and following the European Green Deal, the Commission proposed in March 2020 the European Climate Law to provide the necessary legal framework. The 2050 climate-neutrality objective will also impact the trajectory for achieving this goal. By 2030, for instance, about 50 percent of electricity generation in Europe will be based on wind and solar energy [1]. In particular, the European Commission has high ambitions in terms of further offshore renewable energy development (wind, but also wave and tidal) and this led to the definition of an EU Strategy on Offshore Renewable Energy published end of 2020 [2].

In order to reach these ambitious targets (for offshore but also for other renewable energy sources and the transmission of their power output to the consumption locations), the electrical grid has to be planned in a cost-economic way that allows transmission of energy over long distances while keeping a high security of supply. This is a real challenge in a future power system integrating more intermittent and power electronic interfaced generation. Therefore, the current power system planning methodologies will need to evolve to adapt to the high renewable energy sources landscape. For example, more coordinated grid planning approaches could be envisaged. These approaches could mean sector coupling, more coordination between onshore and offshore planning, or coordinated spatial planning (especially offshore for allocation of areas for offshore plants). For instance, in its proposal for a revision of the TEN-E Regulation (December 2020), the Commission emphasized the need to define offshore renewable generation to be deployed in each sea basin by 2030, 2040 and 2050 and to define integrated offshore network development plans.

Looking at the European network, HVDC is seen as one of the key technologies of the future with several HVDC connections considered in the TYNDP 2020, as shown in Figure 5. It has been generally used for interconnection between the different synchronous areas (e.g. HVDC connections between the Nordic countries, Continental Europe, Great Britain and Ireland), but also to increase the transfer capacity between countries (e.g. Spain and France). Currently, more complex HVDC connections are investigated in order to take advantage of remotely located renewable sources of energy, mainly the vast offshore wind potential in the surrounding seas. In particular, the PROMOTioN project estimated the wind potential in the North Sea to 205 GW. ENTSO-E expects that by 2030 59% of the transmission network investments in Europe will be in HVDC technology. The majority of these new investments is expected to use the VSC technology.

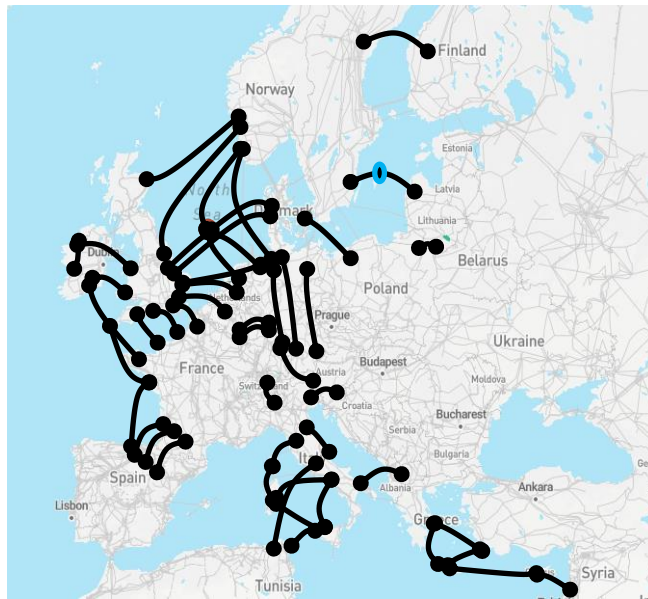


Figure 5 - Subset of HVDC connections in TYNDP 2020 of ENTSO-E

Up to now, the vast majority of HVDC connections in the world consists of point-to-point links, sparsely spread in the power systems. However, with the expected development of HVDC connections, the penetration of HVDC connections will increase with multiple HVDC connections in close proximity and between the same systems. In addition, more complex technologies such as Multi-Terminal DC (MTDC) grids or offshore hubs might become more attractive and be realized.

This transition and integration of HVDC systems is not without its challenges. Technical barriers still have to be surpassed in terms of the protection of such systems – there is still low availability and experience from HVDC circuit breakers – as well as in terms of multi-vendor interoperability – as intellectual property rights between different vendors should be protected. Other important challenges involve the control, operation and planning of such hybrid AC/DC systems, especially when they are combined with high penetration of renewable energy sources. The need for coordination between the TSOs in the above challenges is expected to further increase and be of crucial importance. Operating guidelines, system planning methodologies and market procedures should be revisited and adapted in order to cope with this shift in the power system paradigm.

Regardless of the shape of the future grid topologies, HVDC connections will provide several benefits to the power systems due to their special characteristics such as voltage support, improving stability or providing system services (blackstart, frequency, etc.).

It is however challenging to fully integrate these risks and benefits of new technologies such as HVDC in the planning studies as part of an integrated cost-benefit analysis (CBA), as the initial focus of the European CBA is mainly on energy exchange and on conventional technologies, and less on power system technical aspects and stability. The rapid evolution of the grid and of the technology caused significant changes and therefore more details must be included in the CBA studies to compare appropriately different technological options. This is especially true for meshed HVDC grids, multi-terminal HVDC or for HVDC links embedded within the AC grid.

In order to address these challenges and to allow decision makers to make better informed decisions, this study aims at providing modelling requirements of AC/DC grids and in particular to propose clear guidelines to evaluate, at the planning stage, all benefits that can be provided by HVDC technology in a system with high share of RES.

As such, the main question we are trying to answer can be summarized as: “**Are the existing methodologies, models and tools adequate to capture all risks and benefits when planning AC/DC hybrid grid?**”

The focus of this study is therefore on the planning stage when the evaluation of the costs and benefits of a project candidate takes place. It is important to evaluate whether some of these costs or benefits are under-estimated using classical CBA methodologies. Commonly used CBA methods do not capture all technical risks related to operation of a system with high penetration of IBRs. Therefore, operating conditions considered might not be stable and would require additional investment or redispatch to be viable. VSC HVDC technology can provide system stability services that would allow stable operation at high penetration of IBRs. This must be accounted for in the CBA analysis, in order to correctly capture the benefits of HVDC technology. Also, the lower losses and power flow control capabilities of HVDC technology are not always considered in typical CBA approaches.

This study tries to identify the limitations of the classical CBA methodologies and to provide implementation guidelines. To that end a proof-of-concept optimization model is developed and implemented as an open-source optimization tool and is clearly described in the report. Specific use cases were carefully chosen to test and fine-tune our implementation.

The report is further structured as follows:

- Chapter 5 describes the proposed “enhanced CBA” methodology. First, the existing CBA proposed by ENTSO-E is analysed. Then, additional or updated KPIs are discussed. Next, the recommended methodology is explained in more detail.
- Chapter 6 focuses on the modelling requirements and implementation guidelines. The section starts by a review of the different classes of models and describes which level of detail is recommended depending on the studied phenomenon. The second part of the section details the modelling requirements for the steady-state optimization problem while the last part details the requirements for the stability indicators.
- Chapter 7 shows the simulation results on the selected use cases. First, the use case selection process is described. Different use cases are highlighted to quantify specific indicators with the goal of illustrating the methodology, test the implementation and demonstrate the feasibility of future applications.
- Chapter 8 finally gives an overview of the main findings and recommendations

Additional information on the stakeholder interaction (during a workshop which took place on 31st March 2022), on the use case selection and on the data resources for the zonal economic dispatch model can be found in appendix.

## 5. “Enhanced” CBA methodology

### 5.1. Description of the existing ENTSO-E CBA approach

The following section briefly describes the current CBA methodology employed within the TYNDP process and pinpoints, (1) how the representation of additional benefits and costs through HVDC (grids) can be improved, (2) how some of the KPIs deemed not quantifiable within the current approach could be quantified in a uniform way.

The starting point for the analysis of the CBA KPI is the 3<sup>rd</sup> ENTSO-E Guideline for Cost Benefit Analysis of Grid Development projects [3], currently under public consultation. Figure 6 shows the current set of KPIs defined for conducting the CBA and if the KPIs are computed based on a zonal or nodal model. It is also already outlined that the stability KPIs (B8) are updated in this study.

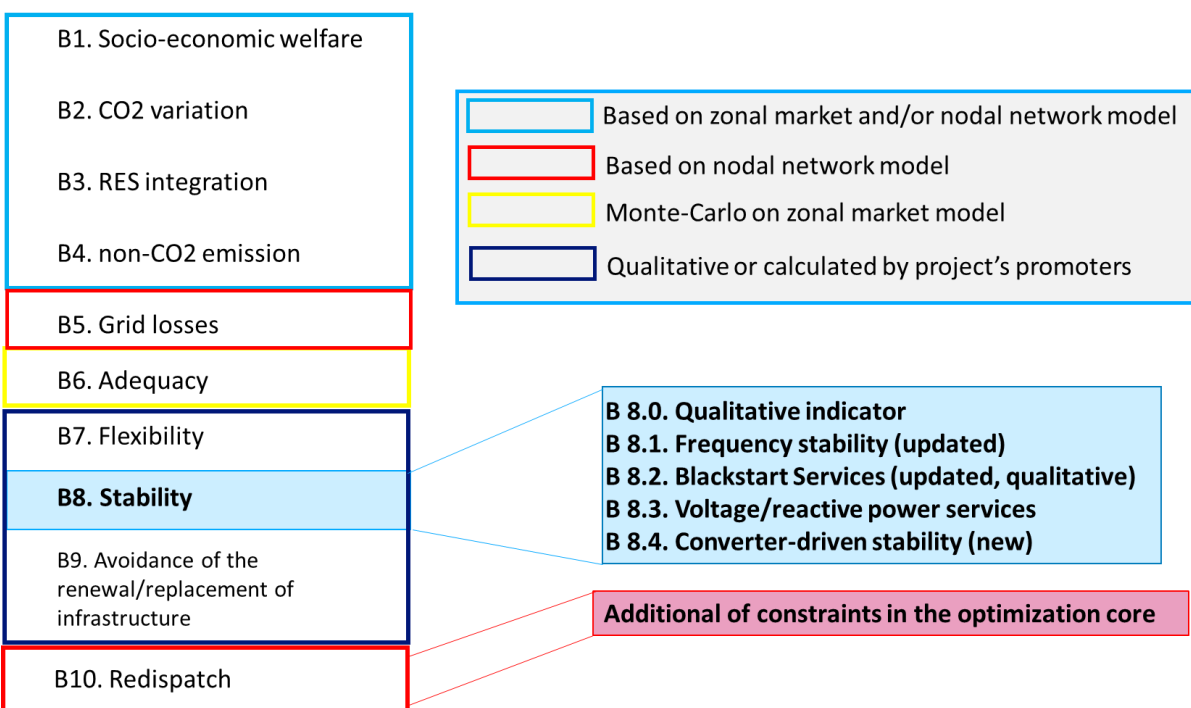


Figure 6 – CBA KPI according to the 3<sup>rd</sup> ENTSO-E guideline for cost benefit analysis of grid development projects

In the following paragraphs, the calculation of the different KPIs will be introduced briefly, for the detailed calculation of the parameters, the readers are referred to [3]. Table 1 gives an overview of the KPIs B1 to B10.

**Table 1 - Overview of KPIs B1 to B10**

Cat.	Name	Unit	Monetized?	Qualitative/Quantitative
B1	Socio-economic welfare	€/yr	Yes	Quantitative
B2	CO2 emissions	t/yr or €/yr	No / Yes	Quantitative
B3	RES integration	MW or MWh/yr	Yes	Quantitative
B4	Non CO2 emissions	t/yr	No	Quantitative
B5	Grid losses	MWh / yr	Implicit or explicit	Quantitative
B6	Adequacy	MWh / yr	Yes	Quantitative
B7	Flexibility	0/+/++	No	Qualitative
B8	Stability	-	No	Qualitative
B9	Avoidance of renewal / replacement	€	Yes	Quantitative
B10	Redispatch reserves	€ / yr	Yes	Quantitative

Although the KPIs B1 – B6 as well as B9 – B10 can be determined in a quantitative way, KPIs B7 and B8 related to enhancing system flexibility and impacting system stability have been defined in a qualitative manner. Table 2 summarizes the computational requirements to calculate the listed KPIs and provides improvement needs for the determination of the KPIs.

**Table 2 - Computational requirements to calculate the listed KPIs**

Cat.	Name	Computational requirements	Improvement needs
B1	Socio-economic welfare	Can be obtained via zonal and/or nodal economic dispatch model depending on use-case, efficiently solvable using linear models	Power flow control through HVDC links in the modelling framework.
B2	CO2 emissions	No additional optimisation needed w.r.t. B2, translation of dispatch to emissions	/
B3	RES integration	No additional optimisation needed w.r.t. B3, translation of dispatch to additional RES integration	/

Cat.	Name	Computational requirements	Improvement needs
B4	Non CO2 emissions	No additional optimisation needed w.r.t. B4, translation of dispatch to emissions.	/
B5	Grid losses	Solution of 'AC' power flow based on dispatch (prone to non-convergence), or estimation of losses with subsequent power flow calculations.	Representation of HVDC converter and line losses.
B6	Adequacy	No additional optimisation needed w.r.t. B6, however explicit demand curtailment to be modelled using VOLL.	/
B7	Flexibility	Stochastic model to determine optimal size of FRR and RR for different climatic conditions and contingencies.	Power flow control through HVDC links in the modelling framework.
B8	Stability	<p>Maximum frequency deviation or minimum inertia constraints within OPF/ED needed for frequency stability for optimisation. As an alternative, dynamic simulations for various operating points can be performed.</p> <p>Voltage stability can be assessed using continuation 'AC' power flow (convergence prone).</p> <p>Black-start modelling is very case specific requiring dynamic/transient models.</p>	Methodology based on stability / inertia constraints to approximate stability constraints based on dimensioning incident.
B9	Avoidance of renewal / replacement	Very project / TSO specific. Can only be modelled using nodal models. Ideally modelled with TNEP model using exclusivity constraints.	Multi-step transmission expansion optimisation to determine potential for investment deferral between multiple options.
B10	Redispatch reserves	Two stage model consisting of market clearing, and detailed redispatch – OPF needed. Detailed information on N-1 contingency set, and control actions needed. Potentially discrete model if topological actions considered (high computational requirement).	Clear guidelines on usage of HVDC for cross-border exchange and as preventive/curative measure needed.

In fact, for the determination of the KPIs B1 throughout B6, the same underlying optimisation model can be used.

**KPI B1 – Socio economical welfare**, is calculated using an economic dispatch or unit commitment model, which can be applied to either a zonal or detailed nodal grid model. The main idea behind such an optimisation model is to determine the least cost generation dispatch (or market outcome) for a given RES and demand scenario. The main inputs to the optimisation problem are the installed generation capacity for different types

of generation in each zone / node, the zonal / nodal electricity demand, the cost of electricity generation for the different generators (generator types), and a network model including the zonal / nodal connectivity of generators and demand. In case of zonal models, the network is often represented with transfer capacities available between the different market zones, whereas in detailed nodal models, the high voltage network is represented through line impedances governing the power flows and the respective line limits. A more detailed explanation of the two types of models is presented within the section 6.2. Thus, KPI B1 is calculated by applying such an optimisation model, where the generation dispatch cost is determined for a number of different operating conditions using RES and demand time series for a number of different climate years. By running the same optimisation model for the case without the investment and with investment and comparing to total electricity generation cost in both cases, the socio – economic benefits of the investments can be obtained. In the case of HVDC technology, its power flow control capability can help to avoid congestion in the system, and so have a higher impact on the minimisation of the total generation dispatch cost. However, this aspect can hardly be captured in zonal models, as in such models, the interzonal transmission capacity is often modelled without accounting for the distribution of power flows and only making of Net Transfer Capacities (NTCs) between the zones, and zones themselves are assumed to be congestion free. As such, this KPI can be improved by applying detailed nodal network models, as well as explicitly modelling the control capabilities of HVDC connections. The NTC based model can be improved using power transfer distribution factors (PTDF) which use representative impedances within the zones, and can approximate power flow constraints. However, in presence of controllable devices such models need to be extended with additional distribution factors for PSTs or HVDC links. Section 6.2 shows how such models can be improved using linearized power flow models.

**KPI B2 – CO<sub>2</sub> emissions** is a KPI that can directly be calculated from the output of the optimisation model used for B1. As the dispatch of each generator (type) is optimised on an hourly basis, the emissions of each generator can be calculated in a post-processing step, in case the emission factors of the generators expressed in tCO<sub>2</sub> / MWh are known. Thus, again by comparing the results of the optimisation for the case with and without the investment, the contribution to CO<sub>2</sub> savings can be calculated.

**KPI B3 – RES integration** indicates how many additional MWh of RES generation can be accommodated in the system if the investment takes place. Just as in case of B2, this KPI can be calculated in a post – processing step by comparing the total amount of RES generation between the case with and without the grid investment.

**KPI B4 – Non – CO<sub>2</sub> emissions** is an extension of B2, which also accounts for other types of emissions associated with electricity generation, such as NO<sub>x</sub> and SO<sub>x</sub> emissions. Similar to B2, using appropriate emission factors tNO<sub>x</sub> / MWh and tSO<sub>x</sub> / MWh for conventional generators, the non-CO<sub>2</sub> emissions between the case with and without the grid investment can be compared.

**KPI B5 – Grid losses** can be calculated in several different ways. If a detailed network model and a lossy power flow formulation are used, the transmission losses attributed to AC and DC grid components will be implicitly considered by the optimisation model as will be explained in section 6.2 in detail. However, such models are usually nonlinear and nonconvex in nature, and as such are seldom applied to large power systems, for many different generation and demand scenarios as being done within the TYNDP CBA process. Thus, even if detailed nodal grid model is used, very often a linearised power flow (DC) formulation is used in practice to conduct the socio-economic welfare optimisation, which neglects the network losses. When zonal models are used, generally losses cannot be accounted for. One way of calculating the transmission losses is to perform power flow calculations using the obtained generation dispatch as a starting point. In the power flow calculation, a subset of the generators in the system are defined as

slack generators which can provide the additional energy to compensate for losses. This way a feasible system state fulfilling the nonlinear nonconvex equations is determined. Another possible way of calculating the transmission losses is to start from the transmission line flows obtained in the first optimisation stage, and to multiply these with certain loss factors in order to estimate the actual amount of expected losses. Although this approach is widely used for AC lines, there are standardised loss factors which are being used for HVDC connections.

**KPI B6 – Adequacy** relates to the expected energy not served, due to unavailability of generation sources in certain parts of the grid and lacking transmission capacity to supply these parts from neighbouring parts. This KPI can be calculated by extending the model briefly introduced for B1. Therefore, a zonal / nodal demand curtailment variable is introduced to the optimisation problem, to reduce the demand in hours where there is not enough generation and transmission capacity available. Obviously, the cost of such demand curtailment should be very high, to be only used as last resort action. In practice, the value of lost load is considered to be 1-2 order of magnitude higher than the generation costs. The zonal optimisation model with such a demand curtailment model is outlined in detail in section 6.2.

**KPI B7 – Flexibility** is only considered to be a qualitative parameter in the proposed CBA framework. This KPI related to the usage of unused zonal capacity to exchange balancing energy across national balancing markets. System balancing can be provided by different types of reserve products such as automatic or manual frequency restoration reserves (aFRR, mFRR) or replacement reserves (RR), often also called tertiary reserves. The calculation of the improvement of system flexibility through grid investments requires the utilisation of optimisation models, which can incorporate redispatch actions from generators. Also, considering the stochastic nature of system imbalance, either through deviations from forecasted generation and demand values or through system outages, a probabilistic calculation of redispatch needs is required to quantify flexibility improvement.

**KPI B8 – Stability** indicates the change in system stability as a result of grid reinforcement from the perspective of transient stability, voltage stability, frequency stability and provision of system restoration services, e.g., black start capability. Generally, dynamic analysis is required in order to assess the stability of the system. HVDC connections can provide improvements in all aforementioned aspects, and such, a quantitative analysis of this indicator would highlight the benefits of HVDC technology. However, generally, detailed time-consuming dynamic simulation studies are required to assess the stability of the system (provided that adequate dynamic model is used). Thus, such analysis cannot be conducted for a large number of operational states, such as different grid loading conditions or different contingencies.

**KPI B9 – Avoidance of renewal / replacement cost of infrastructure** indicates the avoidance of new investments in generation capacity, refurbishment of existing generation fleet or avoidance in construction of other transmission / distribution lines. Aspects related to generation expansion can be derived from the outcome of the socio – economic welfare model, by analysis of the utilisation of generators in the system. In order to assess the avoidance of transmission line replacements, dedicated transmission expansion optimisation models would be required, which treat different expansion options as candidates, and select the most suitable set of candidates considering their investment costs. However, such approach implicitly performs a CBA within optimisation model, to select the best subset of candidate lines. As such, in practise this type of quantification is only be done on a case-by-case approach, by adding (or removing) additional grid expansion, replacement options besides the actually analysed investment.

**KPI B10 – Reduction of necessary reserve for redispatch power plants** can be calculated by extending the model used for B1 by means of a redispatch optimisation as

outlined in section 6.2.3. In this case, for all operating conditions throughout a year, the maximum amount of required redispatch power within the year is calculated. By comparing the maximum redispatch requirement for the case with and without the grid investment, it can be determined if the redispatch need is increased or decreased, as well as what the costs (benefits) of the increase (decrease) would be. HVDC connections can help to decrease the redispatch need, due to the power flow control capability they offer, and therefore this KPI is important to be quantified to highlight the benefits of HVDC technology.

## 5.2. Drivers for an “enhanced” CBA approach

As highlighted in the introduction, the goal of this work is to adequately capture all risks and benefits in an enhanced CBA for planning an AC/DC hybrid grid with high penetration of IBRs. Before giving an overview of this enhanced CBA and the proposed additional or updated associated KPIs, the following section provide first an overview of the benefits, costs and risks of HVDC together with the stability challenges in a system with high IBR penetration. Also, some new or updated stability KPIs are introduced which will be incorporated in the “enhanced” CBA.

### 5.2.1. Benefits from HVDC functionalities

**Power flow control capability:** The power flow control capability is one of the most valued technical features of HVDC technology for grid expansion. The fast power control capability of HVDC can help to avoid congestion, optimize use of existing assets and increase RES integration, reduce system losses and reduce redispatch needs. Although benefits with respect to congestion management and RES integration are already accounted for within KPI B1, KPI B10 could be assessed in a different way to explore the benefits of power flow control capability of HVDC to reduce redispatch costs. In this respect, instead of only comparing the redispatch needs with and without the HVDC investment, the comparison can be done threefold, (1) determination of redispatch need without the HVDC investment, (2) determination of the redispatch need with the HVDC investment without power flow control, (3) determination of the redispatch need with the HVDC investment with power flow control.

**Inertial response provision capability:** HVDC can offer benefits through asynchronously connected HVDC systems with respect to inertia provision (or fast frequency reserves). Using dynamic simulations, the rate of change of frequency (ROCOF) can be determined for a number of predefined dimensioning incidents and operational conditions. As quantitative KPI, different metrics such as the inertia provision speed in MW / s, the inertia provision capability in MW / Hz and/or the improvement of the ROCOF in Hz / s can be provided. However, it is difficult to monetize the inertial response provision capability from HVDC systems due to the stochastic nature of the incidents happening in system operation, and the large number of possible system operational states. In this study we use minimum inertia constraints, which are based on a given allowable ROCOF in the network and determine the generation dispatch costs for the cases (1) without the inertia constraint, (2) with the inertia constraint but no contribution from HVDC and (3) with an inertia constraint which considers HVDC contribution. By analysing the difference in costs, we can derive the benefits of inertial response provision.

**Improvement of resilience:** HVDC technology can help to increase the resilience of the power system in two fundamental ways.

Firstly, by decreasing the vulnerability of the system, by for instance improving system stability through more robust control and application of special protection schemes. HVDC can act as firewalls between different parts of the power system and help to isolate

healthy parts of the system in a fast way, in case of wide-spread disturbances in the system. Other technical features, such as oscillation damping, provision of short circuit current, and voltage control, can further improve the quality of service and the system.

Secondly, the resilience of the system can be improved through faster system restoration after major events, for instance through provision of black-start services. When equipped with grid forming functionality, HVDC converters can provide a stable voltage reference, to which other parts / devices of the system can be synchronized to.

Although in theory quantitative KPIs such as MWh / year of avoided service interruptions, or their societal cost in € / year, can be defined, the calculation of such KPIs is very difficult. To analyze the improvement of the system vulnerability, detailed dynamic simulations can be performed for a number of critical contingencies and operating conditions. This way the frequency and voltage stability of the system can be assessed.

For the improvement of the system restoration, even though a number of steady-state analysis tools exist to analyse the system restoration from the power flow and power balance points of view, the main challenge in system restoration is ensuring dynamic stability. As such many different types of dynamic simulations would be required to analyse the system restoration process in detail, covering different operational scenarios as well a number of emergency situations, such as different system restoration sequences. Considering that black start services could be delivered by different HVDC connections to different countries at the same time, large scale simulation models would be needed. As such, this KPI better is suited to be defined in a qualitative manner for high level CBA, whereas TSOs can quantify this parameter through more detailed simulation models for known system restoration sequences.

**Improvement of system stability:** HVDC converters can provide several system services that will improve system stability. These services, such as voltage control, frequency response or grid forming controls can be beneficial for the system and reduce the need of investment in other assets. It is important to note that the classical zonal approach typically ignores network constraints. Therefore, additional constraints or nodal network model would need to be considered, to observe the benefits of HVDC technology for improving system stability. It must also be kept in mind that the goal is to integrate more RES in the system and that more IBR based RES poses challenges to system stability. Therefore, this KPI can be quantified by evaluating the percentage of operating conditions which are at risk of being unstable.

**Public acceptance:** HVDC technology overhead lines have a smaller footprint than AC overhead lines. Also, HVDC cables (underground or undersea) can be used on much longer distance than AC cables. It is therefore believed that HVDC will be more easily accepted by the public and that the permitting process will potentially be quicker than for AC lines. Such public acceptance is very difficult to be translated in a quantitative KPI, but should be taking into account in future CBA in a qualitative manner when comparing different network expansion options. Although not further elaborated in this report, public acceptance may become one of the bottlenecks/key decision points in future network expansion.

### 5.2.2. Risks and Costs of HVDC

**HVDC protection strategy cost:** The costs for AC protection systems are relatively low when compared to the total investment cost of grid expansion. However, HVDC circuit breakers can be costly, and especially in large multi-terminal and meshed HVDC grid expansion projects, their costs should be taken into account. This can be done based on existing studies on HVDC protection systems, such as proposed within the PROMOTiON project [4].

**Interoperability:** Multi-vendor interoperability of HVDC systems is, at the time of writing of this document, still an important challenge. There are several ways to de-risk potential interoperability problems, but some include additional costs (e.g. use of replica). As it is not clear what will be the best way to mitigate interoperability issues, no additional cost is foreseen in our calculation.

**Extendibility<sup>4</sup>:** HVDC systems are currently not built to be extended. Allowing extendibility might require additional costs (e.g. spare place on DC-busbar, spare place for DCCB, etc.) and also clear specifications for the control systems. For modelling, an additional margin on the cost could be considered to allow for future extension.

**Technology maturity:** The technology is still evolving (e.g. DCCB, XLPE cables, converters, etc.) and is not yet at a fully mature stage. However, it is assumed that the technology will be ready at the time horizon considered in this project (i.e. 2030 onwards).

### 5.2.3. System stability challenges with high penetration of IBRs

Stability of power systems with high penetration of IBRs is an important challenge which might require mitigation means such as new investments (e.g. synchronous condensers, BESS, etc.), advanced controls (e.g. grid forming) and/or operational constraints. In [5], it is noted that “*In the midterm, until new technical solutions are implemented, it may be necessary to take additional measures (e.g. RES curtailment or power flow limitations) to ensure system security. As such, there is a need to work decisively on the target solutions and to make them available when necessary, so that the midterm and probably costly limitations does not last too long*”. There is therefore uncertainty on costs for securing future system operations with high RES, which will require more simulations, advanced control loops, operational measures and/or additional assets.

The main technical challenges related to stability in power system with high IBR penetration are the following:

- **Reduced inertia** and frequency stability
- Low system strength<sup>5</sup> which can impact:
  - Functioning of protection devices
  - Power Quality
  - Transient stability of synchronous machines
  - **Converter-driven stability**
- Voltage control
- Potential control interactions

The currently proposed stability KPIs in the ENTSO-E methodology are qualitative and are based on the theoretical benefits of a technology with respect to transient, voltage and frequency stability [3]. While this provides some information, it is important to not only focus on the technology but also to consider some more project-specific characteristics. Moreover, the KPIs used by ENTSO-E focus on classical stability aspects (i.e. Transient, Voltage and Frequency) while the stability challenges of IBRs in weak grid has to also be specifically considered.

Table 3 proposes therefore two additional KPIs allowing to quantify the risks related to a grid with high penetration of power electronics. The quantification is based on the number of hours where the system is considered at risk. It should be noted that the KPI B.4

<sup>4</sup> Extendibility defined as “The design should allow for the forecast need for future extensions” (from National Grid ESO, <https://www.nationalgrideso.com/industry-information/codes/security-and-quality-supply-standards/code-documents>)

<sup>5</sup> system strength refers to the “*characteristic of an electrical power system that relates to the size of the change in voltage following a fault or disturbance on the power system*” [32]

(converter-driven stability) is really a new KPI, while the assessment of existing KPI 8.1 frequency stability is extended/updated with some new metrics.

**Table 3 - Proposed Stability KPIs to be incorporated in the “enhanced” CBA**

Proposed KPI	Metrics	How to calculate?	Comments
B 8.1. Frequency stability: Percentage of hours per year where frequency stability is at risk	Estimated inertia	Unit dispatch	Simplified time-domain simulations on single-node network can be used but lead generally to optimistic results.
	RoCoF	Use of swing equation	
B 8.4. Converter-driven stability: Percentage of hours or RES energy per year where converter-driven stability is at risk	Frequency nadir	Use of (simplified) time-domain simulations	Risk indicator  Indicator considering not only grid strength but also IBR control loop  To be used on a selection of operating conditions and with adequate model parameters.
	Percentage of hours at risk	Use of time-domain simulations or use of inertia/RoCoF constraint	
	SCR	Using network static data	
B 8.4. Converter-driven stability: Percentage of hours or RES energy per year where converter-driven stability is at risk	Converter-driven instability risk indicator	Using network static data and simplified grid following control parameters	Risk indicator  Indicator considering not only grid strength but also IBR control loop  To be used on a selection of operating conditions and with adequate model parameters.
	Converter-driven instability from RMS simulation	Using RMS simulations	
	Converter-driven instability (EMT + modal analysis)	Using EMT simulations + frequency-scan	

In the example of the **reduced inertia challenge**, it is therefore needed to estimate the inertia of each operating condition and also the minimum inertia constraint. The proposed KPIs require to therefore evaluate the percentage of operating conditions being below the inertia constraint. A monetary value can also be linked to this KPI by adding a stability constraint based on an allowable minimum inertia level within economic dispatch or redispatch calculations (as described in section 6.2).

Regarding the **KPI for converter-driven stability (in weak grid)**, it is also proposed to quantify the number of operating conditions or the amount of energy produced by RES for which a stability risk was identified. The stability of inverter based resources is driven by their control loops. With that regards, typical controls of inverters are grid-following and require therefore a stable source of voltage to synchronize to the grid. Theoretically, the stability of IBRs has to be assessed via EMT simulations. This is the only type of simulations which can fully capture the potential instability in the different control loops and in the dynamics of the inverters. However, accurate models, which are typically not available at the CBA stage of projects, are required. Another option would be to use RMS simulations to capture some aspects of converter-driven instability (such as stability of the PLL in weak grid). However, RMS simulations also require adequate models (including PLL control loops of grid following inverters, current limiter loops and grid forming implementations). While having limitations, the mostly used indicator is the short-circuit level which represents the “strength” of the network. Therefore, it is proposed to use indicators such as the short-circuit ratio (SCR) or more advanced metrics considering the SCR but also some basic control loops of the inverters and their setpoint (such as the CCT-IBR described in [6] [7]). Based on these metrics, a threshold can be used (e.g. SCR < 3) and the number of operating conditions for which the threshold is not reached are

considered as at risk of being unstable. Figure 7 illustrates that there are more stability challenges when the SCR is below 3 and that advanced controls or even new assets/hardware are required when SCR goes below 2. Since converter-driven instability can also affect HVDC systems, from the same figure it becomes evident that grid forming control in HVDC can increase their range of stable operating conditions and therefore allow to integrate more RES.

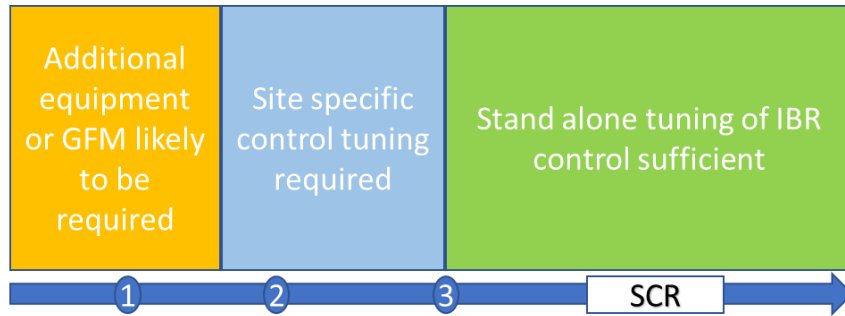


*Figure 7 - Impact of SCR on Converter-driven stability (from [8])*

### 5.3. Overview of “enhanced” CBA approach

The “enhanced” CBA as proposed in this work has two main aspects. First of all, it introduces new KPIs or updates existing ones to capture not only the benefits, but also the cost and risks associated with HVDC. An overview of the way the benefits provided by HVDC are incorporated in the “enhanced” CBA is presented in Table 4 at the end of the section (not all of them will be further elaborated in this project, but a first proposal has been included on future KPIs). The computational requirements, e.g. the way to monetize the corresponding KPIs are also presented in this table.

Secondly, as it is a fact that operating a system with high penetration of power electronics interfaced devices is a fundamental shift from the current system operations, the question is to know which assets will be required, which functionalities are required in order to ensure security and reliability of the system and, last but not least, which tools and methodologies are required to study them. Therefore, the “enhanced” CBA sets also a framework to assess the KPIs in future power systems building upon the existing CBA approach, see also Figure 8.

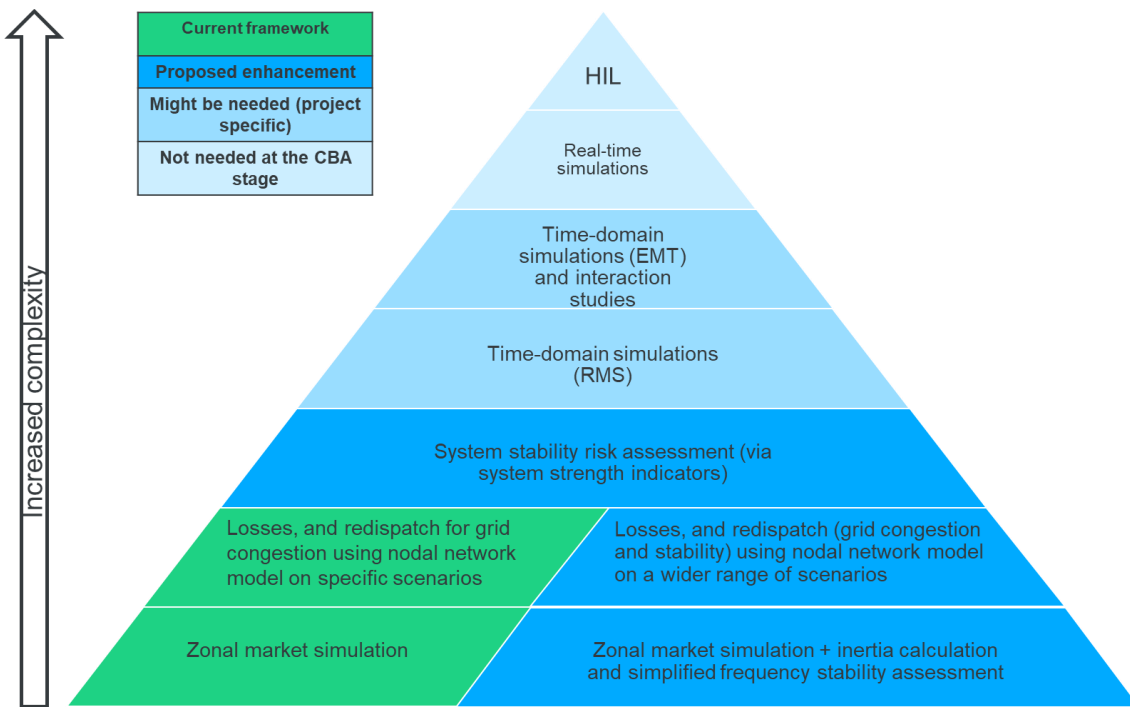


Figure 8 - Overview "enhanced" CBA approach

As shown in this figure, the existing framework focuses on zonal market simulations. This is the basis of the pyramid and stays the main key element in the CBA assessment. However, there are some additional aspects that should be evaluated. In particular, it is needed to verify whether large power flows over long distance do not cause any thermal violations and whether system stability is maintained for a wide range of operating conditions.

Section 5.2.3 described the additional stability KPIs that we recommend for integrating in the "enhanced CBA" while sections 6.2 and 6.3 provide more details on how to compute them. It is important to note that the proposed approach has several layers of complexity and it is shown how the complexity of the model should be increased to compute additional KPIs or to quantify KPIs that are currently assessed only in a qualitative manner.

The first layer of the proposed approach is the zonal market simulation. On this aspect there is no change compared to the existing CBA framework (i.e. energy simulations, minimizing the overall dispatch costs with transfer capacity constraints). It is recommended to complement this zonal market simulation step by an inertia calculation and simplified frequency stability assessment. The main reason is that reduced inertia presents a significant challenge for future system operations and it is important to at least identify whether the planned operating conditions will be at risk or not.

The second layer consists of nodal market simulations based on the European static network model. It is understood that the European network model is currently not widely used during the CBA calculation, except for calculation of losses or redispatch simulations in a limited number of operating conditions. It is proposed to considerably extend this second layer by:

- Including power flow control capabilities of HVDC
- Adding stability constraints (such as inertia)

Therefore, the network model needs to be more intensively used in the economic dispatch optimization. This will allow to quantify the redispatch costs for each thermal and/or stability constraint, and by consequence, give a clear order of magnitude on what mitigation actions need to be put in place to ensure stability. More mathematical details on the implementation of the network model optimization problem can be found in section 6.2.

The third layer which is recommended in this work, consists of a more detailed stability assessment. As already outlined, stability of systems with high penetration of IBRs is currently a challenge. It is also commonly agreed that the converter-driven stability must be assessed using very detailed and representative models that are typically not available when performing a CBA study. Our approach is thus to use indicators that can represent operating conditions at risk of being unstable. More details on these indicators are presented in section 6.3.2.

On top of these recommended three first layers, additional more complex layers are proposed. These include time-domain simulations in RMS or EMT domain. As illustrated in Figure 9, RMS simulation (also called phasor-mode simulation) is suitable for the classical types of power system stability and slow interactions, whereas EMT is necessary for faster stability phenomena.

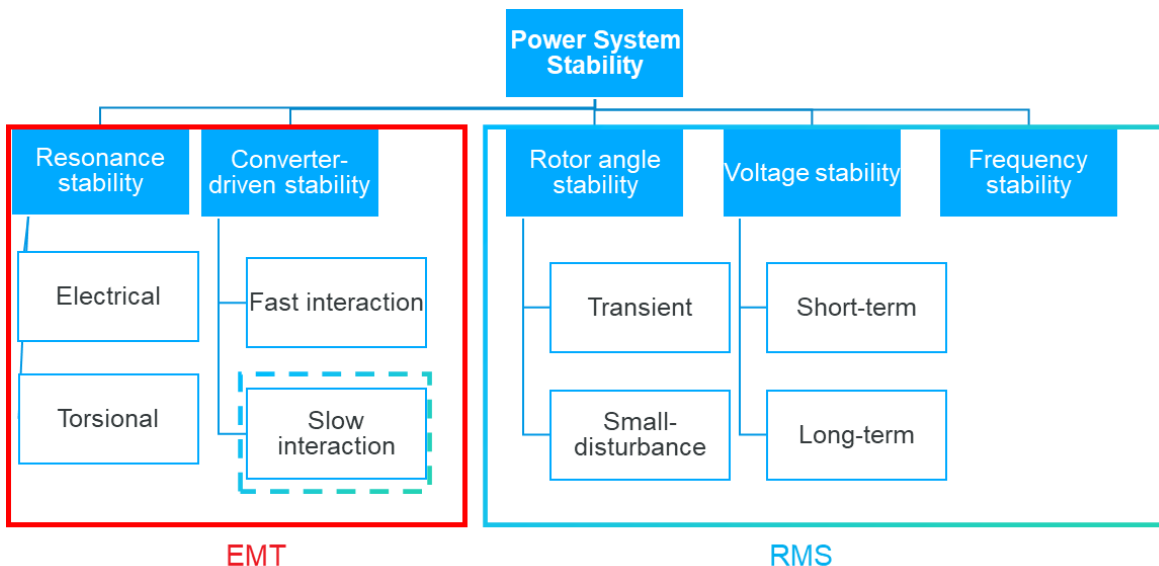


Figure 9 - Power system stability classification and simulation type for each type of stability (Figure inspired by [8] and [9])

It must be evaluated for each project which simulations are required. These simulations will typically be performed closer to the design stage of the project and therefore after the CBA approach which is the scope of this report. It is however important that, during the CBA, projects which will require more advanced simulations are identified. This will allow to include a cost margin for further studies and de-risking potential stability issues.

Finally, the use of real-time simulations or even hardware-in-the-loop is recommended when knowing the design of the project under consideration. These simulations are extremely important for understanding the behaviour of power electronics assets in weak grids. Also, the use of replica for HVDC systems has shown great benefits to prevent adverse interactions or for root-cause analysis, and for allowing simulations on the protection system design of multi-terminal HVDC and HVDC grids. However, these simulations are project specific and not to be used at a European scale CBA.

**Table 4 - Benefits provided by HVDC incorporated in “enhanced” CBA**

<b>Additional benefits considered in this work</b>	<b>Unit</b>	<b>Monetized</b>	<b>Qualitative/ Quantitative</b>	<b>Computational requirements</b>	<b>Comments</b>	<b>Link to KPI</b>
Power flow control capability	€ / year	Yes	Quantitative	Redispatch OPF for a set of N-1 contingencies, similar to B10. Two sets of calculations, with and without HVDC set point changes. Possibly SCOPF.	Would be too excessive to calculate for N-1 contingency sets and large number of operating conditions. Sampling/clustering would be needed. No unified definition of the SCOPF.	B.10
Improvement of frequency stability	Percentage of operation conditions / year	No	Quantitative	Dynamic simulations or swing equation needed to determine ROCOF.	Swing equation can be used in "conventional" systems where the main inertia provision comes from rotating masses. Frequency time-domain simulations recommended in systems with high penetration of virtual inertia or fast-frequency responses. For monetizing, inertia constraints can be embedded in steady state optimisation models.	B.8 or B.10
	Or			Provision of inertial or fast-frequency response through asynchronous HVDC. Addition of inertia constraint in redispatch calculation needed if monetary is required.		
	€ / year (if redispatch)	Yes	Quantitative			
Improvement of converter-driven stability	Percentage of operation conditions / year	No	Quantitative	Simplified assessment, RMS or EMT simulations required depending on the phenomenon under	"New" type of stability classification. The most important is to identify risk of instability operating conditions. Depending on the project, simplified or more detailed assessment can be performed. For monetizing, stability constraints can be embedded in steady state optimisation models.	B.8 or B.10
	Or			assessment and available dataset..		
	€ / year (if redispatch)	Yes	Quantitative			

Additional benefits to be assessed in future work	Unit	Monetized	Qualitative/Quantitative	Computational requirements	Comments	Link to KPI
Resilience improvement	MWh/year € /year	Yes	Quantitative	Dynamic simulations for firewalls. Black-start simulations. In both cases the avoided expected energy not served through HVDC could be used as KPI	Difficult to model in detail in a harmonised way. Future work needed to have a common agreement by stakeholders on what to include in resilience assessment.	/
Public acceptance and permitting	-	No	Qualitative	Expected duration for permitting process	Non-technical indicator, very project specific.	/
Protection system cost and extendibility as part of CAPEX	€	Yes	Quantitative	Additional cost of protection system or multi-terminal readiness as part of the CAPEX.	Reliable cost data (projections) on HVDC equipment needed.	C.1

## 5.4. Data for determining CBA-KPIs of the selected use cases

The data being used in the optimization process from the following sections are coming from the ENTSO-E database. In fact, the reference grid, generation and demand data are taken from the TYNDP 2020. The reference grid data help to give an overview about how the transmission lines are connected in the system. Knowing the level of interconnection between areas is fundamental to evaluate the effects of new investments on the grid. Regarding generation, the installed capacity for each bidding zone in the European system is used as input data. Information regarding renewables, conventional generators, power to grid technologies (P2G) and flexibility providers such as electric storage and demand side response (DSR) are listed based on the DE2040 scenario from [10]. Among the renewables (RES), data can be found for wind (offshore and onshore), solar PV, solar thermal, hydro reservoir and run-of-river. All the other RES sources are grouped in ‘other RES’. On the conventional generators side, the sources being included are coal lignite (new and old 1-2), hard coal new and old (1-2- +Bio), gas (conventional old 1-2, CCGT, CCGT new CCS and present 1-2 CCS, OCGT new and old), oil (heavy, light and shale new), PS (closed and open) and nuclear power plants. All the other kinds of conventional generator capacities are summed up in ‘Other non-RES’. The demand data contain the load for each bidding zone for an entire climate year, i.e. 8760 hours.

When developing a nodal balance model, it becomes clear how there is a lack in precise data for each node in the system. As anticipated, the ENTSO-E data set is based on the European zonal model, which assumes the electricity price to be constant for buses in the same bidding zone. Furthermore, the Kirchoff's and Ohm's laws behind the nodal model are not considered. The only limiting factor for the power transfer is the computed NTC for the different zones. In order to have a better overview about the status of the power grid, the demand and generation data need to be distributed to the nodes in each zone. With such a nodal balance model, the loading of each line is analyzed and the power flows to each bus are investigated. The main reason to use this kind of model is the more reliable picture of the power system that is computed. As a result, it is possible to study the cost of electricity in a more detailed way and spot possible additional benefits of HVDC technologies which cannot be fully grasped in the original zonal model. For example, a selected line which is not considered in the zonal model could turn out to be overloaded for most of the time in the nodal balance model. For this reason, installing a new HVDC link near the selected line could lead to a more optimal power dispatch in the grid and improve results for both reliability indexes and the computed KPIs.

## 5.5. Interface between steady-state optimization and power system simulations

The highly detailed European high voltage network model (which can be obtained from ENTSO-E under confidentiality agreement) consists of more than 7000 substations and 10000 transmission lines (and cables) and 7000 generating units. The calculation of the CBA-KPIs by applying hourly optimal power flow calculations on this large network model would be too time consuming on the one hand, and has a higher risk of non-convergence on the other. As such, a two-step approach is used for determining the CBA-KPIs.

First, the NTC based economic dispatch model as described in section 6.2.1 is solved for the whole European region to determine the hourly dispatch of each generation type on an hourly basis, for the selected scenarios and planning horizons. This way, the net positions of each market zone, and the total power exchange between the market zones are determined. All data to conduct this zonal analysis are publicly available at ENTSO-E and the location of data is provided in the appendix. The data contain the aggregated generation capacity per generation type for each market zone per planning year, climate year and scenario. Additionally, time series for RES capacity factors and demand are available for each market zone.

In a second step, the detailed high voltage network model is used to perform OPF calculations where controllability of HVDC can be taken into account. Depending on the use case, e.g., the location of the HVDC link, the detailed networks of the countries where the HVDC connections are located are used. All other countries/market zones are represented by equivalent single nodes. For instance, for the Navarra – Landes link connecting Spain and France, it is sufficient to use the detailed network models for Spain and France, and use equivalent nodes for all other neighbouring networks. In order to maintain consistency between the zonal and the nodal network models, a disaggregation of the zonal model is performed which is described in section 7. The demand is disaggregated linearly from the zonal model to the nodal model, whereas the hourly generation dispatch is disaggregated based on the maximum generation capacity of each unit.

Beside the nodal and zonal simulations, also a sequential approach is applied by means of an iterative procedure between optimal power flow calculations and the dynamic simulation performed for validating system stability. This procedure is visualized in Figure 10.

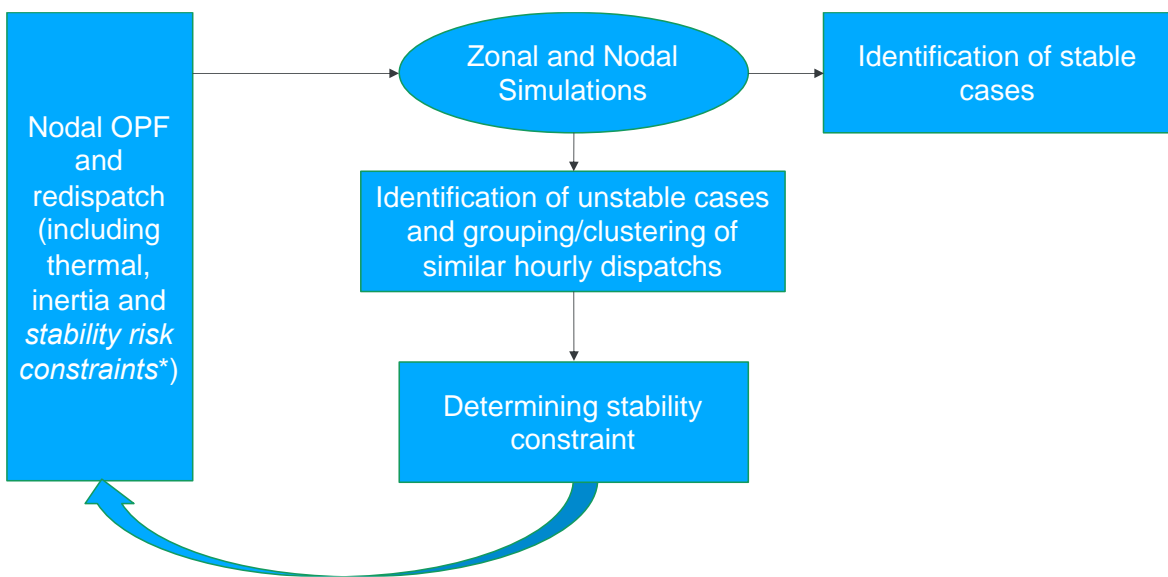


Figure 10 - Iterative procedure between steady state and dynamic calculations

In the first instance, optimal power flow calculations are used (either on zonal or nodal network models depending on the nature of the use case), which determines the generation set points under various operational conditions. Using this information dynamic simulations are performed to identify potentially unstable cases, as well as the required level of system inertia to ensure system stability in such cases. This information is passed back to the steady state calculation routine, which can determine a new set of generator and HVDC converter set points considering the inertia constraints.

Dynamic simulations are performed on the results of the AC/DC grid OPF described in section 6.2. It is hence expected to receive from the OPF a series of generation dispatches optimized on an hourly basis for at least one year which yields 8760 different network conditions. It is not relevant nor realistic to perform the time-domain simulations on each dispatch, for the following reasons:

- The interest of the time-domain simulations lies in the identification of weaknesses in the grid leading to instabilities. These weaknesses can only be highlighted during periods of significant stress on the system, which should occur only during a limited period of time throughout the year. In other words, most generation dispatches extracted from the OPF will be far away from the stability limits of the system and hence bring limited added value to the time-domain results.
- Most dispatches will be redundant, for instance due to daily, weekly or monthly periodicity.
- Considering the size of the systems envisaged (multi-country scale), the time-domain simulations will be time-extensive. It is key to reduce the number of simulations required for efficiency purposes.

Consequently, the time-domain simulations are performed on a selection of cases amongst the hourly dispatches provided by the OPF. The dimensions used to perform the selection will be key to ensure that the simulations consider the worst-case dispatch scenarios for each instability envisaged. For instance, the total inertia of the system is to be considered if frequency stability is of concern. For the purpose of AC/DC system studies, the following dimensions are suggested:

- Level of AC short-circuit at key nodes of the network;
- Power Flow through the DC link(s) and on parallel AC lines (if relevant);
- Overall demand of the system;
- Ratio RES production over overall demand;
- System inertia (in MW.s);

Once the N dimensions have been selected, each dispatch scenario is then associated to a n-tuple and might have to be processed into a normal distribution for uniformity of dimensions purposes. Finally, each n-tuple can be plotted in a multi-dimensional environment where each axis corresponds to one dimension, then we can use clustering methods to select either representative scenarios (which lie in “the middle of the cloud” of points), or extreme scenarios (which lie at the edge of the cloud of points).

Two clustering methods have been used in this work. The first clustering method is based on the K-means algorithm and aims at grouping similar operating conditions into clusters. The main goal is to perform more advanced simulations on representative samples from each cluster rather than on each operating point. These advanced simulations can be power system time-domain simulations or redispatch calculations. When using this clustering technique, it is recommended to set a relatively high number of clusters (ideally equal to the highest number of advanced simulations that can be handled by the user).

The second clustering technique is based on the DBSCAN algorithm. This algorithm analyses the density of points in the n-dimensional space. It is therefore a good algorithm to identify a representative set of operating conditions (i.e. operating conditions that occur regularly over the year). The overall methodology is summarized in Figure 11. The clustering process itself is illustrated in Figure 12 and Figure 13, which show the different types of results obtained by the two proposed clustering approaches.



Figure 11 – Dispatch scenario selection process

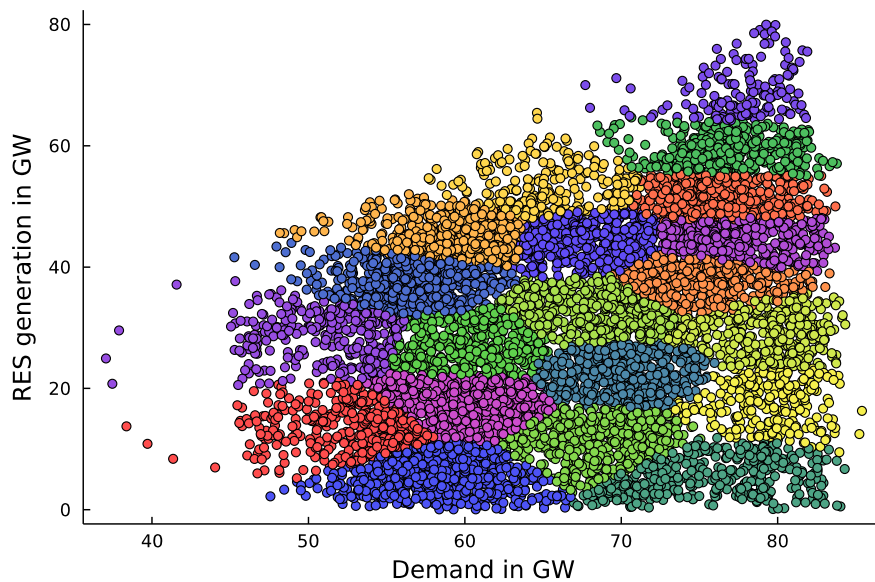


Figure 12 – Example of an hourly dispatch selection through K-means clustering. This example counts 20 cluster (each cluster is indicated by a color). Advanced simulations can be performed on each of these clusters.

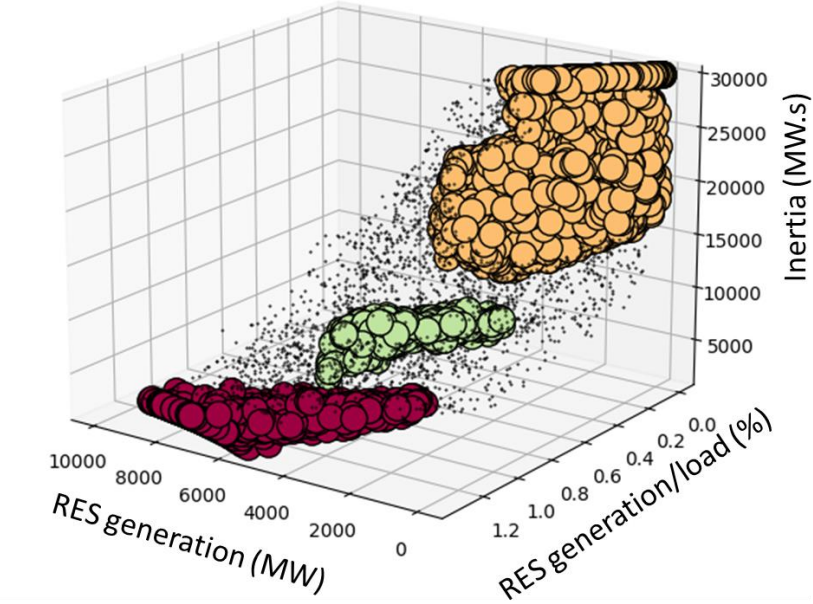


Figure 13 – Example of an hourly dispatch selection through DBSCAN clustering. This example counts 3 representative clusters (e.g. low, intermediate and high RES penetration). It can be seen that a significant number of points are not assigned to these clusters.

## 6. Modelling and implementation guidelines

### 6.1. Technical Aspects of HVDC and Modelling Requirements

#### 6.1.1. HVDC technologies, configurations, and technical features

Two dominant HVDC technologies are used currently: Line Commutated Converter (LCC) and Voltage Source Converter (VSC). Most of the HVDC connections in operation worldwide use the LCC technology, which relies on thyristor semiconductor switches. Their power and voltage ratings keep increasing over time with voltages up to 1100 kV and rating up to 10 GW in China. On the other hand, VSCs have gained momentum during the recent years and are the most used technology in Europe. VSCs rely on Insulated Gate Bipolar Transistors (IGBT) for the conversion process, which allows to generate an independent AC voltage waveform.

Although LCC technology is mature and offers several benefits, VSC technology offers additional advantages, such as [11]:

- **Four-quadrant operation:** LCCs consume large amounts of reactive power. In contrast, VSCs can absorb or consume reactive power depending on the system requirements, thus achieving independent active and reactive power control.
- **Power reversal:** VSCs can almost instantaneously change the power flow direction, whereas in LCC connections this requires shutting down the link and reversing the DC voltage polarity.
- **Possibility to connect to weak AC grids:** LCCs require a strong enough AC grid to operate correctly. VSCs do not necessarily face such a limitation.
- **Grid forming and black-start capability:** VSCs can generate a voltage output to which other devices can synchronize. This makes it extremely attractive for offshore applications.
- **Fault-ride through capability:** VSCs can ride through low AC voltages, whereas LCCs are prone to commutation failures.
- **Harmonics:** VSCs generate less harmonic content than LCCs. Therefore, the need for AC and DC filters is smaller.
- **Footprint:** VSC stations are generally less bulky than LCC stations of the same rating, mainly due to the smaller requirements for filters.
- **Cheaper cables:** VSCs can be connected with XLPE cables, instead of the oil-based (mass impregnated) cables required for LCC connections.

The state-of-the-art ratings currently considered in Europe for offshore VSC-HVDC transmission are 2 GW at  $\pm 525$  kV assuming a bipolar topology and Modular Multilevel Converters (MMC).

Attractive system-level features and the related functionalities that VSC-HVDC can offer are key to many of the drivers for the increasing use of HVDC systems. Many of these features are beneficial to increased system flexibility, controllability, resilience, and security as time constraints to get system back to normal operating conditions are becoming tighter. Nevertheless, these benefits are often not properly reflected in holistic planning approaches such as CBAs that is key to adopting and investing in HVDC technologies at the planning stages. Thus, the benefits and potential cost impacts are often not completely captured.

The precursor to assessing how the current CBA should be extended is highly dependent on the foreseen impact on the system by a feature and its functionalities, and how these may influence analyses. The benefits of HVDC technologies for hybridization are not in question as they are well-promoted and are major drivers for these technologies. The major challenge is the potential cost implications (savings or expenditure) and how these

trades-off with the potential benefits, and by how much these costs are high enough to influence the CBA. Importantly, the system impact is dependent on the expected functionality, implementation details (generic or specific), initial speed of response, duration of response, and repeatability. These in turn influence modelling requirements, tools, and necessary studies — all related.

This section aims at highlighting some of the most important features and functionalities, and some key benefits they provide. Subsequently, the minimum modelling requirements to adequately represent and capture the benefits of these features and typical tools to adopt in representing them are discussed relative to the desired level of detail. Some of the most important features and the related functionalities of each (traditional and emerging) include:

1. Frequency regulation and inertia-emulation.
2. Voltage regulation and reactive support.
3. Power flow control and transient stability enhancement.
4. Black-start capability
5. Grid-forming capability

Considering that the response and behavior of HVDC systems are inherently control driven, many of the features and functionalities are at the lowest levels implemented by device-control structures based on a hierarchical structure. Figure 14 shows a high-level block diagram from the external terminals of the HVDC converter to the inner-most control block that actuates the converters. The figure also roughly highlights in color the level of detail generally required to represent these blocks in simulations. However, from another perspective it also suggests which blocks are generally not required to be modelled in basic simulations; by basic we mean first-level representations for high-level insights. In the following, we dive deeper into each feature identified previously, short description of each, typical related functionalities under each feature, and generic implementation details.

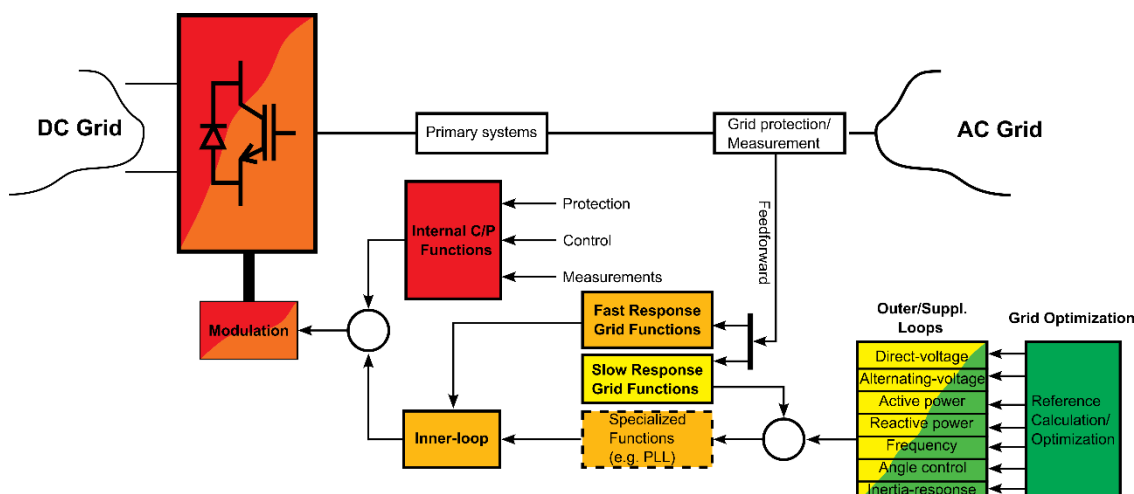


Figure 14 – High-level abstract of an HVDC converter from external terminals to inner-most functionalities

**Table 5 – Color legend for qualitative level of details**

	<b>Frequency spectrum of phenomena</b>	<b>Remarks</b>
<b>A+</b>	> 10 kHz	A high-level of detail is required to fully capture the phenomena that most characterize the said component or their system-level impact.
<b>A</b>	< 10 kHz	Further simplifications to previous level, though the level of detail is still significantly high.
<b>B</b>	100 – 1 kHz	Level of detail required to capture the behaviour of control structures typical of PE and their system impact. The system is correspondingly modelled.
<b>C</b>	< 500 Hz	Typical level of detail required in EMT simulations to model generic PE devices, their controllers, and system impact.
<b>D</b>	1- 10 Hz	Traditional domain of RMS simulation.
<b>D-</b>	< 1 Hz	Lowest level of detail. Traditional domain of system-adequacy and load-flow tools. This level of detail is synonymous with typical CBA.

### 6.1.2. Frequency Regulation and Inertia-emulation Capabilities from HVDC

Frequency regulation is at the core of power system operation and security in its entirety. In the conventional system, synchronous generators have been at the core of nearly all frequency regulation activities — inertia, frequency response, balancing, reserves, etc. Large-scale efforts aimed at transitioning the system to a renewable-based system is leading to a progressive decommissioning of these generators, while replacing them with power electronic (PE) interfaced generation without a natural capability to regulate system frequency. Thus, the system is being deprived of its natural capability to regulate frequency. On the other hand, these PE interfaces can be purposefully designed to support and regulate system frequency with superior flexibility and controllability than conventional generators.

Frequency regulation with HVDC systems is generally achieved by the adjustment of power flow between areas interfacing converters and the availability of containment reserves or access to readily available energy sources. This adjustment can be automated based on pre-defined system conditions, manually activated, or both depending on circumstances, timing of operations, and energy reserves at the moment of activation. The activation of frequency regulation by asynchronous HVDC systems results in a coupling of the frequency of the two synchronous areas. The actual type of coupling could be static (stepwise adjustment) or dynamic, as defined by ENTSO-E in [13]. The latter could fall into one of the following three classes i.e.: frequency containment reserves (FCR) exchange, frequency netting or frequency optimization.

Specific functionalities related to frequency regulation capabilities include:

- Generic frequency control including frequency containment, frequency restoration.
- Fast-frequency regulation.
- Inertia response and emulation.
- Grid-forming.

## Implementation

Frequency regulation activities can be broadly split into short-term (in order of seconds), mid-term (in order of minutes), and long-term (in order of hours or longer). In conventional generators, short-term typically involves inertia and primary frequency response. Immediately following this is the mid-term period marked with a sustained period of power injection, maintained for up to a few minutes before tertiary reserves are activated to return the system close to the pre-disturbance status.

Since HVDC systems do not have a natural rotary dynamic and cannot independently generate power, there are several ways in which frequency regulation activities can be implemented. In most implementations of this feature in HVDC systems, at least one control loop is invariably involved in the most basic of cases as shown in Figure 15. From the perspective of HVDC control design, the control system can be designed to have responses that range from milliseconds (ms) to several minutes to flexibly mimic the short and mid-term responses of synchronous generators. Additionally, these responses can be implemented either as a step, ramp, or proportional-based responses in any of these temporal periods.

## Benefits

The core of the benefits of frequency regulation from HVDC systems are the speed, flexibility, and controllability of responses, while improving frequency stability properties of the host network. Generally, HVDC can provide a tuneable and arbitrarily fast response that can arrest frequency deviation faster than synchronous generation (containment) and that can support multiple networks simultaneously (containment and restoration). Furthermore, considering that the physical implementation is inherently based on control systems, it is always possible to include damping functionalities without additional costs. With additional investments in dedicated energy storage for instance, even additional flexibility and controllability can be achieved and more functionalities can emerge whose cost can be compensated by the added benefits.

## Modelling Requirements

Frequency control which includes generic frequency control and inertia responses, fast-frequency response, are usually implemented in HVDC systems as a supplementary control at a higher hierarchical level to local control. Due to hierarchical considerations and the relatively slow behaviour of AC system frequency ( $\Delta f$ ), the control system is at the very least an order of magnitude slower than the next group of downstream controllers.

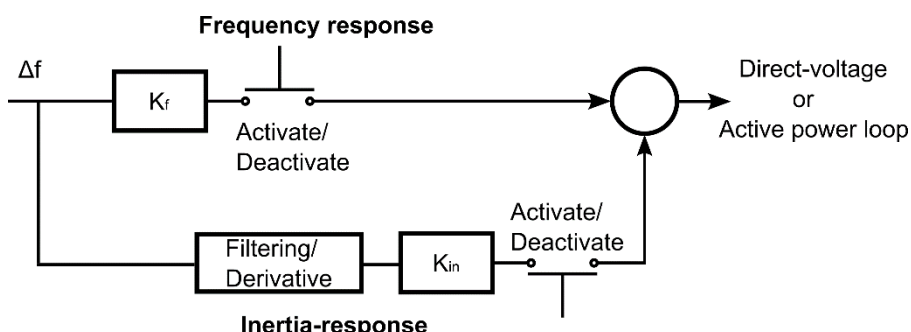


Figure 15 – Generic block-diagram of frequency and inertia-response control

There are several factors that can influence the level of detail required to represent the behaviour of frequency regulation functionality and this includes the expected system impact and the desired study of interest, and by extension the modelling requirements. Table 6 provides the minimum modelling requirements and a qualitative labelling of the level of modelling details required relative to CBA analysis. That is, for greenish coloured labels, generic models may suffice, and they require less detail in representation. These are typically adequate for CBA and should be reflected in the modified CBA. Whereas the brighter colours (orange, red) indicate that generic models may no longer be sufficient if the corresponding studies are required to establish the potential costs and benefits. However, more often than not, these levels of details are not necessary for first-level CBA at the planning stage unless they are shown to affect investment choices.

**Table 6 - Minimum modelling requirements for frequency regulation and inertia-emulation capabilities**

System impact	Typical studies of interest	Minimum modelling requirements	Qualitative level of details
Area power exchanges	System adequacy: - load-flow	Fundamental frequency models (voltage and current sources)	D-
Frequency stability and transient power exchange	Transient stability: - Angle stability	Phasor based models	D
	Dynamic stability: - dynamic performance - oscillatory phenomena	AVM models of outer loops and cables up to a bandwidth of 100 Hz	C
Control interactions	Dynamic stability: -oscillatory phenomena -resonances -interaction risks -harmonic stability	- More accurate AVM models of outer loops and cables - possibly inner-loops (up to bandwidth of 500 Hz) depending on system peculiarities.	B
Synchronization, fast-frequency response, and voltage source behaviour	Dynamic stability	High-fidelity models are recommended depending on implementation details. Model detail of class B at the minimum.	A

System impact	Typical studies of interest	Minimum modelling requirements	Qualitative level of details
Momentary overloading		Any of the above depending on time duration of overloading	

### 6.1.3. Voltage regulation and reactive power support capabilities from HVDC

With as much importance as frequency regulation in a hybrid AC/DC system, voltage regulation is also at the core of power system operation, security, and power quality. With the proliferation of PE interfaced systems, HVDC inclusive, it is now being demanded that these devices should in the least not contribute to detrimental behaviours that may lead to voltage collapse and at the same time contributing to valuable voltage stability.

Voltage regulation by HVDC is achieved by the adjustment of reactive current/power (absorption or generation) through dedicated control strategies which is possible independent of active power flow (within the converter's capability). Thus, voltage regulation and reactive support can, in general, be decoupled from other features without need for coordination.

Specific functionalities related to voltage regulation and reactive power support include:

- Fast static and dynamic voltage regulation.
- Reactive power control.
- Generation of network driving voltage — grid-forming functionality.
- STATCOM operation.

#### Implementation

Voltage regulation activities can be broadly split into static regulation and dynamic regulation. The former requires relatively static setpoints for operation based on fixed reactive power or voltage references. Implementation examples include, but not limited to reactive power control, AC voltage control (local and area mode and/or STATCOM operation), and power factor control. Whereas, the dynamic voltage regulation allows on-the-spot regulation of voltage depending on the network and pre-defined conditions, with possibilities to include fixed setpoints. Implementation examples include, but not limited to, droop-based/supplementary control-based structures, fast current injection mechanisms, and grid-forming control approaches to voltage generation and support.

## Benefits

While synchronous generators generally have a good control of network voltages, the increasing adoption of intermittent power sources and PE interfaces is resulting to voltage control issues that synchronous generators are not adequately equipped to mitigate. However, PE devices themselves such as HVDC systems can be designed to mitigate emerging voltage and power quality issues with a superior speed of response and flexibility than synchronous generators without additional costs. Importantly, the capability to fully decouple active and reactive power control in the case of VSC technology provides more flexibility especially in emergent conditions. Furthermore, HVDC systems, can potentially save on costs of investing in additional equipment. For instance, a VSC-HVDC converter can reliably operate in STATCOM mode even when the DC-side is out of service, which can reduce the need for additional physical component in proximity to support reactive power. Overall, HVDC systems can support and improve the voltage and transient stability of a network better than an equivalent synchronous generation. With additional investment, there is further potential for additional functionalities to enhance the performance of the network across varying temporal periods; for example, the VSC can be upgraded to provide active harmonic filtering capability and act as a harmonic sink to improve power quality. Therefore, when the HVDC system is properly located, the benefits for voltage and reactive power support can be immense.

## Modelling Requirements

Voltage regulation involves all activities aimed at maintaining the evolution of voltages within acceptable bounds in normal and emergency conditions. Like frequency regulation activities, several factors will influence the level of detail required to represent voltage regulation capabilities mainly due to the significant flexibility afforded by PE. As a result, there is no fixed or clear-cut minimum modelling requirement without additional information, particularly, the system impact and study of interest.

**Table 7 – Minimum modelling requirements for voltage regulation and reactive support capabilities**

System impact	Typical studies of interest	Minimum modelling requirements	Qualitative level of details
Long-term power transfer capability	System adequacy: - load flow	Fundamental frequency models (voltage and current sources)	D
Voltage and rotor-angle stability	Transient stability	Phasor based models	D-
Short-term power transfer capability	Dynamic stability: - dynamic performance - oscillatory phenomena - multi-infeed stability	AVM models of outer loops and cables up to a bandwidth well below 100 Hz especially if grid expected to be weak.	C
Control interactions	Dynamic stability: - dynamic performance - oscillatory phenomena - faster interactions	- AVM models of outer loops and cables up to a bandwidth well below 100 Hz. - detailed dc-side	C B

System impact	Typical studies of interest	Minimum modelling requirements	Qualitative level of details
		model if POC is expected to be weak. NB: Overall transfer capability of the hybrid system is limited in weak condition without additional investment e.g., specialized non-generic control.	
Transient over-voltages	EMT studies: - resonances - harmonic coupling - some protection studies	- detailed model of surrounding AC network and components in proximity. - high-fidelity models of inner and outer loops involved in voltage control up to bandwidth of 1 kHz	A
Harmonic propagation	EMT studies: - harmonics	- network harmonic impedance model - switched model of the converter - detailed inner loops (up to 10 kHz)	A+

#### 6.1.4. Power flow control and transient stability enhancement Capabilities

Without a possibility to control the power flow in transmission paths, the natural power transfer capability of a network is generally limited. The implementation of dedicated power flow control devices in a conventional grid has been shown to significantly enhance the capabilities and stability properties of the system. In today's networks, PE devices have been at the core of sophisticated power flow control mechanisms. Therefore, an HVDC system can inherently contribute with little to no modification. On the long term, this power flow capability of HVDC will reduce the need for investments elsewhere for dedicated power flow controlling devices and is thus a feature of significant interest. For HVDC in particular, one of the most important characteristics of power-flow control is the superior speed of response that can be flexibly set to meet demanding conditions during emergencies.

Specific functionalities related to power-flow control capabilities include:

- Fast power flow reversal and ramp facilities.
- P/Q modulator and emergency power control.
- AC-line emulation (HVDC links).
- Provision of an asynchronous tie.

## Implementation

There are several ways in which power flow may be enforced from an HVDC. Known techniques include (but not limited to) emulation of an AC line (by an HVDC link), setpoint enforcement according to a centralized control, manual adjustment of setpoints (as in redispatch cases), keeping the power setpoints constant, among others. Power flow control capability may involve one converter and its adjacent AC grid, or multiple converters and their adjacent AC grids. Furthermore, power flow in other lines in the system can be indirectly influenced by a converter providing dynamic reactive power so those lines can be loaded up to their thermal limits, e.g., long parallel AC lines. Another method for implementation of power flow control from HVDC is through the manipulation of firing angle of the converter. However, this implementation is only applicable for LCC implementations based on thyristor technology. Power flow control can also be implemented on the DC-side using dedicated, fractionally rated current flow controllers that offer more capabilities and functionality.

## Benefits

When properly utilized, power flow control capability is one of the most powerful benefits of HVDC systems. In addition to obvious improvement in transient stability properties and better utilization of network capacity, other benefits from power flow control include, but not limited to:

- Arbitrary control of active power in either direction.
- Fast and full reversal of power flow in normal and emergency conditions.
- Significant improvements in network flexibility and controllability.
- Mitigation of power flow constraints on AC corridors.
- Full independent control at each AC terminal in any of the four quadrants.

## Modelling Requirements

The modelling requirements for power flow control will depend on the required functionality and the actual implementation of the mechanism. Considering that power flow control mainly impacts on the transient stability properties of a network in normal and emergency conditions, its impacts often transcend the actuating device and can be felt in the entire network depending relative size of the HVDC system. In essence, this requires an extensive model of the network or the part of the network where the impacts are most felt. Therefore, at the initial stages of development, fundamental frequency models are required for system adequacy studies and at the minimum phasor-based models to assess angle-stability and damping properties in response to power flow changes enforced by the HVDC system. At a second stage, AVM models of outer control loops (up to a bandwidth of 100 Hz) are required to assess the impact of power flow control on stability properties when a faster than normal response is desired e.g., fast power flow reversals, emergency power control, or in the moments after unexpected conditions occur. Table 8 summarizes the minimum modelling requirements based on potential system impacts and the related study.

**Table 8 – Minimum modelling requirements for power flow control**

<b>System impact</b>	<b>Typical studies of interest</b>	<b>Minimum modelling requirements</b>	<b>Qualitative level of details</b>
Power flow control capability	System adequacy : - load flow	Fundamental frequency models (voltage and current sources)	D
	Transient stability	Phasor-based models	D-
Stability	Dynamic stability : - dynamic performance - oscillatory phenomena - multi-infeed stability	AVM models of outer loops and cables up to a bandwidth well below 100 Hz.	C

### 6.1.5. Blackstart Capabilities

Since 2017, the network code on electricity emergency and restoration [12] has become part of the European Commission regulation, setting the rules and responsibilities of each Member state (MS) in case of a blackout. In case of a blackout in Europe, either complete or partial, each of the MSs must have a restoration plan in place in order to progressively restore its network to the normal operating state, thus minimizing customer interruption.

Each MS typically considers two approaches for the restoration of its system or a combination of these two approaches. The first and most commonly used is the so-called “bottom-up” approach. This approach relies on a restoration using internal energy sources without any external support from other MSs. The internal sources should be equipped with the black-start functionality that allows them to form a stable voltage waveform of constant magnitude and frequency, to which the rest of the system (loads, generators, transmission elements) can synchronize/connect. The TSO responsible for the restoration should thus have available at all times a minimum number of units capable of black-starting the system. Hydro and gas units are commonly used in a bottom-up approach.

The second method is the “top-down” approach where the restoration is performed using external sources. In this case, interconnections are utilized to energize the backbone of the transmission system, with internal equipment being progressively synchronized. AC interconnections and embedded HVDC links can be used in case of a partial blackout (i.e. when only a part of a synchronous area is blacked out). However, it is rather uncertain whether in case of a black out, the other end of an embedded HVDC link is healthy. On the other hand, asynchronous HVDC interconnections can be more reliably used as black start units taking into account that the probability of two different synchronous areas suffering a blackout at the same time is negligible. An agreement between the MSs is required in such a case for provision of the required restoration power.

The capability of HVDC to provide black start services was first field-tested in 2008 by ABB [13]. A successful black-start test with Skagerrak 4 establishing and supplying a load of approximately 100 MW has been reported in the literature [14]. According to the European regulation, the black-start capability of an HVDC link should be tested at least once every three years [12].

Considering that complete black-start capability from HVDC is still at a relatively developmental stage, desirable functionalities may include:

- Black-start control mode, i.e. possibility to generate a voltage waveform of specific magnitude and frequency.
- Parallel operation with other units in black-start mode.
- Soft and/or hard energization.
- Fast voltage and frequency control to limit the voltage and frequency transients.
- Fast DC voltage control from the VSC-HVDC on the healthy side of the link (requires a relatively stiff AC system).
- Availability of back-up power source (e.g. small battery) sufficient to power the auxiliary equipment (such as control and protection systems) of the HVDC station.

## Implementation

In short, the black-start capability of an HVDC converter is provided by the manufacturer, if requested in the specifications stage of the HVDC project. HVDC systems based on the LCC technology cannot provide black-start services because they need a strong grid in order to operate. Nevertheless, LCC links can still support in the faster restoration of the network after a stable voltage has been established.

There should be at least one HVDC converter connected to a healthy AC system in order to be able to provide this service. The black-start functionality refers to an additional control mode of the VSC that allows it to use the DC voltage to generate a voltage waveform of a pre-defined magnitude and frequency. The VSC should be able to withstand the connection of the rest of the system elements (transformers, loads, etc.) by injecting the required current and power while ensuring that the system variables (frequency, voltage) remain between limits. Parallel operation with other generating units should be possible and stable. A VSC can perform hard and soft energization. In case of hard energization, the VSC should be able to provide the inrush currents during line and transformer connection. Such currents can be minimized by using the soft energization functionality, where the VSC progressively ramps up the voltages in the grid. Soft energization also allows to energize multiple elements at once. However, in such a case it is necessary to coordinate the protection relays to avoid protection actions that inadvertently trip the equipment to be energized.

## Benefits

- The capability to perform both soft and hard energization (not always possible with other conventional black-start units)
- Possibility to blackstart from another asynchronous AC area (not the case with AC connections), which is unlikely to have suffered simultaneously a blackout.
- HVDC systems have in general very high availability.
- Very fast voltage and frequency control that leads to better system performance.
- No diesel generators are required to start-up, except for small units (diesel or batteries) to start up the auxiliaries.
- Possibility to provide black-start capability in a system without synchronous machines.
- Due to the absence of mechanical parts, multiple self-start attempts can be made at a very short time [15].
- The black-start capability from an HVDC system can be provided without significant additional investment cost.

## Modelling Requirements

In order to capitalize on the benefits of black start services from HVDC, it is a prerequisite that the HVDC is included in the restoration plan established by the responsible TSO. Devising such a restoration plan requires dedicated studies that demonstrate its feasibility

to manage the system transients taking place during the switching events of the restoration sequence. As discussed in [16], a black-start involving an HVDC converter requires very detailed simulations using either a real-time simulator or an offline EMT-type simulation tool, also shown in Table 9.

**Table 9 – Minimum modelling requirements for black-start simulation study**

System impact	Typical studies of interest	Minimum modelling requirements	Qualitative level of details
Power system restoration	EMT study, switching transients	- Real-time model with actual control and protection replica of HVDC equipment - Simplified representation of the system part that is involved in the restoration scenario	A+
		- Offline EMT simulation tools with the black-start control mode of the HVDC link - Generic representation of the connected system	A

A simplification could be considered at this point, assuming that a feasible restoration plan can be set-up including the HVDC link. As a result, the study of the benefits from black start by HVDC would be restricted to a much simpler economic analysis, where the HVDC system would replace the black start service of another, more expensive, black start unit. Obviously, this would require incorporating in the current CBA methodology the costs of having black-start units (and the cost of the black-start service from the HVDC).

As illustrated in [17] and [18], there is no clear trend neither on the method the black-start service is sourced (mandatory service, tendered service, bilateral agreements, etc.) nor on how and if the method is remunerated. As a result, this makes it particularly challenging to develop a generic enough method to include black start costs in the ENTSO-E CBA methodology. Assessing the benefits of black start services from HVDC is even more difficult since they will be connected between different zones, so information on the cost of this service is needed.

### 6.1.6. Grid-Forming Capabilities

Most of the existing IBR generation and HVDC converters uses the so-called grid-following control mode, where the converter measures the grid voltage and frequency and adjusts the injected currents in order to reach the desired active and reactive power setpoints. In order to enable such sources to contribute to the system security and stability during voltage and frequency excursions, the TSOs developed specific requirements in the grid codes. Nevertheless, the control structure of these converters remained largely the same. As has been highlighted in several parts of this document, the replacement of conventional generating units by such PE-based sources poses several challenges in the planning and operation of power systems. Amongst others, ENTSO-E has identified these challenges in a technical report [19] and has described a roadmap to address them in the short and long-term. For example, the behavior of grid following converters becomes more important in case of weak grids, i.e. when the short circuit level at the point of connection of the HVDC converter is low in relation to the size of the converter. A typical rule of thumb specifies that a system is weak if the short circuit power is less than two or three

times the rating of the converter. In such operating conditions the behavior of grid following converters cannot be ensured and instability might arise. The use of grid forming control on HVDC systems (along with other PE-based sources) appears as a promising countermeasure in the long-term.

The grid forming control refers to a different control philosophy for the converter that allows it to form its own voltage and frequency and is expected to lead to better system performance. The early generation of grid forming control from HVDC converters has already seen some applications. Offshore wind systems require that the offshore HVDC converter forms the offshore AC grid for the wind turbines to synchronize and produce power. In addition, the black-start control mode described previously is also a type of grid forming control, employed in special circumstances. However, there are very few grid forming control applications in bulk power systems, which concern (mainly) Battery Energy Storage Systems (BESS) and not HVDC converters. The current generation of grid forming control is expected to allow better coupling of the converter to a large AC grid consisting of several other grid forming elements and synchronous machines. For example, the converter can be controlled to behave virtually as a synchronous machine, as shown in Figure 16.

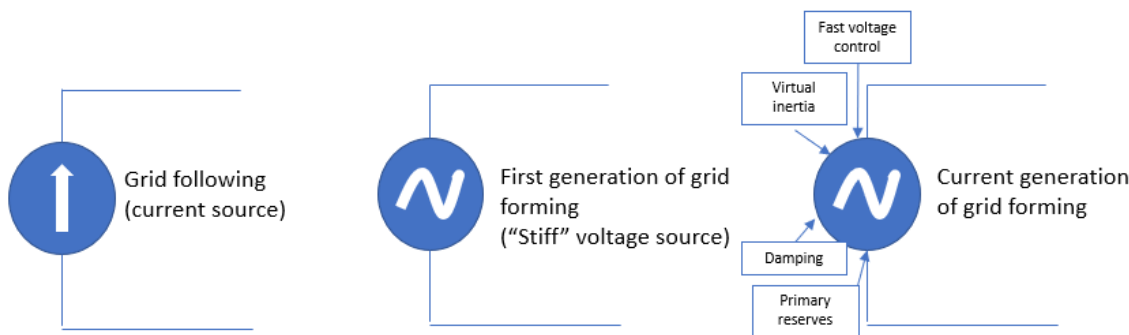


Figure 16 – Grid following and Grid forming inverter types [20]

Similar to black-start capability, grid-forming capability from PE is still at the developmental stages with several large-scale demonstrations completed or in operation (see WP3, Deliverable 3.2 of the OSMOSE project [21]) to validate proof-of-concept. Hence, desired functionalities include, but not limited to:

- Enforcement of network driving voltages, synchronizing angle, and frequency;
- Reliable voltage source behaviour;
- The current limitation strategy;
- Short circuit current contribution and any temporary overload capability;
- Fast-frequency regulation and inertia response capabilities.

## Implementation

The grid forming control requires implementing different control algorithms inside the converter. There have been several methods proposed in the literature [22] [23] [24], such as the Power Synchronization Loop (PSL) or the so-called Virtual Synchronous Machine (VSM) scheme, where the converter is controlled to behave as a synchronous generator. Each of these methods comes with its own benefits and drawbacks. This document will not go through the details of such schemes, which can be found in the provided references. However, the general principle is similar in all methods. In contrast to grid following converters that rely on a Phase-Locked Loop (PLL) scheme for synchronization and to calculate the phase angle of the injected current, grid forming converters generate a voltage waveform of specific magnitude and frequency. Then, the magnitude and the phase of this voltage are adjusted to control the reactive and active power injected into the network, respectively. During faults in the system, the grid forming converter should be able to ride-through without disconnecting or any equipment damage, and minimal time to

full power transfer recovery. A grid forming converter should also be able to provide short-circuit current. Typically, the contribution of converters to short circuit level is much smaller compared to synchronous machines (~1.2 pu instead of ~6-7 pu). Hence, if higher short circuit current is required, investments in hardware would be needed. It should be noted that the rest of the features described in this chapter (i.e., frequency/voltage regulation, power flow control) can be also provided by a converter operated in grid forming mode. The main difference would be in the (short-term) dynamic performance of the converter, where the grid-forming scheme is expected to be superior, especially in weak grid conditions.

The actual implementation is expected to vary from manufacturer to manufacturer and on a case-by-case basis. It has to be noted though that grid forming control for bulk power systems is a relatively new feature and there are currently no clear requirements regarding the performance that should be satisfied. This also makes the modelling and tuning of such converters for inclusion in planning studies more challenging. To define such requirements and allow large scale deployment of grid forming converters, close cooperation between system operators and manufacturers is critical in the near future [25].

## Benefits

In principle, a grid following converter can provide the same features as a grid forming converter (e.g. frequency/voltage control, oscillation damping, etc.). However, according to the current industry practice, a grid following converter cannot reliably operate in case of low system strength, whereas a grid forming converter does not face such a limitation.

Although it is still not certain if grid-forming capability will be offered predominantly as a grid service and/or as a standard feature and when, it is at present being considered as one of the most important features of next generation converters. The foremost important benefit of grid-forming as a feature is the capability to replicate grid-control functions provided by synchronous generators. Thus, in line with hybridization efforts and decommissioning of existing synchronous generators, system reliability and security can be maintained. Furthermore, since implementation will be in PE converters, most benefits of PE apply. More specific benefits with respect to HVDC include, but not limited to:

- Increase of stable operating region of HVDC converter. The converter can operate reliably and transfer more power in operating points with low short circuit level and low system inertia.
- Decrease of need to invest in means to ensure stable system operation, such as synchronous condensers.
- Apart from the connection of the HVDC converter, grid forming control can enable higher penetration of other PE-sources, which would not be possible with a grid following HVDC converter.
- Operation of islanded systems without must-run synchronous units.

## Modelling Requirements

The modelling requirements of a grid forming converter do not significantly differ from what has already been listed in the previous sub-sections for frequency and voltage control. The main difference lies in the control structure of the converter, which should correspond to the grid forming type. As already discussed, the modelling and control of grid forming HVDC converters is an ongoing research topic that has received significant attention in the recent years. A generic model of an HVDC grid forming converter is shown in Figure 17. It includes:

- The outer loops:
  - a. The power synchronization loop that provides the internal phase angle and frequency of the converter. If frequency regulation capability is required, it

- can be achieved by selecting appropriately the parameters of this loop. Regulation of DC voltage can be also added (not shown in Figure 17).
- b. The voltage profile management that provides the magnitude of the voltage output of the converter. Reactive power control or terminal voltage control is performed through this loop, if required.
  - The inner loop receives as inputs the outputs of the outer loops and the currents of the converter. The outputs are the modulation signals that are passed to the internal switching logic of the converter. An important part of the inner loop is the current limitation strategy, that is activated in case of overcurrent (e.g. during a nearby fault).

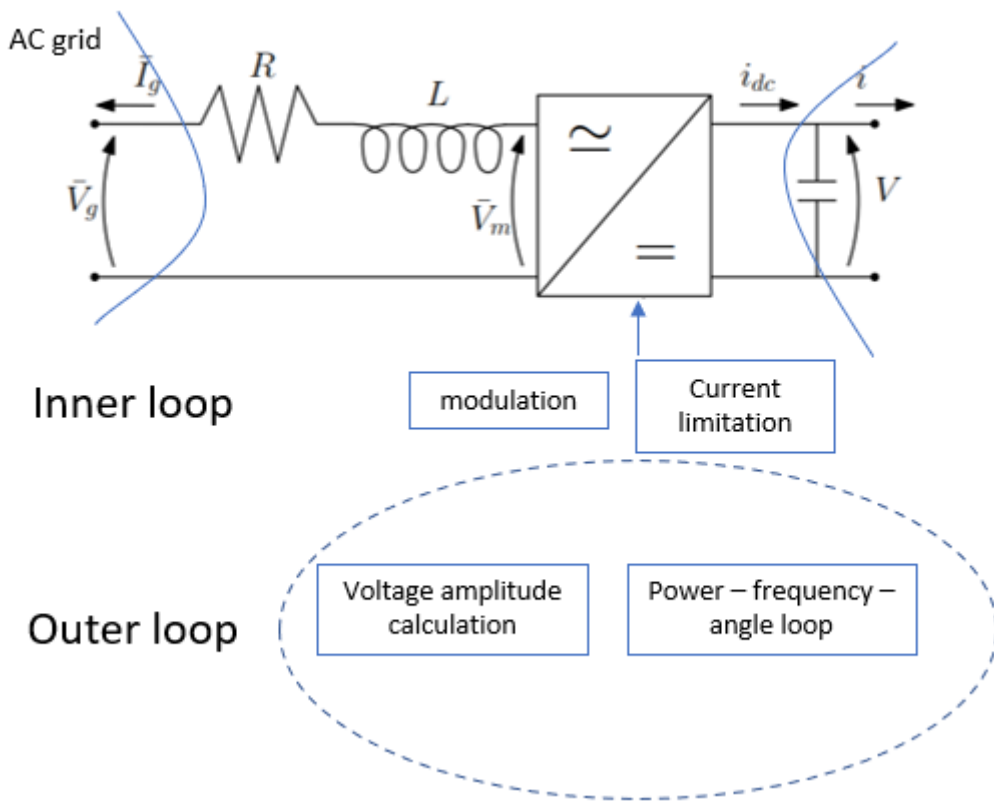


Figure 17 – Generalized control structure of grid forming converter (inspired from [26])

The level of detail that is required depends on the phenomenon of concern. For example, RMS simulations are sufficient to investigate the classical types of power system stability, i.e. frequency, voltage and angle stability. Hence, a simplified model of the converter that ignores the very fast dynamics of the inner loop and focuses on frequency/voltage regulation could be sufficient. However, for the investigation of faster phenomena, such as the response to AC and DC faults or the possible interactions between several converters in proximity (especially in weak systems), the modelling of converters in detail for the use in EMT tools is necessary. Typically, such problems are solved during the project design phase. However, even if they cannot be fully addressed during the system planning, the operator should be able to detect the possibility of such problems arising and set appropriately the system requirements and specifications.

### 6.1.7. HVDC grid protection aspects

The protection of HVDC grids is a challenging part of their operation that has received significant attention in the literature, but has not seen extended practical applications yet. In contrast to AC grids, where there is a natural zero crossing of the current that allows to open the protection breakers in case of faults, the breaking of DC faults is much more

complex and challenging, since it requires to employ measures that bring the DC fault current to zero first before opening the breakers.

In contrast to the previously discussed functionalities, it is uncertain whether HVDC grid protection will bring additional benefits to the AC system. However, it can have a significant impact on the cost and risk of HVDC projects.

On the one hand, if an HVDC system is planned from the beginning with the final topology in mind, its protection costs can also be incorporated and optimized from the beginning. On the other hand, the connection of several pre-existing HVDC point-to-point links to form an HVDC grid may come with a much larger (or even prohibitive) cost. The reason for this is that typically, point-to-point HVDC did not require any dedicated HVDC protection apart from conventional AC breakers. Such systems were usually turnkey projects, optimized for a particular configuration, and no arrangements were made to accommodate extension to HVDC grids (e.g. no additional space for DC breakers was foreseen).

## Implementation

Design of HVDC grid protection requires two choices, i.e., choice of protection philosophy and choice of technology within the protection philosophy.

Within the protection philosophy, three main options exist. First, the fully selective protection philosophy works similar to the present practice in AC systems, that is, considering each transmission line and bus as independent protection zones. This option requires DC-side breakers at every transmission line end and makes sure that continuity of supply within the HVDC grid is guaranteed. Second, a non-selective protection philosophy can be used, where the entire HVDC grid is treated as one protection zone. This requires equipment to interrupt fault currents at each converter station, e.g., AC breakers, DC breakers or converters with fault blocking capability. A fault at the DC side results in a temporary loss of the entire HVDC grid. Third, an intermediate strategy is putting DC-side breakers at strategic locations in the HVDC grid, forming protection zones consisting of multiple transmission lines and buses. In case of a DC-side fault, only the affected protection zone is temporarily lost, whereas other protection zones continue operation.

As an alternative to HVDC grids, the option to form reconfigurable point-to-point or multi-terminal HVDC systems also exists. In this option, HVDC links can be grouped in small multi-terminal systems and reconfigured according to the system needs for power transfer.

To interrupt DC-side fault currents, several technologies exist, which are listed below:

- AC-side circuit breakers: can be used at the AC-side of every converter, in a non- or partially selective protection philosophy
- Converters with fault blocking capability, such as hybrid or full-bridge modular multilevel converter, which can be used in a non- or partially selective protection philosophy
- DC-side circuit breakers, such as resonance-type or hybrid DC circuit breakers, which can be used in any protection philosophy. DC-side circuit breakers are more complex and bulky counterparts compared to AC-side circuit breakers because of additional circuitry (resonant circuits or power-electronic circuits, surge arresters) and the need for series inductors.
- DC-DC converters with fault blocking capability, which can be used in any protection philosophy

Each philosophy with used technologies will lead to a profile of “loss of active power transfer” and “loss of reactive power transfer” at HVDC nodes, which will allow to quantify

the impacts of a DC-side fault on the AC- and DC-systems connected to the faulted component or protection zone.

## Costs

Cost drivers of HVDC grid protection can be classified into capital expenditures and operational expenditures.

Non-negligible capital expenditures related to HVDC grid protection are:

- DC-side circuit breakers: DC-side circuit breakers are typically more expensive compared to their AC counterparts and require more space in substations or platform space offshore.
- Converters with fault blocking capability typically require a higher amount of power electronics compared to their non-fault blocking counterparts.

Non-negligible operational expenditures related to HVDC grid protection are:

- DC-side circuit breaker losses: certain DC-side circuit breakers insert power-electronics in the main circuit, incurring extra losses in the system.
- Converters with fault blocking capability are typically less efficient compared to their non-fault blocking counterparts.
- AC-side impact: HVDC grid protection philosophies that shut down the entire or part of the HVDC system may have an impact on dimensioning of frequency reserves.
- DC-side impact: HVDC grid protection philosophies that shut down part of the HVDC system may have an impact on the dimensioning of DC-side voltage balancing reserves.

## Modelling Requirements and Studies

To identify the most suitable protection strategy, design the equipment, and minimize the costs, several studies have to be performed. These are listed hereafter:

- *Short-circuit studies at the DC-side*: Short-circuit studies at the DC side should be performed using either EMT-type simulation tools (time domain) or frequency domain studies. The most important aspects to gather from these studies (considering low-impedance grounded systems) are the rate-of-rise of the DC-side current and the value of the DC-side current. Analytical solutions have been proposed in the literature but are either not accurate or confined to specific systems. These studies will feed into the CBA as “cost of DC breaker” or as a variable that should be checked against the constraint on short-circuit currents in the DC system. The cost of the DC breaker will depend on the current rate-of-rise and value of the current at interruption time. These variables will provide inputs to the required size for series inductors, breaker interruptible capacity and surge arrester energy.
- *Short-circuit studies at the AC-side*: Short-circuit studies at the AC-side may reveal the AC-side breaker requirements and the impact on AC-side protection. First, steady-state AC-side short-circuit studies can be performed, to check in a CBA for compatibility against minimum and maximum AC-side short-circuit currents.
- *Dynamic studies at AC- and DC-side*: Dynamic studies checking the needs for AC frequency regulation and DC voltage regulation will feed in the CBA as costs

incurred when adopting a certain HVDC grid protection strategy, especially for non-selective or partially selective protection methods. These dynamic studies can be performed by considering loss of infeed of the terminals that are grouped within one protection zone. The studies can be performed using the profiles for loss of active power associated with the chosen HVDC grid protection philosophy and technology.

- *Dynamic studies on transient AC stability:* Simultaneous loss of multiple HVDC nodes may result in loss of AC system stability. Therefore, dynamic studies may feed in the CBA as to check for stability limits of certain system states.

### 6.1.8. Overview of Typical Tools Based on Recommended Level of Detail

Tools for power system simulation range from those adopted for system planning, decades before the actual commissioning, to those adopted in real-time operational scenarios, and many in between these extremes. One key defining paradigm of these tools is the level of detail they require to provide accurate, plausible, and reasonable conclusions subject to the study at hand. The size and complexity of the power system has meant that modelling at a mathematical level has been at the core of power system analysis. Due to these complexities, simplifications at various levels are of utmost necessity to represent various phenomena. Traditionally, when representing these phenomena, the philosophy of timescale separation has been adopted (as illustrated in Figure 18), which allows to neglect very fast phenomena when slow dynamics are of interest and vice versa. This results in a simplified model and reduced computation time.

As a result of this separation, dedicated software routines have been developed specifically to exploit this philosophy. Thus, phenomena that require fairly simple models are treated as such, resulting in a model that is computationally tractable. However, they may lack generality and can only be applied specifically to these phenomena that occur within the timescale of the studied dynamics. On the other hand, phenomena that require more detailed model can be handled by another class of software routine designed to cater for these. However, computational tractability is often lost, and it could take hours to complete a few seconds of simulations.

Nevertheless, the advent of PE devices today is challenging this timescale of separation idea as PE devices can influence dynamics across the entire spectrum of power system dynamics. As a result, simple models are becoming inaccurate, resulting in misleading or incomplete conclusions, and fine-grained model are too detailed and computationally intractable to model long-term behaviour. Although there are advancements today in computational tractability of fine-grained models, the cost is still significant.

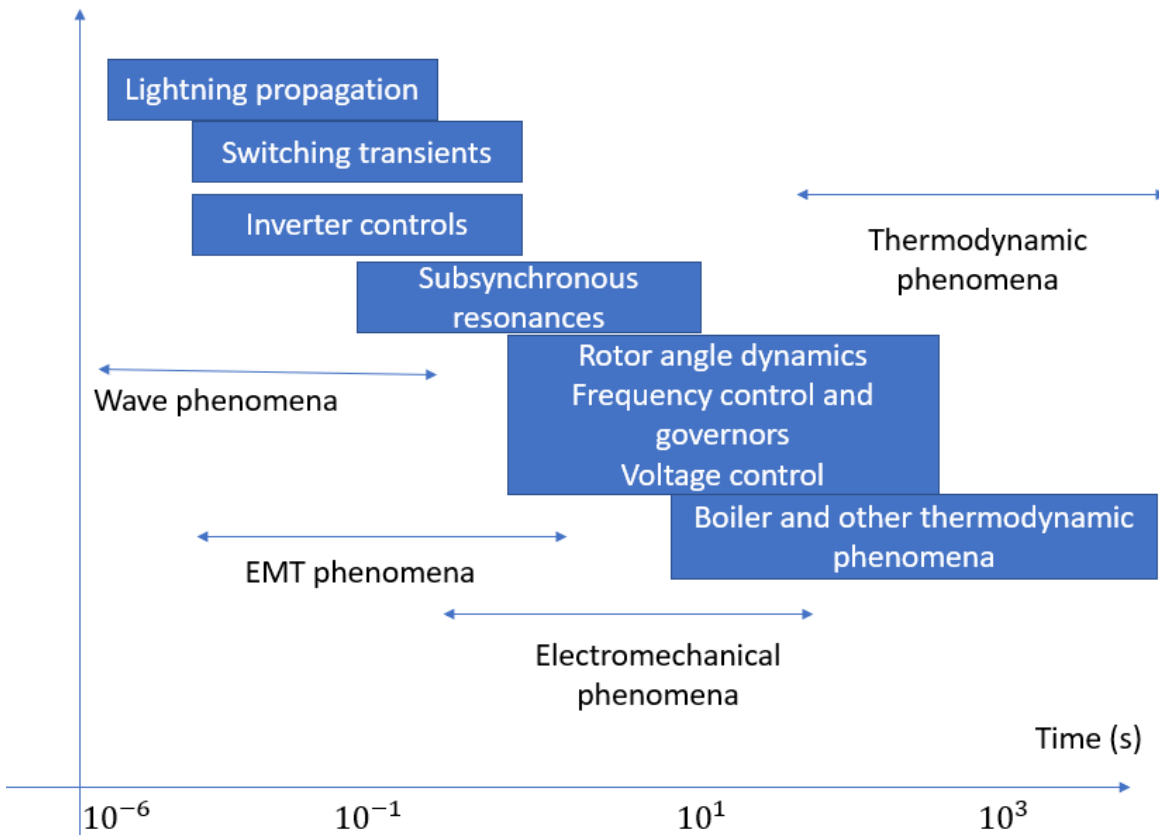


Figure 18 – Power system time scales [27]

In terms of long-term system planning, when several scenarios are considered with high uncertainty, it makes little sense to pursue such high accuracy using high-fidelity simulation models. This is further supported by the fact that the technology of converters has undergone tremendous developments in the latest 30 years in hardware and software, and more developments are on the way. As a result, modelling the current state-of-the-art of control and functionalities of converters in high detail and investing significant effort for high-fidelity simulations is of questionable benefit. Nevertheless, it is of utmost importance to be able to identify cases of concern based on simplified metrics derived from static calculations (load flows) or from dynamic simulations (i.e. phasor-mode simulations). In essence, great skill is required in selecting the most appropriate tool given accuracy and computational tractability subject to the requirements of the study in question.

**Table 10 – Summary of typical tools subject to the level of detail**

Qualitative level of details/Model classes	System impact	Typical tools	Update potential	Remarks
A+	- Harmonic propagation - Harmonic stability issues with frequency > 5-10 kHz - power quality	- EMT tools + real-time tools - emerging high fidelity frequency domain tools	Currently the state-of-the art	Not recommended for CBA except if initial analysis show a need for a very small subset of scenarios to be verified.

Qualitative level of details/Model classes	System impact	Typical tools	Update potential	Remarks
A	- Resonance - Harmonic coupling - extremely fast control interactions (< 10 kHz) - Transient overvoltages due to control and peculiar network	- EMT tools - emerging high-fidelity small-signal tools	Currently the state-of-the art	Not necessary for CBA unless specificity of implementation warrants such studies. This is the case as of these impacts may have cost implications if they must be mitigated with additional investments (which may be significant enough) to get the full benefits of a feature.
B	- Converter-driven control interactions - dynamic performance - oscillatory phenomena (< 1 kHz)	- High-fidelity small-signal tools - AVM for control design/studies	State-of-the-art	Possible for a slightly larger subset of scenarios considering the increasing adoption of converters
C	- dynamic performance - fast converter driven oscillatory phenomena (bandwidth < 500 Hz)	Standard small-signal tools	Can be upgraded to have a configurable bandwidth of accuracy	Recommended depending on the expected number of HVDC system and their role in the network. The more the number of converters and system functionalities required, the more the need for a reasonably accurate small-signal analysis
D-	Transient, voltage & frequency stability in the presence of HVDC systems	Standard RMS tools	Can be upgraded to include better representative models of PE systems	Highly recommended for coarse-grained stability metrics for hybrid AC/DC grids that can establish if simulation with higher model classes is required.
D	System adequacy	Load-flow tools	Can be upgraded to include some details regarding converters or high-level system computations such as inertia estimation	Already part of CBA

Although hybrid AC/DC grids are still emerging in power system infrastructure and still far from being fully adopted, the previous subsections show that the benefits that can be derived even today are significant. Table 11 summarizes the generic implementation methods of the previously discussed features and their related functionalities, and the high-level system impacts.

**Table 11 – Summary of technical features, functionalities, and basic modelling requirements**

Technical feature	Related functionalities	Generic implementation methods	Overview of System impacts
Frequency regulation	Generic frequency control	Step, ramp, or proportional-based control: - Inertia emulation strategies (with and without storage) - Supplementary frequency control	Frequency stability Power exchange: - Transient exchange - Area exchanges Control interactions Momentary overloading (ms-s)
	Fast-frequency regulation	Feedback-based control: - Closed-loop synchronizing frequency and angle - Closed-loop inertia emulation strategies	
	Inertia response and emulation		
	Frequency balancing		
	Grid-forming		
Voltage regulation	Static and dynamic voltage regulation	Static control: - Reactive power - Voltage - Power factor	Stability - Voltage stability - Rotor-angle stability
	Reactive power control	Dynamic control: - Grid-forming approaches - Fast current injection - Droop/supplementary control-based	Control interactions (AC-AC, AC-DC) Harmonic propagation System dynamic performance Nonlinear impacts: - limits - Transient over-voltages
	Generation of network driving		
	Harmonic sink/filtering		
	Reactive power support		
Power flow control and transient stability enhancement features	Fast power flow reversal	Closed-loop P/Q modulator	- Transient stability
	Dynamic reactive power control	Ramp functions	- Damping properties
	Provision of an asynchronous tie	Angle/AC-line emulation (HVDC links)	- Power balance
	Fast speed of response	Dedicated DC-side power flow control	- Network dynamic performance
	P/Q modulator		- Network power routing flexibility
	Emergency power control		- Damping properties
	Provision of damping		- Shorter
Blackstart	Blackstart control mode	- Inclusion of HVDC converter in	

Technical feature	Related functionalities	Generic implementation methods	Overview of System impacts
capabilities	Parallel operation during synchronization	restoration plan - Capability to provide inrush currents - Capability to inject/absorb reactive power during energization	restoration times - Adjustment of protection settings - Less investment in synchronous condensers - Higher penetration of RES
	Fast voltage/frequency control		
	Soft/hard energization		
	DC voltage control from healthy side of link		
	Small back-up power source		
Grid-forming capabilities	<ul style="list-style-type: none"> <li>- Synchronization control scheme</li> <li>- Frequency/voltage and other supplementary control loops</li> <li>- Current limitation strategy</li> <li>- Overload capability</li> </ul>	<ul style="list-style-type: none"> <li>- Virtual synchronous machine, power synchronization loop, etc.</li> <li>- hardware oversizing</li> <li>- switch to grid following during faults, virtual impedance</li> </ul>	<ul style="list-style-type: none"> <li>- Operation in operating points with lower short-circuit and inertia levels</li> <li>- Higher stress on DC-side variables</li> </ul>

## 6.2. Steady-state Optimization: Modelling Requirements to determine Techno-economic KPIs

A number of different steady state optimization models can be used to determine specific KPIs of the CBA. Firstly, an NTC based zonal economic dispatch model can be used to determine the expected interzonal flows between different market zones, using the installed generation capacity and RES and demand time series as inputs. This provides a base case where the generation dispatch is determined per generation type, and zone as well as expected interconnector flows.

Secondly, an optimal power flow model (OPF) can be used, to determine the generation dispatch and the line flows within the high voltage network(s) of different zones. To do that, a detailed nodal network model is needed, including a nodal mapping of installed generation capacities and nodal demand and RES time series. The OPF model then determines the least cost generation dispatch considering Ohm's and Kirchhoff's laws and technical limits of grid equipment, such as current/power flow limits in transmission lines, or nodal voltage limits. Within such an OPF model, different possible control actions can be modelled, such as optimizing tap settings of PST, and active and reactive power control of HVDC converters.

An optimal power flow model can also be used to determine the optimal amount of redispatch need, either for balancing the system w.r.t. forecast errors between day-ahead and real-time operation, or to compensate for outages of transmission lines or generators. As such, a basic redispatch optimal power flow model is introduced, with the objective of minimizing the redispatch w.r.t. a reference generation dispatch, to compensate for system imbalances due to RES and demand forecast errors or generation outages. The following paragraphs will outline the mathematical formulations of the different optimization models.

### 6.2.1. NTC based zonal economic dispatch model

In this model, each market zone is represented by a single node. As such we can denote the set of zones as  $z \in Z$ , where  $z$  represents a particular market zone, within the given set of market zones  $Z$ . Further, the installed generation capacity per generation type  $gt \in GT$  is known for each zone, where  $GT$  is the set of different generation types. The objective of the optimization is to minimize the cost of generation for each hour  $t$  of a given time horizon  $T$ , e.g., 8760 hours. Two additional components namely, demand response actions  $DR_z$  and possible demand curtailment  $Curt_z$  should be accounted for to avoid model infeasibility in cases of adequacy problems.

The objective of the optimization can be written as:

$$\min \sum_{z \in Z} \sum_{gt \in GT} C_{gt,z,t} P_{gt,z,t} + DR_{z,t} C_{dr,z,t} + Curt_{z,t} VOLL_{z,t} \quad \forall t \in T$$

where  $P_{gt,z,t}$  denotes the power generation of type  $gc$  in zone  $z$  for the time point  $t$ , and  $C_{gt,z,t}$  its associated generation cost. Similarly,  $DR_{z,t}$  is the amount of demand response activation within zone  $z$  in time point  $t$ , and  $C_{dr,z,t}$  is its associated cost. Lastly,  $Curt_{z,t}$  the amount of possible demand shedding in zone  $z$  in time point  $t$ , with the associated value of lost load  $VOLL_{z,t}$ .

The following optimization constraints need to be fulfilled. Firstly, the nodal power balance in each zone needs to be respected as given below:

$$\sum_{gc \in GC} P_{gc,z,t} + DR_{z,t} + Curt_{z,t} - D_{z,t} - \sum_{z=i,j \neq z} Pf_{ij,t} = 0 \quad \forall z \in Z, t \in T$$

where  $D_{z,t}$  denotes the expected total zonal demand in zone  $z$  in time point  $t$ , and  $Pf_{ij,t}$  denotes the power flow from zone  $z$  to any other connected zone  $j$ .

Secondly, the power flows between different zones need to be limited by the given net transfer capacity (NTC) as follows:

$$-NTC_{ij} \leq Pf_{ij,t} \leq NTC_{ij} \quad \forall (i,j) \in Z, t \in T$$

Finally, capacity limits for the different generator types in each zone as well as limits for providing demand response as well as demand curtailment need to be defined as follows:

$$0 \leq DR_{z,t} \leq DR_z^{max} \quad \forall z \in Z, t \in T$$

$$0 \leq Curt_{z,t} \leq Curt_z^{max} \quad \forall z \in Z, t \in T$$

$$0 \leq P_{gc,z,t} \leq P_{gc,z}^{max} \quad \forall gc \in GC^{nonres}, z \in Z, t \in T$$

$$0 \leq P_{gc,z,t} \leq P_{gc,z}^{max} \quad \forall gc \in GC^{res}, z \in Z, t \in T$$

Note that in this case a distinction between RES generation and non-RES generation needs to be made, as the maximum generation capacity for RES generators in each hour is determined by the hourly solar irradiation and wind speeds.

As there are no time coupling constraints, e.g., to model storage or specific unit commitment constraints, the optimization problem is solved as a sequence of hourly optimization problems. Figure 19 shows the outcome of the optimization model, applied to the zonal TYNDP model under the Global Ambition (GA) scenario. The figure depicts the

total amount of demand across all European market zones for each hour of the planning year 2030, for which the RES generation and demand time series have been based on the climate year 1982. The figure also depicts the amount of curtailed RES generation on an hourly basis due to limited transmission capacity between the market zones, as the RES generation costs have been modelled as the cheapest option. The detailed description of all input data is provided in Appendix III.

In comparison, in Figure 20 we can observe a much higher RES curtailment need for the planning year 2040, where the total installed RES generation capacity is 300 GW higher than in 2030, namely 1032 GW in 2040 instead of 737 GW in 2030. This is also reflected in the interzonal flows. Figure 21 and Figure 22 show the number of hours within a year, where the interconnection flows are larger than 90% of the interzonal NTC values. We can observe that the number of hours where the NTC between the zones is utilized fully, increases with the amount of RES in the system, especially observable between the Nordic region and Continental Europe, in the Balkan region and around Germany.

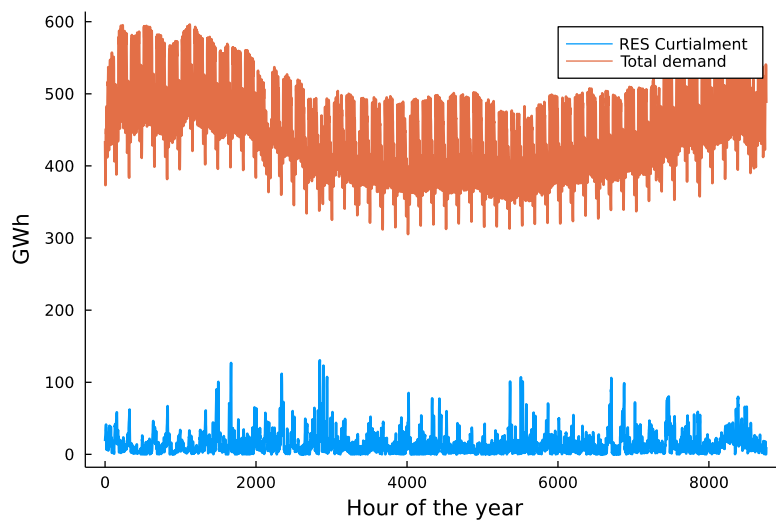


Figure 19 – Total demand and RES curtailment for the GA2030 scenario, for climate year 1982

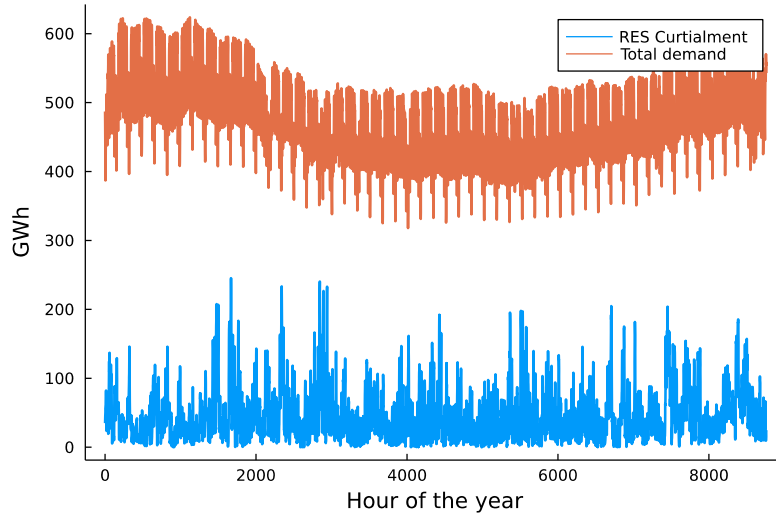


Figure 20 – Total demand and RES curtailment for the GA2040 scenario, for climate year 1982

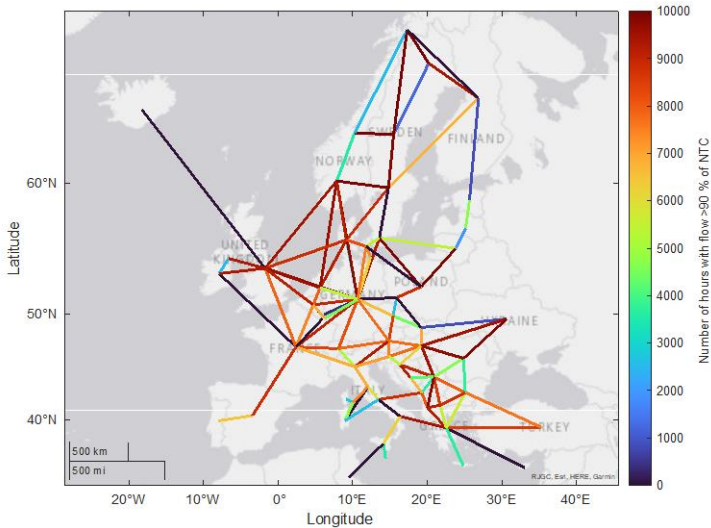


Figure 21 – Number of hours with interconnection flow larger than 90% of NTC for GA2030 scenario, climate year 1982

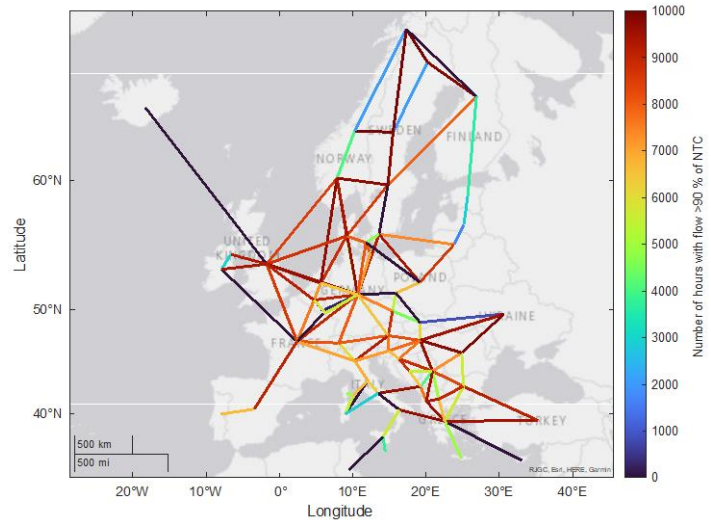


Figure 22 – Number of hours with interconnection flow larger than 90% of NTC for GA2040 scenario, climate year 1982

In order to determine the generation dispatch while considering the power flows on both the interconnectors as well as within the market zones, an optimal power flow model is needed, which determines the least cost generation dispatch in a given hour, while respecting Ohm's and Kirchhoff's laws and the operational and technical limits in the system. By doing so, also the optimal set points for HVDC converters and PSTs can be determined to maximally utilize the transmission lines, thus reduce congestion, and achieve a lower total generation cost in the system.

### 6.2.2. AC/DC grid optimal power flow modelling

Firstly, the most detailed generic nonlinear, nonconvex (NLP) optimal power flow model is introduced which is able to represent the nonlinearity of the system, when reactive power and voltage magnitudes are considered, and transmission losses are considered in the network equations. This OPF model is applicable on a nodal level, where the total generation cost in the transmission system is minimized while considering the circuit physics and limits of the network. The objective function of the optimization problem is given as:

$$\min \sum_{g \in S_g} C_g P_{g,t} + \sum_{u \in S_u} (C_u^{dr} P_{u,t}^{dr} + VOLL_u P_{u,t}^{curt}) \quad \forall t \in T$$

where  $g \in S_g$  denotes the set of generators in the system,  $P_{g,t}$  denotes the dispatch of generator  $g$  at time point  $t$ ,  $C_g$  denotes the cost of generator  $g$  in €/MWh,  $u \in S_u$  denotes the set of loads,  $P_{u,t}^{dr}$  the demand response of load  $u$  at time point  $t$  with the associated cost  $C_u^{dr}$ , and  $P_{u,t}^{curt}$  denotes the possible demand curtailment of load  $u$  at time point  $t$  with the associated value of lost load  $VOLL_u$ . Note that to represent the active power generation cost, also polynomial or other types of nonlinear cost functions can be incorporated in the optimization model.

To model all network constraints, we first start with the modelling of AC nodes. Each AC node is characterized with a complex valued nodal voltage  $U_k \angle \theta_k, k \in S_n^{ac}$ , where  $S_n^{ac}$  is the set of network nodes. The operational limits of the AC nodal voltages are defined as follows:

$$U_{m,t,y}^{\min} \leq U_{m,t,y} \leq U_{m,t,y}^{\max} \quad \forall m \in S_n^{ac}, \forall t \in T$$

$$\theta_{m,t,y}^{\min} \leq \theta_{m,t,y} \leq \theta_{m,t,y}^{\max} \quad \forall m \in S_n^{ac}, \forall t \in T,$$

where these operational limits need to hold for each time step of each planning horizon considered. An AC branch connects two different AC nodes  $k$  and  $m$ . As such, the AC branch model consists of AC lines and cables and power transformers, e.g., found in primary substations. A generic PI-model representation of AC branches is chosen, as depicted in Figure 23.  $g_l$  and  $b_l$  are the resistive and inductive series admittances, whereas  $bc_l$  is the shunt susceptance. For the representation of power transformers, the AC branch model is generalized with an ideal transformer with the voltage tap ratio  $\tau_l$ . For an AC line or cable,  $\tau_l = 1$  holds.

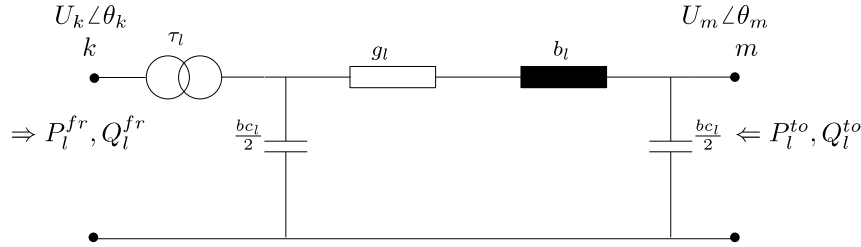


Figure 23 – Generic AC branch model for optimal power flow models

The active and reactive power flow through an existing AC branch in the *from* direction  $k \rightarrow m$  are defined as follows:

$$P_{l,t}^{fr} = g_l \left( \frac{U_{k,t}}{\tau_l} \right)^2 - g_l \frac{U_{k,t} U_{m,t}}{\tau_l} \cos(\theta_{k,t} - \theta_{m,t}) - b_l \frac{U_{k,t} U_{m,t}}{\tau_l} \sin(\theta_{k,t} - \theta_{m,t}) \quad \forall l \in S_l^{ac}, t \in T$$

$$Q_{l,t}^{fr} = -b_l \left( \frac{U_{k,t}}{\tau_l} \right)^2 + b_l \frac{U_{k,t} U_{m,t}}{\tau_l} \cos(\theta_{k,t} - \theta_{m,t}) - g_l \frac{U_{k,t} U_{m,t}}{\tau_l} \sin(\theta_{k,t} - \theta_{m,t}) \quad \forall l \in S_l^{ac}, t \in T$$

where,  $P_{l,t}^{fr}$  and  $Q_{l,t}^{fr}$  are the active and reactive power flows through the line  $l$  in time point  $t$  respectively. Similarly, the active and reactive power flow through an existing AC branch in the *to* direction  $m \rightarrow k$  are defined as follows:

$$P_{l,t}^{to} = g_l \left( \frac{U_{m,t}}{\tau_l} \right)^2 - g_l \frac{U_{k,t} U_{m,t}}{\tau_l} \cos(\theta_{m,t} - \theta_{k,t}) - b_l \frac{U_{k,t} U_{m,t}}{\tau_l} \sin(\theta_{m,t} - \theta_{k,t}) \quad \forall l \in S_l^{ac}, \forall t \in T$$

$$Q_{l,t}^{to} = -b_l \left( \frac{U_{m,t}}{\tau_l} \right)^2 + b_l \frac{U_{k,t} U_{m,t}}{\tau_l} \cos(\theta_{m,t} - \theta_{k,t}) - g_l \frac{U_{k,t} U_{m,t}}{\tau_l} \sin(\theta_{m,t} - \theta_{k,t}) \quad \forall l \in S_l, \forall t \in T$$

The apparent power flow through AC branches is bounded by the MVA rating of branch the branch  $S_l^{rated}$  as follows:

$$(P_{l,t}^{fr})^2 + (Q_{l,t}^{fr})^2 \leq (S_l^{rated})^2 \quad \forall l \in S_l^{ac}, \forall t \in T$$

$$(P_{l,t}^{to})^2 + (Q_{l,t}^{to})^2 \leq (S_l^{rated})^2 \quad \forall l \in S_l^{ac}, \forall t \in T$$

Additionally, voltage phase angle deviation limits across AC nodes can be defined, which are used as a proxy of dynamic stability limits, where  $\Delta\theta_l^{max}$  denotes the maximum allowable phase angle deviation across an AC branch:

$$\theta_{k,t} - \theta_{m,t} \leq \Delta\theta_l^{max} \quad \forall l \in S_l^{ac}, \forall t \in T$$

$$\theta_{m,t} - \theta_{k,t} \leq \Delta\theta_l^{max} \quad \forall l \in S_l^{ac}, \forall t \in T$$

A phase shifting transformer (PST) which can be used to provide power flow controllability, can be represented by a series impedance connected in series to an existing transmission line as shown in Figure 24. Where  $g_b$  denotes its series conductance and  $b_b$  denotes its series admittance. The PST adds an additional variable phase shift  $\varphi_b$  to control the power flow through the in series connected branch.

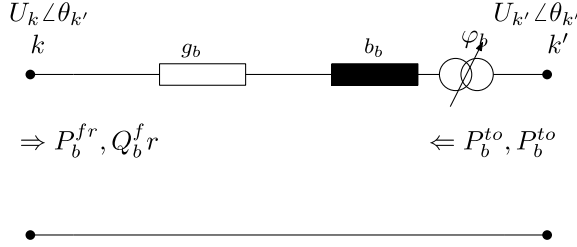


Figure 24: Steady state PST representation for OPF modelling

The PST is located between the nodes  $k$  and  $k'$  connected in series with a line  $k' \rightarrow k$ . A PST introduces a voltage angle shift  $\varphi_b$  along the PST impedance, such that the power flow through an existing PST becomes,

$$P_{b,t}^{fr} = g_b (U_{k,t})^2 - g_b U_{k,t} U_{k',t} \cos(\theta_{k,t} - \theta_{k',t} + \varphi_{b,t}) - b_b U_{k,t} U_{k',t} \sin(\theta_{k,t} - \theta_{k',t} + \varphi_{b,t}) \quad \forall b \in S_b, \forall t \in T$$

$$Q_{b,t}^{fr} = -b_b (U_{k,t})^2 + b_b U_{k,t} U_{k',t} \cos(\theta_{k,t} - \theta_{k',t} + \varphi_{b,t}) - g_b U_{k,t} U_{k',t} \sin(\theta_{k,t} - \theta_{k',t} + \varphi_{b,t}) \quad \forall b \in S_b, \forall t \in T$$

$$P_{b,t}^{to} = g_b(U_{k',t})^2 - g_b U_{k,t} U_{k',t} \cos(\theta_{k',t} - \theta_{k,t} - \varphi_{b,t}) \\ - b_b U_{k,t} U_{k',t} \sin(\theta_{k',t} - \theta_{k,t} - \varphi_{b,t}) \quad \forall b \in S_b, \forall t \in T$$

$$Q_{b,t}^{to} = -b_b(U_{k',t})^2 + b_b U_{k,t} U_{k',t} \cos(\theta_{k',t} - \theta_{k,t} - \varphi_{b,t}) - g_b U_{k,t} U_{k',t} \sin(\theta_{k',t} - \theta_{k,t} - \varphi_{b,t}) \quad \forall b \in S_b, \forall t \in T.$$

The phase angle shift is bounded with the maximum and minimum phase angle shift of the PST,

$$\varphi_b^{min} \leq \varphi_{b,t} \leq \varphi_b^{max} \quad \forall b \in S_b, \forall t \in T.$$

Also, the apparent power flow across the PST is bounded by its MVA rating  $S_b^{rated}$  as follows,

$$(P_{b,t}^{fr})^2 + (Q_{b,t}^{fr})^2 \leq (S_b^{rated})^2 \quad \forall b \in S_b, \forall t \in T$$

$$(P_{b,t}^{to})^2 + (Q_{b,t}^{to})^2 \leq (S_b^{rated})^2 \quad \forall b \in S_b, \forall t \in T$$

According to Kirchhoff's current law, all active and reactive power injections in a node  $m$  need to balance to zero,

$$\sum_{gm \in T^{gen}} P_{g,t} + \sum_{cme \in T^{acdc}} P_{c,t}^{ac} - \sum_{lmk \in T^{ac}} P_{l,t}^{fr} - \sum_{bmk \in T^b} P_{b,t}^{fr} - \sum_{um \in T^{load}} P_{u,t} = 0 \quad \forall m \in S_m, t \in T$$

$$\sum_{gm \in T^{gen}} Q_{g,t} + \sum_{cme \in T^{acdc}} Q_{c,t}^{ac} - \sum_{lmk \in T^{ac}} Q_{l,t}^{fr} - \sum_{bmk \in T^b} Q_{b,t}^{fr} - \sum_{um \in T^{load}} Q_{u,t} = 0 \quad \forall m \in S_m, t \in T$$

where,

- $P_{g,t}$  and  $Q_{g,t}$  are the active and reactive power injections of generators connected to node  $m$ , in time point  $t$ , where  $gm \in T^{gen}$  represents the nodal connectivity of generators
- $P_{c,t}^{ac}$  and  $Q_{c,t}^{ac}$  are the AC side active and reactive power injections of HVDC converters connected to node  $m$ , in time point  $t$ ,  $cme \in T^{acdc}$  represents the nodal connectivity of HVDC converters between AC nodes  $m$  and DC nodes  $e$
- $P_{l,t}^{fr}$  and  $Q_{l,t}^{fr}$  are the active power flows leaving from node  $m$ , in time point  $t$ , where  $lmk \in T^{ac}$  represents the nodal connectivity of AC branches between AC nodes  $m$  and  $k$
- $P_{b,t}^{fr}$  and  $Q_{b,t}^{fr}$  are the active flows and reactive power flows of PSTs leaving from node  $m$ , in time point  $t$ , where  $bmk \in T^b$  represents the connectivity of PST between nodes  $m$  and  $k$

- $P_{u,t}$  and  $Q_{u,t}$  are the active and reactive power demands of loads connected to node  $m$ , in time point  $t$ , where  $um \in T^{load}$  represents the nodal connectivity of loads

Both dispatchable and renewable generators are subject to operational limits,

$$P_{g,t}^{min} \leq P_{g,t} \leq P_{g,t}^{max} \quad \forall g \in S_g, t \in T$$

$$Q_{g,t}^{min} \leq Q_{g,t} \leq Q_{g,t}^{max} \quad \forall g \in S_g, t \in T$$

where the active and reactive power limits of the renewable generators are defined by the climatic conditions at time instance  $t$ . Similarly, the nodal demand including demand response and possible demand curtailment can be modelled using following relationships:

$$P_{u,t} = P_{u,t}^{ref} - P_{u,t}^{dr} - P_{u,t}^{curt} \quad \forall u \in S_u, t \in T$$

where  $P_{u,t}^{ref}$  is the reference demand of load  $u$  at time point  $t$ , and  $P_{u,t}^{dr}$  and  $P_{u,t}^{curt}$  are the demand response and curtailment, respectively. Similarly, the reactive power demand is modelled using :

$$Q_{u,t} = Q_{u,t}^{ref} - Q_{u,t}^{dr} - Q_{u,t}^{curt} \quad \forall u \in S_u, t \in T$$

Active and reactive demand response, as well as curtailment are subject to upper and lower bounds:

$$0 \leq P_{u,t}^{dr} \leq P_{u,t}^{ref} \quad \forall u \in S_u, t \in T$$

$$0 \leq P_{u,t}^{curt} \leq P_{u,t}^{ref} \quad \forall u \in S_u, t \in T$$

$$0 \leq Q_{u,t}^{dr} \leq P_{u,t}^{ref} \quad \forall u \in S_u, t \in T$$

$$0 \leq Q_{u,t}^{curt} \leq P_{u,t}^{ref} \quad \forall u \in S_u, t \in T$$

where the reference power factor is preserved through  $\frac{P_{u,t}^{dr}}{Q_{u,t}^{dr}} = \frac{P_{u,t}^{ref}}{Q_{u,t}^{ref}}$  and  $\frac{P_{u,t}^{curt}}{Q_{u,t}^{curt}} = \frac{P_{u,t}^{ref}}{Q_{u,t}^{ref}}$   $\forall u \in S_u, t \in T$ .

Figure 25 depicts the HVDC converter station model as part of the AC/DC grid optimal power flow model. The generic converter station model consists of a converter transformer, an inductive and capacitive filter, and the power electronic HVDC converter itself.

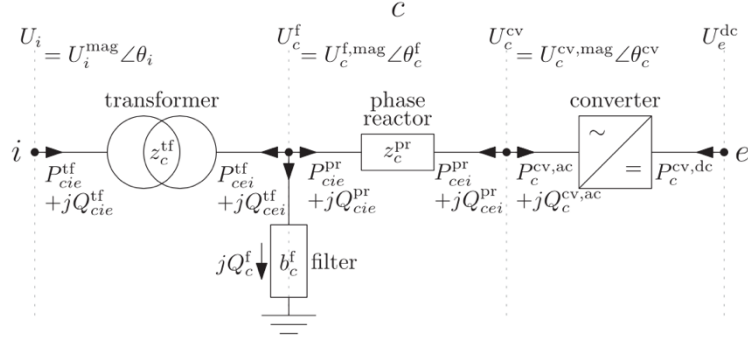


Figure 25 - Generic HVDC converter station model

The depicted converter station is located between an AC node  $i$  and a DC node  $e$ . On the AC side, the converter is characterized by the complex voltage  $U_i$  of the AC node  $i$ , the complex voltage after the converter transformer  $U_c^f$  and the complex voltage observed on the AC side of the power electronic converter  $U_c^{cv}$ .

Using the AC side voltages, the power flows through the converter transformer of each converter station  $c \in S_c$ , for each time point  $t \in T$  are calculated using for the *from* direction  $i \rightarrow e$ :

$$P_{cie,t}^{tf} = g_c^{tf} \left( \frac{U_{i,t}^{mag}}{\tau_c} \right)^2 - g_c^{tf} \frac{U_{i,t}^{mag} U_{c,t}^{f,mag}}{\tau_c} \cos(\theta_{i,t} - \theta_{c,t}^f) - b_c^{tf} \frac{U_{i,t}^{mag} U_{c,t}^{f,mag}}{\tau_c} \sin(\theta_{i,t} - \theta_{c,t}^f) \quad \forall c \in S_c, t \in T$$

$$Q_{cie,t}^{tf} = -b_c^{tf} \left( \frac{U_{i,t}^{mag}}{\tau_c} \right)^2 + b_c^{tf} \frac{U_{i,t}^{mag} U_{c,t}^{f,mag}}{\tau_c} \cos(\theta_{i,t} - \theta_{c,t}^f) - g_c^{tf} \frac{U_{i,t}^{mag} U_{c,t}^{f,mag}}{\tau_c} \sin(\theta_{i,t} - \theta_{c,t}^f) \quad \forall c \in S_c, t \in T$$

And the *to* direction  $e \rightarrow i$ :

$$P_{c,t}^{ac} = P_{cei,t}^{tf} = g_c^{tf} \left( \frac{U_{c,t}^{f,mag}}{\tau_c} \right)^2 - g_c^{tf} \frac{U_{i,t}^{mag} U_{c,t}^{f,mag}}{\tau_c} \cos(\theta_{c,t}^f - \theta_{i,t}) - b_c^{tf} \frac{U_{i,t}^{mag} U_{c,t}^{f,mag}}{\tau_c} \sin(\theta_{c,t}^f - \theta_{i,t}) \quad \forall c \in S_c, t \in T$$

$$Q_{c,t}^{ac} = Q_{cei,t}^{tf} = -b_c^{tf} \left( \frac{U_{c,t}^{f,mag}}{\tau_c} \right)^2 + b_c^{tf} \frac{U_{i,t}^{mag} U_{c,t}^{f,mag}}{\tau_c} \cos(\theta_{c,t}^f - \theta_{i,t}) - g_c^{tf} \frac{U_{i,t}^{mag} U_{c,t}^{f,mag}}{\tau_c} \sin(\theta_{c,t}^f - \theta_{i,t}) \quad \forall c \in S_c, t \in T$$

where,  $g_c^{tf}$  denotes the series conductance of the transformer,  $b_c^{tf}$  denotes its series admittance, and  $\tau_c$  denotes the tap setting of the transformer. In case, the converter station does not contain a transformer, the equations can be placed by:

$$P_{cie,t}^{tf} + P_{cei,t}^{tf} = 0 \quad \forall c \in S_c, t \in T$$

$$Q_{cie,t}^{tf} + Q_{cei,t}^{tf} = 0 \quad \forall c \in S_c, t \in T$$

$$U_{i,t}^{mag} = U_{c,t}^{f,mag} \quad \forall c \in S_c, t \in T$$

$$\theta_{i,t} = \theta_{c,t}^f \quad \forall c \in S_c, t \in T$$

The reactive power injected by the capacitive part of the filter is defined as, with  $b_c^f$  as the susceptance of the capacitive filter:

$$Q_{f,t}^c = -b_c^f (U_{c,t}^{f,mag})^2 \quad \forall c \in S_c, t \in T$$

The nodal power balance at the filter node  $f$  is defined as:

$$P_{cie,t}^{pr} + P_{cei,t}^{tf} = 0 \quad \forall c \in S_c, t \in T$$

$$Q_{cie,t}^{pr} + Q_{cei,t}^{tf} + Q_{c,t}^f = 0 \quad \forall c \in S_c, t \in T$$

As the inductive part of the converter station filter behaves similar to the converter transformer (with the exception of the transformer tap  $\tau_c$ ), the active and reactive power flows across the inductive filter can be written down as with  $g_c^{pr}$  and  $b_c^{pr}$  as the series conductance and susceptance of the inductor:

For the *from* direction  $i \rightarrow e$ :

$$\begin{aligned} P_{cie,t}^{pr} &= g_c^{pr} (U_{c,t}^{f,mag})^2 - g_c^{pr} U_{c,t}^{f,mag} U_{c,t}^{cv,mag} \cos(\theta_{c,t}^f - \theta_{c,t}^{cv}) \\ &\quad - b_c^{pr} U_{c,t}^{f,mag} U_{c,t}^{cv,mag} \sin(\theta_{c,t}^f - \theta_{c,t}^{cv}) \quad \forall c \in S_c, t \in T \end{aligned}$$

$$\begin{aligned} Q_{cie,t}^{pr} &= -b_c^{pr} (U_{c,t}^{f,mag})^2 + b_c^{pr} U_{c,t}^{f,mag} U_{c,t}^{cv} \cos(\theta_{c,t}^f - \theta_{c,t}^{cv}) - g_c^{pr} U_{c,t}^{f,mag} U_{c,t}^{cv} \sin(\theta_{c,t}^f - \theta_{c,t}^{cv}) \quad \forall c \\ &\in S_c, t \in T \end{aligned}$$

And the *to* direction  $e \rightarrow i$ :

$$\begin{aligned} P_{cei,t}^{pr} &= g_c^{pr} (U_{c,t}^{f,mag})^2 - g_c^{pr} U_{c,t}^{f,mag} U_{c,t}^{cv} \cos(\theta_{c,t}^{cv} - \theta_{c,t}^f) \\ &\quad - b_c^{pr} U_{c,t}^{f,mag} U_{c,t}^{cv,mag} \sin(\theta_{c,t}^{cv} - \theta_{c,t}^f) \quad \forall c \in S_c, t \in T \end{aligned}$$

$$\begin{aligned} Q_{cei,t}^{pr} &= -b_c^{pr} (U_{c,t}^{f,mag})^2 + b_c^{pr} U_{c,t}^{f,mag} U_{c,t}^{cv,mag} \cos(\theta_{c,t}^{cv} - \theta_{c,t}^f) \\ &\quad - g_c^{pr} U_{c,t}^{f,mag} U_{c,t}^{cv,mag} \sin(\theta_{c,t}^{cv} - \theta_{c,t}^f) \quad \forall c \in S_c, t \in T \end{aligned}$$

According to the notation in Figure 25, the AC side active and reactive power of the HVDC converter have opposite signs as the power through the inductive filter, e.g.,

$$P_{cei,t}^{pr} + P_{c,t}^{cv,ac} = 0 \quad \forall c \in S_c, t \in T$$

$$Q_{cei,t}^{pr} + Q_{c,t}^{cv,ac} = 0 \quad \forall c \in S_c, t \in T$$

The AC and DC side power of the power electronic converter can be linked via the converter losses, e.g.,

$$P_{c,t}^{cv,ac} + P_{c,t}^{cv,dc} = P_{c,t}^{cv,loss} \quad \forall c \in S_c, t \in T$$

with the losses defined as a quadratic function of the current through the power electronic converter  $I_c^{ac} = I_c^{ac,mag} \angle \theta_c^i$ :

$$P_{c,t}^{cv,loss} = a_c + b_c I_{c,t}^{ac,mag} + c_c (I_{c,t}^{ac,mag})^2 \quad \forall c \in S_c, t \in T$$

The active and reactive power of the converter are linked to the converter current and voltage through:

$$(P_{c,t}^{cv,ac})^2 + (Q_{c,t}^{cv,ac})^2 = (I_{c,t}^{ac,mag})^2 \cdot (U_{c,t}^{cv,mag})^2 \quad \forall c \in S_c, t \in T$$

All active and reactive power terms as well voltage magnitudes and currents are subject to operational bounds:

$$(P_{cie,t}^{tf})^2 + (Q_{cie,t}^{tf})^2 \leq (S_c^{tf,rated})^2 \quad \forall c \in S_c, t \in T$$

$$(P_{cei,t}^{tf})^2 + (Q_{cei,t}^{tf})^2 \leq (S_c^{tf,rated})^2 \quad \forall c \in S_c, t \in T$$

$$(P_{cie,t}^{pr})^2 + (Q_{cie,t}^{pr})^2 \leq (S_c^{pr,rated})^2 \quad \forall c \in S_c, t \in T$$

$$(P_{cei,t}^{pr})^2 + (Q_{cei,t}^{pr})^2 \leq (S_c^{pr,rated})^2 \quad \forall c \in S_c, t \in T$$

$$0 \leq Q_{c,t}^f \leq Q_c^{f,max} \quad \forall c \in S_c, t \in T$$

$$U_c^{f,min} \leq U_{c,t}^{f,mag} \leq U_c^{f,max} \quad \forall c \in S_c, t \in T$$

$$U_c^{cv,min} \leq U_{c,t}^{cv,mag} \leq U_c^{cv,max} \quad \forall c \in S_c, t \in T$$

$$I_c^{cv,min} \leq I_{c,t}^{cv,mag} \leq I_c^{cv,max} \quad \forall c \in S_c, t \in T$$

$$P_c^{dc,min} \leq P_{c,t}^{cv,dc} \leq P_c^{dc,max} \quad \forall c \in S_c, t \in T$$

The HVDC branches, e.g., lines and cables can be modelled using the single line diagram shown in Figure 26, which represents the DC branch as a resistance between two DC grid nodes  $e$  and  $f$ . For monopolar HVDC configurations, the power will flow through a single conductor, whereas for symmetrical monopoles or bipolar HVDC schemes, the power flow through a branch is distributed equally between the two conductors, assuming they have the same resistance ( $r_d$ ) / conductance ( $g_d$ ).

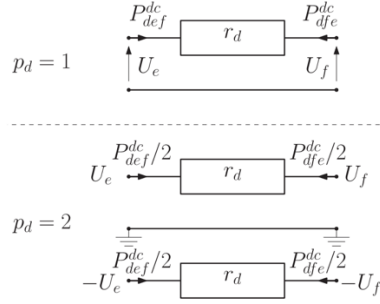


Figure 26 – Generic DC branch model for monopolar and bipolar HVDC

Considering the number of poles  $N_d$  ( $N_d = 1$  for monopolar and  $N_d = 2$ , for symmetrical monopolar or bipolar configurations), the power flows through the DC branches can be calculated with the Ohm's law using the nodal DC grid voltages for both directions  $e \rightarrow f$  and  $f \rightarrow e$ :

$$P_{def,t}^{dc} = N_d g_d U_{e,t}^{dc} (U_{e,t}^{dc} - U_{f,t}^{dc}) \quad \forall d \in S_d, t \in T$$

$$P_{dfe,t}^{dc} = N_d g_d U_{f,t}^{dc} (U_{f,t}^{dc} - U_{e,t}^{dc}) \quad \forall d \in S_d, t \in T$$

with the DC branch power flow limits

$$-P_d^{rated} \leq P_{def,t}^{dc} \leq P_d^{rated} \quad \forall d \in S_d, t \in T$$

$$-P_d^{rated} \leq P_{dfe,t}^{dc} \leq P_d^{rated} \quad \forall d \in S_d, t \in T$$

Finally, defining Kirchhoff's current law for DC nodes completes the AC/DC grid optimal power flow model, where  $S_e$  denotes the set of DC nodes, and set  $T^{dc}$  denotes the connectivity set of DC branches to DC nodes:

$$\sum_{cme \in T^{acdc}} P_{c,t}^{dc} - \sum_{def \in T^{dc}} P_{def,t}^{dc} = 0 \quad \forall e \in S_e, t \in T$$

As in the case of the NTC based zonal model, also this optimization model does not include any time coupling constraints, and as such can be solved for all the hours in a planning year separately. In case unit commitment constraints or storage models are introduced in model, time coupling constraints would be needed, and as such, the problem would become a single optimization problem solved for the entire planning year. Even if solved for each time step (hour) separately, the problem remains a highly nonlinear and nonconvex problem. Although such problems can be solved efficiently with interior point optimization solvers, still for large and especially ill conditioned cases, convergence problems or long calculation times can occur. Thus, as a mitigation, the power flow equations can be linearized, providing a much more tractable and compact model, under the following assumptions, which are very well known for the linearized power flow formulation, often called "DC OPF" (which does not relate to DC grids).

Firstly, it is assumed that the magnitudes of the nodal AC and DC grid nodal voltage magnitudes across the network will only differ slightly such that it can be assumed:  $U_{m,t} = U_{k,t} = U_{ac} \quad \forall m, k \in S_n^{ac}$  and  $U_{e,t} = U_{f,t} = U_{dc} \quad \forall e, f \in S_e$ . Another assumption is that the AC grid voltage angle differences are so small such that  $\sin(\theta_{m,t,y} - \theta_{k,t,y}) \approx \theta_{m,t,y} - \theta_{k,t,y}$

and  $\cos(\theta_{m,t,y} - \theta_{k,t,y}) \approx 1$  can be assumed. Additionally, the resistive part of the series admittance  $g_l = 0$  is neglected under the assumption that the inductance of AC branches is dominant, which is a valid assumption for overhead lines, resulting for AC branches in:

$$\begin{aligned} P_{l,t,y}^{fr} &= b_l \frac{U_{ac}^2}{\tau_l} (\theta_{m,t} - \theta_{k,t}) \quad \forall l \in S_l^{ac}, \forall t \in T \\ P_{l,t}^{to} &= b_l \frac{U_{ac}^2}{\tau_l} (\theta_{k,t} - \theta_{m,t}) = -P_{l,t}^{fr} \quad \forall l \in S_l^{ac}, \forall t \in T \\ Q_{l,t}^{fr} &= Q_{l,t}^{to} = 0 \quad \forall l \in S_l^{ac}, \forall t \in T, \end{aligned}$$

which means that all reactive power related terms disappear in the used model. **As the resistive part of the impedance/admittance is neglected, this representation also neglects the network losses occurring.** In this case, branch flows are only bound by the maximum voltage angle differences and the thermal limits of the AC branches are defined in terms of active power only:

$$\begin{aligned} \theta_{k,t} - \theta_{m,t} &\leq \Delta\theta_l^{max} \quad \forall l \in S_l^{ac}, \forall t \in T \\ \theta_{m,t} - \theta_{k,t} &\leq \Delta\theta_l^{max} \quad \forall l \in S_l^{ac}, \forall t \in T \\ -P_l^{rated} &\leq P_{l,t,y}^{fr} \leq P_l^{rated} \quad \forall l \in S_l^{ac}, \forall t \in T \\ -P_l^{rated} &\leq P_{l,t,y}^{to} \leq P_l^{rated} \quad \forall l \in S_l^{ac}, \forall t \in T \end{aligned}$$

Similarly, to AC branches, also the linearized equations for PSTs can be written using  $U_{k,t,y} = U_{k',t,y} = U_{ac} \forall k', k \in S_n^{ac}$ ,

$$\begin{aligned} P_{b,t}^{fr} &= b_b U_{ac}^2 (\theta_{k,t} - \theta_{k',t} + \varphi_{b,t}) \quad \forall l \in S_l^{ac}, \forall t \in T \\ P_{b,t}^{to} &= b_b U_{ac}^2 (\theta_{k',t} - \theta_{k,t} - \varphi_{b,t}) \quad \forall l \in S_l^{ac}, \forall t \in T \\ -P_b^{rated} &\leq P_{b,t}^{fr} \leq P_b^{rated} \quad \forall l \in S_l^{ac}, \forall t \in T \\ -P_b^{rated} &\leq P_{b,t}^{to} \leq P_b^{rated} \quad \forall l \in S_l^{ac}, \forall t \in T \\ \varphi_b^{min} &\leq \varphi_{b,t} \leq \varphi_b^{max} \quad \forall l \in S_l^{ac}, \forall t \in T. \end{aligned}$$

The AC nodal power balance is only written in active power:

$$\sum_{gm \in T^{gen}} P_{g,t} + \sum_{cme \in T^{acdc}} P_{c,t}^{ac} - \sum_{lmk \in T^{ac}} P_{l,t}^{fr} - \sum_{bmk \in T^b} P_{b,t}^{fr} - \sum_{um \in T^{load}} P_{u,t} = 0 \quad \forall m \in S_m, t \in T$$

Similarly, all equations describing the HVDC converter station can be linearized and written in “active power only” terms as follows:

$$P_{cie,t}^{tf} = -b_c^{tf} U_{ac}^2 \sin(\theta_{i,t} - \theta_{c,t}^f) \quad \forall c \in S_c, t \in T$$

$$P_{c,t}^{ac} = P_{cei,t}^{tf} = -b_c^{tf} U_{ac}^2 \sin(\theta_{c,t}^f - \theta_{i,t}) \quad \forall c \in S_c, t \in T$$

$$P_{cie,t}^{pr} + P_{cei,t}^{tf} = 0 \quad \forall c \in S_c, t \in T$$

$$P_{cie,t}^{pr} = -b_c^{pr} U_{ac}^2 \sin(\theta_{c,t}^f - \theta_{c,t}^{cv}) \quad \forall c \in S_c, t \in T$$

$$P_{cei,t}^{pr} = -b_c^{pr} U_{ac}^2 \sin(\theta_{c,t}^{cv} - \theta_{c,t}^f) \quad \forall c \in S_c, t \in T$$

$$P_{cei,t}^{pr} + P_{c,t}^{cv,ac} = 0 \quad \forall c \in S_c, t \in T$$

Considering that the AC grid and AC equipment of the HVDC substations are considered to be lossless, and the power electronic converter losses are assumed to be zero as well resulting in:

$$P_{c,t}^{cv,ac} + P_{c,t}^{cv,dc} = 0 \quad \forall c \in S_c, t \in T$$

Also, all equipment limits within the HVDC substation can be defined via the active power bounds as:

$$-P_{c,t}^{tf,rated} \leq P_{cie,t}^{tf} \leq P_{c,t}^{tf,rated} \quad \forall c \in S_c, t \in T$$

$$-P_{c,t}^{tf,rated} \leq P_{cei,t}^{tf} \leq P_{c,t}^{tf,rated} \quad \forall c \in S_c, t \in T$$

$$-P_{c,t}^{pr,rated} \leq P_{cie,t}^{pr} \leq P_{c,t}^{pr,rated} \quad \forall c \in S_c, t \in T$$

$$-P_{c,t}^{pr,rated} \leq P_{cei,t}^{pr} \leq P_{c,t}^{pr,rated} \quad \forall c \in S_c, t \in T$$

$$-P_c^{ac,rated} \leq P_{c,t}^{cv,ac} \leq P_c^{ac,rated} \quad \forall c \in S_c, t \in T$$

$$-P_c^{dc,rated} \leq P_{c,t}^{cv,dc} \leq P_c^{dc,rated} \quad \forall c \in S_c, t \in T$$

As for the DC branches, considering that the voltage difference between the nodes reduces to zero, the DC power flow reduces to a network flow model, i.e., an NTC based model which is a valid approximation under the assumption that the injections from the converters can be controlled largely,

$$P_{def,t}^{dc} + P_{dfe,t}^{dc} = 0 \quad \forall d \in S_d, t \in T$$

$$-P_d^{rated} \leq P_{def,t}^{dc} \leq P_d^{rated} \quad \forall d \in S_d, t \in T$$

$$-P_d^{rated} \leq P_{dfe,t}^{dc} \leq P_d^{rated} \quad \forall d \in S_d, t \in T$$

The DC grid nodal power equations remain unchanged:

$$\sum_{cme \in T^{acdc}} P_{c,t}^{dc} - \sum_{def \in T^{dc}} P_{def,t}^{dc} = 0 \quad \forall e \in S_e, t \in T$$

It needs to be noted that in the literature many different formulations of the power flow equations exist, which lead to different computational complexities, accuracy in system representation and computation time. The introduced OPF models can further be extended in order to model different aspects of system operation. For instance, one such application is the determination of the optimal redispatch actions both for balancing the power mismatch stemming from the day ahead renewable forecast error as well as in cases of outages.

### 6.2.3. AC/DC grid optimal redispatch power flow modelling

Considering possible outages in the network, or potential inertia constraints, an optimal redispatch model can be used to determine the minimal redispatch to be performed to avoid thermal overloads in the grid due to outages, or potential dispatch/start-up of conventional synchronous machine based generation to ensure a minimum inertia level in the grid.

Let us first start with the case of possible contingencies in the grid. In case of a line contingency, the power flows in the grid will be changed due to the change in the grid impedances. This could potentially lead to overloading of other lines in the system, e.g., most notable on parallel lines which are highly loaded. In such cases, the active power set points of generators, PSTs and HVDC links can be changed in order to obtain a power flow solution which respects thermal line limits. In order to minimize the necessary active power re-dispatch costs, the following model can be utilized.

Starting from the pre-contingency (N-0) situation, e.g., the solution of the optimal power flow problem denoted with the superscript *ref*, we can deactivate a critical set of transmission lines one-by-one in the system, e.g., create a number of n-1 contingency situations. In this case, our objective is to minimize the cost for upwards and downwards redispatch which is denoted by  $\Delta P_{g,t}^{up}$  and  $\Delta P_{g,t}^{down}$ . Thus, the objective function of the optimisation model becomes:

$$\min \sum_{g \in S_g} (C_g^{up} \Delta P_{g,t}^{up} + C_g^{down} \Delta P_{g,t}^{down}) + \sum_{u \in S_u} (C_u^{dr} P_{u,t}^{dr} + VOL_u P_{u,t}^{curt}) \quad \forall t \in T,$$

with the two newly introduced variables  $\Delta P_g^{up} \geq 0$  and  $\Delta P_g^{down} \geq 0$ . We can then write the relationship between the active power generation and the redispatch need with respect to the reference (N-0) case as:

$$P_{g,t} = P_g^{ref} + \Delta P_g^{up} - \Delta P_g^{down} \quad \forall g \in S_g, t \in T$$

By adding further constraints to the optimization problem defined in the previous section for not altering the net position of a certain market zone the redispatch – optimization problem is fully defined. These constraints are only defined over a set of interconnecting AC and DC lines of the considered market zone and given as:

$$\sum_{l \in S_l^{ac}} P_{l,t,z}^{fr} + \sum_{d \in S_d} P_{def,t,z}^{dc} = \sum_{l \in S_l^{ac}} P_{l,t,z}^{fr,ref} + \sum_{d \in S_d} P_{def,t,z}^{dc,ref} \quad \forall t \in T, z \in Z.$$

Note that the above constraint might need to be defined on a zone-by-zone basis if the considered market zone is connected to multiple other market zones, thus for each  $z \in Z$ .

This optimization model is used to determine the benefits of power flow controllability through HVDC links in the Ultranet use case illustrated in section 7.4.

A similar optimisation model can be derived to determine the minimum redispatch/start-up costs conventional generation in order to fulfil minimum system inertia requirements as a proxy for frequency stability.

In this case first a distinction needs to be made for generators that are already online, and thus can provide inertial support, versus generators that are offline and would need to be started up. Therefore, a binary parameter  $s_g$  is introduced which indicates the on/off state of the generator in the reference case (e.g., the solution of the optimal power flow problem). In this case, our aim is to minimize the start-up costs to provide the necessary inertia in the system, thus the objective of the optimisation becomes,

$$\min \sum_{g \in G} P_g^{\text{rated}} \cdot C_g^{\text{start-up}} \cdot (\alpha_g - s_g),$$

where  $P_g^{\text{rated}}$  is the rated active power generation of generator  $g$ , and  $\alpha_g$  is a binary decision variable,  $\alpha_g \in \{0, 1\}$ , for the start-up of a generator. The following additional constraints w.r.t the optimal power flow problem needs to be introduced to ensure that both grid constraints, and inertia constraints are fulfilled. Firstly, the active power generation needs to be limited by

$$\alpha_g \cdot P_g^{\text{min}} \leq P_g \leq \alpha_g \cdot P_g^{\text{max}} \quad \forall g \in G,$$

to indicate that generators with an off status cannot generate power.

Secondly, the constraint  $\alpha_g \geq s_g$  needs to be introduced to make sure that generators which were online in the reference case, are not switched-off. Finally, a minimum inertia constraint is introduced, which ensures that the total inertia in a given synchronous zone  $z$  is larger or equal to a given minimum inertia limit  $H_z^{\text{min}}$ ,

$$\sum_{g \in G} P_{g,z}^{\text{rated}} \cdot H_g \cdot \alpha_g \geq H_z^{\text{min}} \quad \forall z \in Z,$$

where  $H_g$  is the inertia constant of generator  $g$ .

Here it should be noted that the above-described model does not consider any additional constraint for technical characteristics of conventional power plants w.r.t., start-up times, and minimum down times, and as such can only be used as an approximation.

The above described model can be used both in the NTC based formulation (section 6.2.1) as well as the linearized power flow formulation (section 6.2.2) and is applied to determine the benefits of inertia support through HVDC links in sections 7.3 and 7.5 (use cases Celtic Interconnector and Eurasian Interconnector).

Within this project, all described optimisation models throughout this section have been implemented as an extension of the open-source AC/DC grid optimal power flow tool PowerModelsACDC.jl<sup>6</sup>. As such, a new software package, CBAOPF.jl has been created which includes all optimisation models explained in this section. The CBAOPF.jl package can be accessed through <https://github.com/Electa-Git/CBAOPF.jl>.

## 6.3. Modelling Requirements to determine proposed stability KPIs

### 6.3.1. Frequency stability KPIs

As indicated in section 5.2.3, frequency stability in a reduced inertia system represents a significant challenge. There are some mitigation actions to ensure stability of low inertia systems but they might require more advanced control loops or additional assets.

First of all, it is important to remind that the system inertia represents the kinetic energy stored in the rotating masses synchronously connected to the grid. Therefore, three

<sup>6</sup> <https://github.com/Electa-Git/PowerModelsACDC.jl>

parameters are required in order to estimate the system inertia (i.e. number of online machines, their MVA rating and inertia constants). Two estimations of inertia were used in the project.

The first estimation is applied to the zonal dispatch when there are aggregated machines connected to each zone. In this case, it is not possible to know the unit dispatch and as such accurately determine the inertia. Therefore, a simplification is made by using the active power dispatched and by approximating the MVA rating per type of generator.

For example, it is expected that nuclear units have a load factor of at least 0.9 at all time. Therefore, if the equivalent machine for nuclear units is dispatched at 900MW, it will be assumed that there are 1000MVA of nuclear units running. This approximation has been used in [28] and provides adequate results for large size systems. Estimated load factor values per generation type can also be found in [28]

$$Inertia_{sys} = \sum H_i * \frac{P_{gen_i}}{Load Factor_i}$$

where  $H$  is the inertia constant of machine  $i$ ,  $P_{gen}$  is the dispatch of machine  $i$  and *Load Factor* is the estimated loading factor of machine  $i$ .

A second estimation of the system inertia has been used for the nodal dispatch. In this case, the optimization problem has been slightly adapted to ensure that only the needed number of machines are considered as online. This allows to estimate the inertia by looking only at the MVA rating and inertia constants of the online machines.

$$Inertia_{sys} = \sum H_i * S_{nom_i} * online_i$$

It can be seen that a binary value (*online*) is used to neglect the offline machines in the system inertia calculation.

Once the inertia is estimated, it allows to approximate the initial RoCoF that will occur in the system after a disturbance (before actions of frequency response services). This can be done using the swing equation formulated as per [29]:

$$RoCoF = \frac{f * \Delta P}{2 * Inertia_{sys}}$$

where  $\Delta P$  represents the difference between generation and loads (in MW), and  $f$  is the nominal system frequency. In case of contingency (e.g. loss of infeed), the  $\Delta P$  will be equal to the loss of infeed. *RoCoF* is the rate of change of frequency (expressed in Hz/s) while the total system inertia is expressed in *MWs*.

It is important to note that using the swing equation assumes the exact same frequency at all times in the network, and should therefore be seen as a representation of the frequency behaviour at the centre of inertia of the network. During a disturbance, the frequency at each node of the network will experience an oscillatory behaviour around the average frequency.

Similarly to [29], an inertia constraint is derived from the swing equation. This is done by considering the highest credible loss of infeed (e.g. largest generating unit) and by assuming a maximum RoCoF withstand capability of assets connected to the system. Using these two parameters will directly provide the minimum inertia required to meet maximum acceptable RoCoF.

In this work, fast-frequency response that can be provided by an (asynchronous) HVDC link has been considered in order to estimate the inertia constraint. Assuming that the frequency response of the HVDC is much faster than the mechanical time constants, the following can be expressed:

$$\Delta P = P_{infeed loss} - \min(P_{mod}, P_{max} - P_{HVDC}),$$

where  $P_{infeed\ loss}$  is the total loss of infeed,  $P_{mod}$  is the active power modulation provided by the HVDC link during disturbance, and  $P_{max} - P_{HVDC}$  is the available headroom on the link. An estimation of the inertia constraint can therefore be done based on the active power modulation capability of the HVDC link. However, because this expression is dependent on the HVDC dispatch, it is proposed to model this using a simplified 2-bus system illustrated in Figure 27 (similarly to what has been done in [30]). Another advantage of this model is that it can also consider virtual inertia contribution from RES and/or BESS. Using this 2-bus model allows to perform a large number of frequency stability simulations in order to evaluate which operating conditions are stable and which ones are unstable.

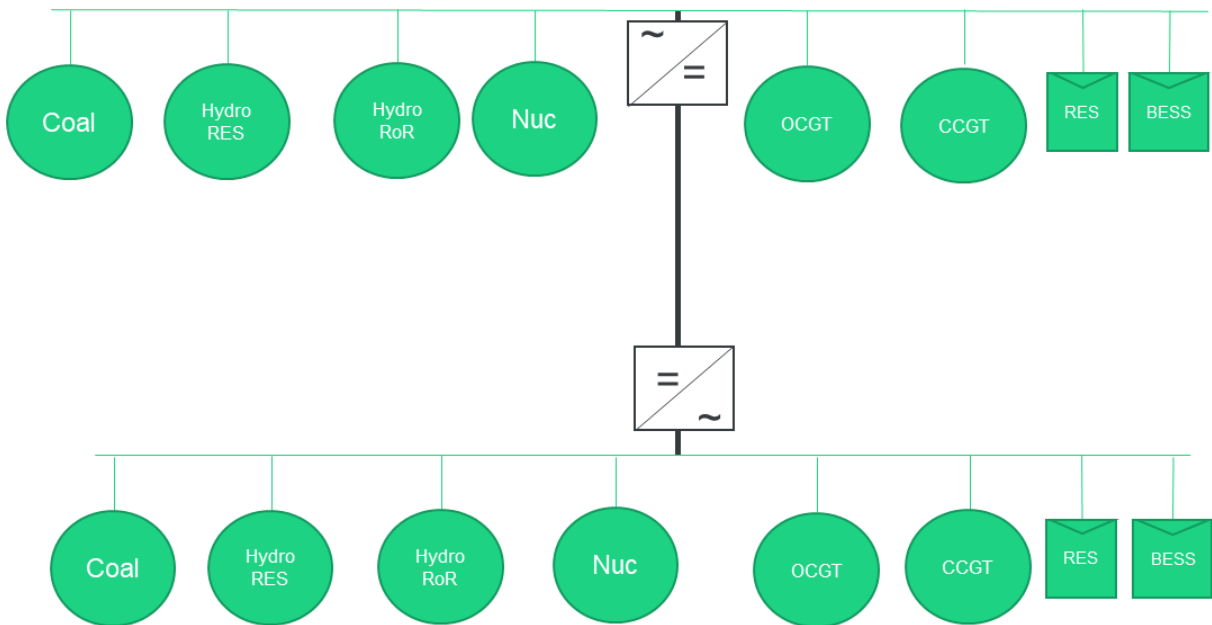


Figure 27 - 2-bus system for simplified frequency stability assessment

It is important to remind that the proposed KPI in section 5.2.3 is the *percentage of hours per year, for which the frequency stability is at risk*. Therefore, if an inertia constraint is used, it simply requires estimating the inertia of each hourly dispatch and to compare this with the pre-determined inertia constraint. The advantage of having an inertia constraint is its simplicity and it also allows to add the constraint into the optimization problem defined in 6.2.3.

If the 2-bus system is used, a representative number of time-domain simulations has to be performed in order to evaluate the number of stable and unstable cases. This representative number can be determined via a clustering technique as presented in section 5.5. This method has the advantage to be more accurate than the inertia constraint because it includes inertia, fast-frequency response, primary frequency response and unit dispatch. However, it requires more interactions with the optimization problem described in 6.2.3.

### 6.3.2. Converter-driven stability KPIs

Converter-driven stability is a major challenge in systems with high IBRs penetration. As stated in [31], “*high-quality vendor-specific EMT models are required [...] as part of the*

*interconnection process to ensure that all resources can reliably operate*". This statement clearly outlines the need to perform EMT simulations to ensure system stability but also emphasizes the need to have detailed EMT models, which are typically not available at the CBA stage of a project<sup>7</sup>. It is also outlined in the same report that RMS simulation can only capture a small subset of the potential instabilities that can be driven by converters. Therefore, in this work, it has been decided to focus on simplified indicators quantifying the risk of instability of IBRs. For example, the system strength, which can be seen as the impact of a fault or disturbance on the change in voltage [32], is a clear candidate that allows to identify this risk. When the grid is "strong", the voltage waveform will be less sensitive to disturbances and therefore the IBRs will be more stable. In "weak" grids, the voltage waveform can be significantly impacted by faults or disturbances, this can cause many consequences to IBRs (e.g., PLL loss of synchronism, AC or DC overvoltage, etc.).

The first proposed indicator for quantifying the risk of converter-driven instability is the **short-circuit ratio (SCR)**, defined as the short-circuit power at the point of connection of the IBR over its rating. High short-circuit ratio means that the grid is strong. As shown in Figure 7, it is generally assumed that when the SCR is above 3 the IBR will be stable while SCR around 1 requires additional assets and/or grid-forming control. To calculate the SCR, the nodal representation of the electrical grid has to be used, including the step-up transformer of each generating unit.

A limitation of the SCR as indicator of converter-driven instability is that it does not include the IBR operating point nor its control loops. Therefore, another indicator, as introduced in [7] and [6], will be applied to complement the SCR. The main objective of this second indicator, referred to in this report as **IBR-CCT (Critical Clearing Time of IBR)**, is to "*Identify operation conditions prone to IBR transient instability following a fault*" [7]. Its advantage compared to the SCR is that it includes two additional components which are:

- The IBR operating points
- Parameters of a simplified PLL control loop

More information can be found in [7] and [6], but in summary the IBR-CCT is an indicator of the transient stability margin of an IBR which can be calculated analytically by taking the operating point, SCR and PLL parameters as main input parameters. The analytical expression is based on the equal area-criterion applied to the PLL dynamics during and after the fault.

It is expected that additional improved indicators will be developed in the future by industry and academia to further assess the stability of converters as well as to also include the contribution of grid forming inverters in the system strength. Therefore, the benefits of grid forming capability as offered by HVDC could be more easily quantified using such stability indicators.

### 6.3.3. Selection of operating conditions

In section 5.5, two clustering techniques have been proposed. The first one, based on K-means, allows to reduce the number of operating conditions for which the stability KPIs have to be estimated. It is recommended to use this clustering technique with a relatively high number of clusters. By doing so, the size of each cluster will be small and it can therefore be assumed that each point of the same cluster will have the same frequency or converter-driven stability performance. Therefore, it allows to simulate a single point within each cluster and then to weight the values obtained by the cluster size. This clustering technique is used for the 2-area frequency stability and for the IBR-CCT assessment.

---

<sup>7</sup> The CIGRE WG C4.60: "Generic EMT-Type Modelling of Inverter-Based Resources for Long Term Planning Studies" is trying to fill the gap and to propose EMT models to be used in long-term planning.

The second approach, based on DBSCAN, allows to identify more dense clouds of points. This should be used when it is required to evaluate more in details (e.g. redispatch, RMS or even EMT-simulations) extreme but yet representative operating conditions. Depending on the size of the clusters obtained via the DBSCAN method, it may be needed to simulate multiple points within each cluster (e.g. extremities).

## 7. Illustration on use cases

This chapter presents first the process for selecting the use cases. It can be seen in section 7.1 that each use case was selected for a particular reason (e.g. embedded HVDC within a single market zone, or HVDC link embedded into AC grid connecting two market zones, or HVDC link connecting two asynchronous areas, etc.). Therefore, the proposed KPIs were not calculated for all use cases. Instead, the goal is to test the implementation of our KPIs among the selected use cases. This is what is presented throughout sections 7.2 and 7.6. Finally, as this work focuses on implementation and modelling guidelines, the main challenges encountered during implementation and analysis of the use cases are presented in section 7.7.

### 7.1. Use case selection

#### 7.1.1. Goal and methodology

The main objective is to select relevant and representative use cases to which the developed extended CBA approach can be applied and tested.

Different steps, which are presented in the schematic overview of Figure 28, are taken to select the final set of use cases. The first step within this approach consists of creating a long list of use cases. The goal is to gather all kinds of projects which can be directly taken from the TYNDP2020 or PCI list (projects of common interest, updated in 2021) but also more academic use cases could be included. Moreover, also variations or combinations of projects (e.g., by adding an HVDC bootstrap to an AC grid, by connecting several PCIs or by connecting offshore windfarms to large load centres further inland) have been integrated as well. Study cases could therefore be fictive cases based on potential future initiatives.

In order to provide a structured overview of the possible projects within the long list, a first high-level classification on the proposed AC/DC systems is applied to split up the list depending on the topology. A preliminary long-list and classification is presented in more detail in section 7.1.2 of this report.

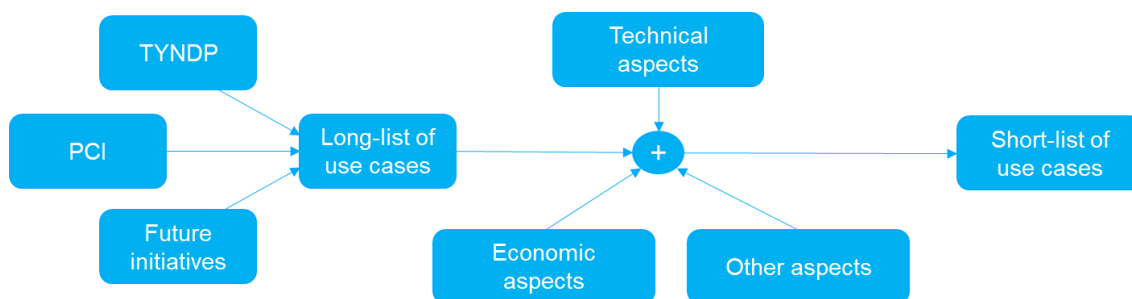


Figure 28 – Use case selection procedure

Next, a selection/screening process is used to narrowing down the long-list and come up with a limited number of relevant use cases. To this end, different selection criteria are defined which are converted to indicators allowing to rank use cases according to their relevance for the study. By applying such indicators, it is ensured that a diverse mix of uses cases is obtained, covering all important aspects (technical, economic, but also the time horizon/geographical aspects...).

To finally select the use cases, a transparent iterative process has been followed which involved regular interactions/discussions with the European Commission in order to make sure a common agreement is made on the selection of use-cases. In addition, a virtual

stakeholder workshop (31/03/2022) has been organized to present the list of selected use cases and to perform adjustments if needed in order to integrate reasoned stakeholders' feedback.

The screening and selection procedure are further elaborated in section 7.1.3 and the five use cases that were selected are described in more detail in section 7.1.4 of this report.

### 7.1.2. Step 1: Long-list of use cases

Numerous examples and uses cases of AC/DC hybrids grids can be found within the TYNDP and PCI list for the short-term time horizon (i.e., commissioned by 2030). In case also the long-term horizon (i.e., 2050) is considered and more academic test cases are considered as well, the number of possible uses cases to select from becomes even higher.

Therefore, instead of arbitrarily adding all projects to the long list, it is chosen to already perform a preselection and to create a well-structured long list which provides a good mix in terms of topology set-up and geographical spread (e.g., South, North, East, Central). To split up the list according to topology, the classification as presented in Figure 29 is applied. As illustrated, HVDC systems are split up in point-to-point connections (PtP) and HVDC grids, which are then further divided into embedded and asynchronous systems. For asynchronous HVDC grids, a further subclassification is defined depending on whether a radial connection or a meshed/interlinked PtP is used. Interlinked PtP is referred to the case where the main (offshore) network is operated in AC with DC links to the surrounding power systems (see also North Sea Wind Power hub for instance). As such, five main topology categories were obtained.

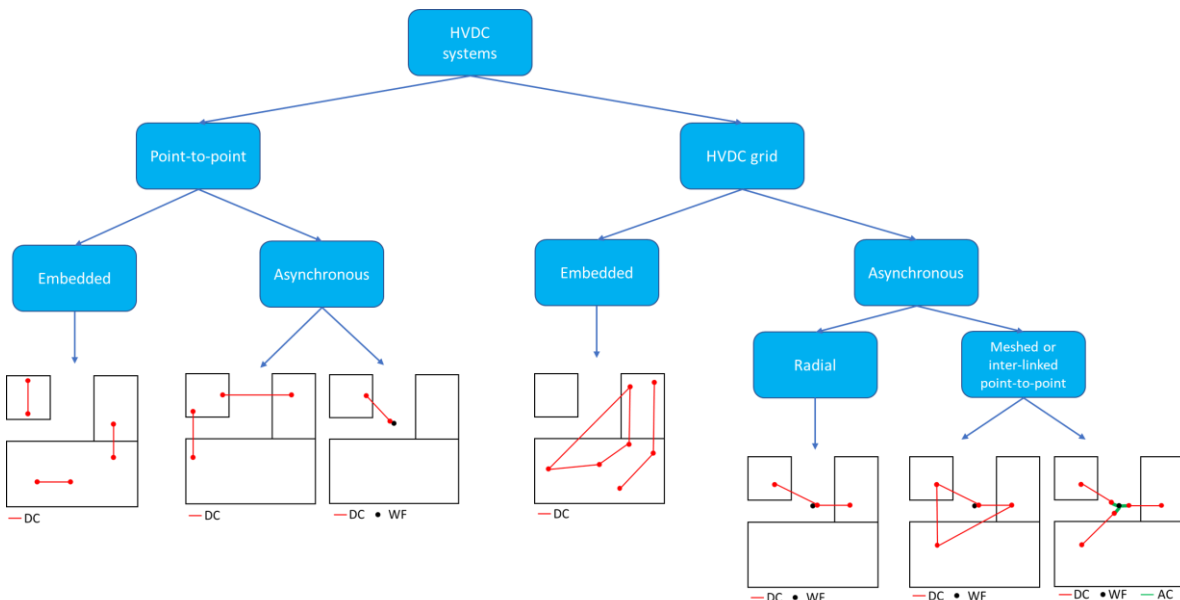


Figure 29 – Topology classification applied to the long-list of use cases (note: if there is even a single offshore WF connected to the HVDC grid, it is considered asynchronous since there is the possibility of frequency support)

The long list, consisting of 15 use cases covering all topology categories and the different areas in Europe, is presented in Table 12. It must be noted that the list is predominantly based on the projects from the ENTSO-E TYNDP 2020. The geographical location and spread of the cases are finally indicated on a map of Europe as given in Figure 30.

**Table 12 - Long list of use cases**

<b>Topology category</b>	<b>Use case</b>	<b>Short description</b>
Embedded PtP	1. Slovenia-Italy link	<p>The project consists of a new HVDC link of 800 MW between Salgareda (Italy) and Divaca/Bericevo (Slovenia) which is planned to be commissioned around 2028.</p> <ul style="list-style-type: none"> <li>• PCI number 3.21 (4<sup>th</sup> list, 31 Oct. 2019)</li> <li>• TYNDP 2020: Project nr. 150</li> </ul>
	2. HVDC SuedOstLink	<p>2 GW HVDC-connection from North-East Germany (Area of Wolmirstedt), an area with high installed capacities of RES, to the South of Bavaria (area of Isar), an area with high consumption and connections to storage capabilities (commissioning foreseen in 2025).</p> <ul style="list-style-type: none"> <li>• PCI number 3.12 (4<sup>th</sup> list, 31 Oct. 2019)</li> <li>• TYNDP 2020: Project nr. 130</li> </ul>
	3. Navarra-Landes Link	<p>A new HVDC interconnection (2x1000 MW) between the Western part of the Pyrenees between Pamplona area (Spain) and Cantegrat (France). The project is foreseen to be commissioned in 2029.</p> <ul style="list-style-type: none"> <li>• PCI number 2.27.2 (4<sup>th</sup> list, 31 Oct. 2019)</li> <li>• TYNDP 2020: Project nr. 276</li> </ul>
	4. MONITA project	<p>The Italy-Montenegro (MONITA) interconnection project includes a new HVDC (LCC) subsea connection between Villanova (Italy) and Lastva (Montenegro). The project is foreseen to be commissioned in 2026 and will have a final capacity of 1.2 GW.</p> <ul style="list-style-type: none"> <li>• TYNDP 2020: Project nr. 28</li> </ul>
Asynchronous PtP	5. Celtic interconnector	<p>Celtic Interconnector will be the first interconnection between Ireland and France. A survey of the route of the HVDC (VSC) link with 700 MW capacity has been done from the southern coast of Ireland to La Martre (Finistère) in France. Interconnection is foreseen to be commissioned in 2026.</p> <ul style="list-style-type: none"> <li>• PCI number 1.6 (4<sup>th</sup> list, 31 Oct. 2019)</li> </ul>

<b>Topology category</b>	<b>Use case</b>	<b>Short description</b>
		<ul style="list-style-type: none"> <li>TYNDP 2020: Project nr. 107</li> </ul>
	6. TUN.ITA.	<p>The project consists of a new interconnection between Tunisia and Sicily to be realized through an HVDC submarine cable with a capacity of 600 MW. The project is foreseen to be commissioned in 2027.</p> <ul style="list-style-type: none"> <li>PCI number 3.27 (4<sup>th</sup> list, 31 Oct. 2019)</li> <li>TYNDP 2020: Project nr. 29</li> </ul>
	7. Viking DKW-GB	<p>2x700 MW HVDC subsea link across the North Seas between Bicker Fen (GB) and Revsing (DK). The project is foreseen to be commissioned in 2023.</p> <ul style="list-style-type: none"> <li>PCI number 1.14 (4<sup>th</sup> list, 31 Oct. 2019)</li> <li>TYNDP 2020: Project nr. 167</li> </ul>
	8. TuNur	<p>TuNur aims at connecting a Concentrated Solar Power plant with storage (total capacity &gt;2000 MW) located in Rejim Maatoug (Kebili, Tunisia) to the Continental European power system. The connection point in Europe is located in Montalto di Castro, North of Rome. The transmission project will consist of a DC overhead line in Tunisia from the power plant to the shoring point and submarine cables from the Tunisian Northern coast to Italy. Project is aimed to be finalized around 2028.</p> <ul style="list-style-type: none"> <li>TYNDP 2020: Project nr. 283</li> </ul>
Embedded MTDC	9. Ultranet + A-North	<p>Ultranet together with A-North form a large-scale transmission link from the North Sea coast to Baden-Württemberg.</p> <p>The Ultranet project consists of a 2 GW HVDC-connection from the Region of Osterath (Rhineland) to the Region of Philippsburg (Baden-Württemberg) and is planned to be commissioned in 2024.</p> <p>A-North on the other hand consists of two new HVDC cables from Emden-East to Osterath. This HVDC link also has a transfer capacity of 2 GW and is planned to be finalized in 2025.</p>

<b>Topology category</b>	<b>Use case</b>	<b>Short description</b>
		<ul style="list-style-type: none"> <li>• PCI number 2.9 (Ultranet) (4<sup>th</sup> list, 31 Oct. 2019)</li> <li>• TYNDP 2020: Project nr. 254 (Ultranet) and nr. 132 (A-North)</li> </ul>
Asynchronous MTDC (radial grid)	10. EuroAsia interconnector	<p>HVDC interconnector between Crete, Cyprus and Israel (Consisting of two stages: final capacity of 2 GW). Interconnection is foreseen to be commissioned in 2026. It is also planned to form a four-terminal MTDC grid in the future with the HVDC link of the Ariadne HVDC connection between Attica and Crete</p> <ul style="list-style-type: none"> <li>• PCI number 3.10 (4<sup>th</sup> list, 31 Oct. 2019)</li> <li>• TYNDP 2020: Project nr. 219</li> </ul>
	11. MaresConnect	<p>MaresConnect is a 750MW HVDC VSC Interconnector between Great Britain and Ireland with three node connections; (i) Bodelwyddan (Wales), (ii) Maynooth (Dublin area, Ireland) and (iii) Bellacorick new node (Mayo area, Ireland). Project is foreseen to be commissioned in 2025.</p> <ul style="list-style-type: none"> <li>• TYNDP 2020: Project nr. 349</li> </ul>
	12. LaSGo Link	<p>LaSGo Link is a new multi terminal HVDC sub-sea interconnector project linking Sweden, the Island of Gotland and Latvia. The project consists of two sections: a 700MW internal grid reinforcement between the Swedish mainland and the island of Gotland and a 500MW cross border connection between the island of Gotland and Latvia. Interconnection is foreseen to be commissioned in 2036.</p> <ul style="list-style-type: none"> <li>• TYNDP 2020: Project nr. 1068</li> </ul>
	13. Nautilus	<p>This project considers the possibility of a multi-purpose HVDC between GB and Belgium with also interconnecting offshore wind farms. The capacity of the is still under review, but is likely to be in the range of 1 GW – 2GW. The project is foreseen to be commissioned in 2028.</p> <ul style="list-style-type: none"> <li>• TYNDP 2020: Project nr. 121</li> </ul>

Topology category	Use case	Short description
Asynchronous MTDC (Meshed grid or interlinked point-to-point grid)	14. MTDC multi-country backbone	Large meshed (asynchronous) HVDC grid connecting different member states which is foreseen on the long-term (i.e. 2050 horizon). A stepwise approach could be taken in which the existing HVDC projects from the 2030 horizon are linked together to form a single meshed system.
	15. North Sea Wind Power Hub (NSWP)	North Sea Wind Power Hub is an international consortium, run by TenneT (Germany), Energinet (Denmark), Gasunie (Netherlands) and Port of Rotterdam (Netherlands), which goal is to develop several farms in the North Sea that are connected to an artificial island (i.e. AC power hub) which has HVDC interconnections to surrounding countries. Foreseen timeline for construction is 2030-2050.

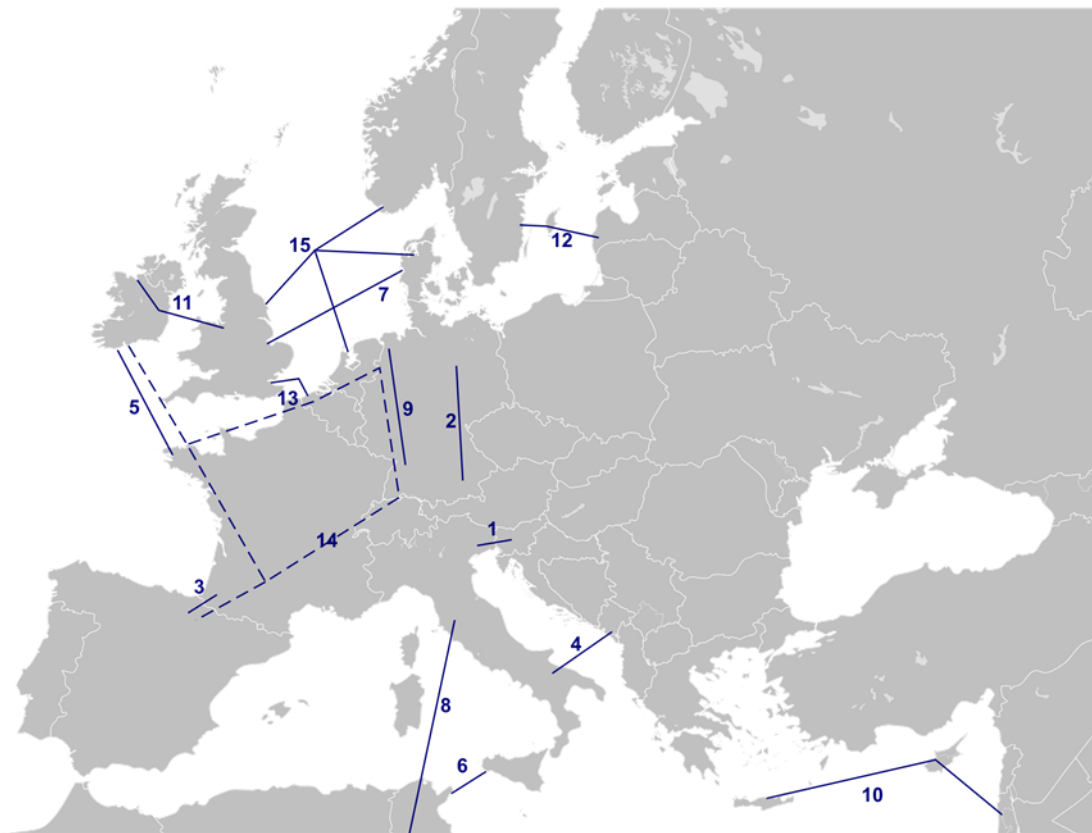


Figure 30 – Geographical location of the different use case from the long-list

### 7.1.3. Step 2: Screening

As previously introduced, the screening process to go from long-list to short-list is done by applying indicators which allow to rank and select use cases according to their relevance for the study. As such, it is ensured that with a limited number of use-cases, all relevant aspects within the scope of this study are covered. In the following subsections, the different indicators are introduced and applied to the long-list of uses cases.

#### 7.1.3.1. Technical indicators

The main technical indicator used in this study is the topology category as defined in the classification of Figure 29. No specific preference is given to a certain set-up, but instead it is aimed to have a good mix of HVDC grids and PtP connections as well as both embedded and asynchronous HVDC connections within the final short-list.

#### 7.1.3.2. Economic indicators

The aim of the economic indicators is to evaluate the additional benefits from HVDC systems through specific capabilities/services to the AC system. These services/capabilities are described in more detail in the previous chapters. For each of the use cases in the long list, a grade of 0 to 5 is assigned to each service depending on the benefit that is expected to be obtained. For example, a grade of 5 for the frequency regulation capability means that significant benefit is expected by considering this service in the CBA. On the other hand, a grade of 0 indicates that the benefit would be negligible.

It has to be noted that in the context of the use case selection, there has been no detailed calculation of the benefit from each service. Instead, this is only a preliminary assessment based on simplified rules, used exclusively for the screening of the use cases. The aim is to make an “educated guess” and to choose the use cases in which including the new services from HVDC would lead to a change in the CBA. The simplified rules are described hereafter:

- **Frequency regulation**
  - For embedded connections there is no benefit
  - For asynchronous point-to-point connections between an area and remote generation some limited benefit is expected
  - For asynchronous point-to-point connections between two areas significant benefit
  - For asynchronous MTDC grids the benefit can be higher depending on the number of connected synchronous areas
- **Voltage regulation:**
  - Embedded point-to-point can provide benefits in voltage regulation through the use of active and reactive power
  - Embedded MTDC grids can provide even better benefits (more options)
  - Asynchronous point-to-point can provide mainly local reactive power regulation (benefit from redirection of active power flow more difficult to assess)
  - The benefits from asynchronous MTDC grids depend on whether they provide parallel paths to AC lines
- **Blackstart:**
  - Very limited and difficult to assess benefit from embedded point-to-point connection
  - Similar benefit from embedded MTDC grids, however the existence of multiple connections provides more options
  - For asynchronous point-to-point connections between an area and remote generation no benefit is expected
  - For asynchronous point-to-point connections between two areas significant benefit

- For asynchronous MTDC grids the benefit can be even higher depending on the number of connected synchronous areas
- **Power flow control:**
  - Similar to the voltage regulation, embedded point-to-point and MTDC grids provide significant benefits
  - Point-to-point connections provided limited benefits
  - The benefits of asynchronous MTDC grids depend on the number of connections and on whether alternative paths to the AC network are provided.
- **Grid forming control:**
  - The benefit from grid forming control in a point-to-point connection between an area and a remote generation (usually offshore wind farm) is expected to be low. In such cases, there is already one grid forming converter (offshore converter), hence it is still unclear whether the onshore one can reliably operate also as grid forming.
  - In all the other cases, the grading depends on a case-by-case basis. In general, if an islanded network is included in the configuration (e.g. Cyprus, Ireland) a higher benefit is expected.

The afore-mentioned rules are summarized in Table 13, where the resulting grades for each topology are also given:

**Table 13 - Preliminary assessment of benefits from HVDC services/capabilities**

HVDC capability	Embedded PtP	Embedded MTDC	Asynchronous PtP		Asynchronous MTDC (radial)	Asynchronous MTDC (meshed)
			Between area and remote generation/load	Between two areas		
Frequency regulation	0	0	2	3	3 to 5	3 to 5
Voltage regulation	4	5	2	2	2 to 5	2 to 5
Black start	1	2	0	3	4 to 5	4 to 5
Power flow control	3	4 to 5	1	2	2 to 5	2 to 5
Grid forming	To be defined on a case-by-case basis	To be defined on a case-by-case basis	1	To be defined on a case-by-case basis	To be defined on a case-by-case basis	To be defined on a case-by-case basis
Total score	8 to 13	11 to 17	6	10 to 16	11 to 25	11 to 25

The following observations are made based on the grading of topologies:

- Embedded configurations are expected to provide benefits in terms of voltage regulation and power flow control
- Connection between asynchronous areas provides higher benefits in terms of frequency regulation and black-start services
- More complex HVDC topologies will in general provide more benefits by combining different aspects

These general rules are then applied to the use cases of the long list, see in Table 25 in Appendix II: use case selection. The sum of the grades for the different benefits is applied to rank the use cases and finally select the ones with a high total score.

### 7.1.3.1. Other indicators

Finally, some other indicators were added to the screening process, namely a geographical and a time horizon indicator. The geographical indicator has been applied to make sure that the final use cases cover the different parts of Europe (i.e., to avoid that all use cases are for instance located in countries around the North Sea) and to ensure that also at least one use case with a connection external to Europe is included.

Looking at the time horizon, it is important to note that some of the operational challenges in power systems, such as operation with reduced grid strength (low inertia and low short-circuit power), are expected to become more prominent on a longer time horizon (i.e., 2050). The corresponding benefits from HVDC (e.g., grid forming capability in this case) are therefore also more relevant/important in the future power system compared to its application today. Therefore, to illustrate/capture these benefits within a CBA analysis, it is proposed to have at least one 2050 (long-term) use case.

An assessment of the use cases within the long list applying these additional indicators is presented in Table 14.

**Table 14 - Assessment of long list considering time horizon and geographical aspects (N=North, E=East, S=South, W=West, C=central)**

Use case	Geographical location within Europe	External connection	Time horizon
1. Slovenia-Italy link	CS	No	2030 (short-term)
2. HVDC SuedOstLink	NC	No	2030 (short-term)
3. Navarra-Landes Link	SW	No	2030 (short-term)
4. MONITA project	SW	No	2030 (short-term)
5. Celtic interconnector	NW	No	2030 (short-term)
6. TUN.ITA.	S	Yes	2030 (short-term)
7. Viking DKW-GB	N	No	2030 (short-term)
8. TuNur	S	Yes	2030 (short-term)
9. Ultranet + A-North	NC	No	2030 (short-term)
10. EuroAsia interconnector	ES	Yes	2030 (short-term)
11. MaresConnect	NW	No	2030 (short-term)

12. LaSGo Link	NE	No	2030 (short-term)
13. Nautilus	NW	No	2030 (short-term)
14. MTDC multi-country backbone	N/E/S/W/C	No	2050 (long-term)
15. North Sea Wind Power Hub (NSWP)	NE	No	2050 (long-term)

#### 7.1.4. Step 3: short-list of use cases

Using the indicators and the assessment of uses cases presented in the long list, five use cases were finally selected:

- 1. Navarra-Landes link**
- 2. Celtic interconnector**
- 3. Ultranet+A-North**
- 4. EuroAsia Interconnector**
- 5. MTDC multi-country backbone**

As highlighted in the table below, the different aspects are well covered by these five uses cases. Looking at the additional benefits (i.e., economic indicator), they all have a medium to high score (adding up the grades given in section 7.1.3.2) and each of the 5 topology categories is represented. Additionally, the geographical locations of the use cases are more or less spread over Europe and there is even one including an external connection. Finally, considering the time horizon, both use cases planned to be built in the short-term (2030) and the long-term (2050) are included in the list. In the following subsections, each of the use cases from the short-list is described in more detail.

**Table 15 - Short-list of use cases and a summary of the different indicators**

	Additional benefits from AC/DC			Topology category				Time horizon		Geographical location				External connections			
	Low (0-8)	Medium (8-16)	High (>17)	Emb. PtP	Asyn. PtP	Emb. MTDC	Asyn. MTDC Radial	Asyn. MTDC Meshed	2030	2050	N	E	S	W	C	Y	N
Navarra-Landes Link	High	Medium	Low	Low	Medium	Low	Low	Low	High	Medium	Medium	Medium	Medium	Medium	Medium	Yes	No
Celtic interconnector	Medium	Low	Low	Low	Low	Low	Low	Low	Medium	Medium	Medium	Medium	Medium	Medium	Medium	Yes	No
Ultranet + A-North	Medium	Low	Low	Low	Low	Low	Low	Low	Medium	Medium	Medium	Medium	Medium	Medium	Medium	Yes	No
EuroAsia interconnector	Medium	Low	Low	Low	Low	Low	Low	Low	Medium	Medium	Medium	Medium	Medium	Medium	Medium	Yes	No
MTDC multi-country backbone	Medium	Low	Low	Low	Low	Low	Low	Low	Medium	Medium	Medium	Medium	Medium	Medium	Medium	Yes	No

#### 7.1.4.1. Navarra-Landes Link

**Description:** A new HVDC interconnection (embedded PtP) between the Western part of the Pyrenees between Pamplona area (Spain) and Cantegrit (France).

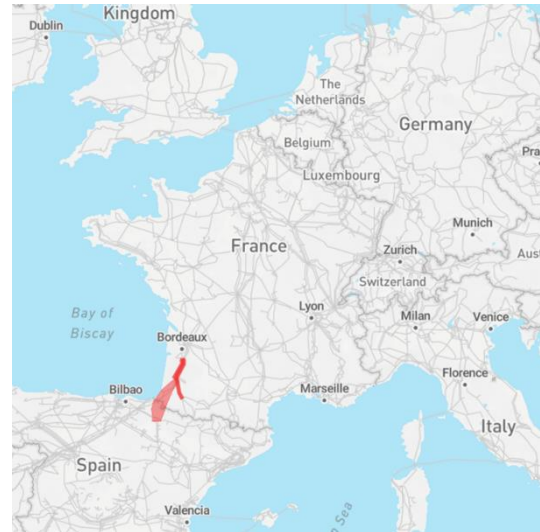
**Capacity:** 2000 MW

**Commissioning year:** 2029

**Promotors:** REE & RTE

**Why is this a good case?**

- Benefits expected from power flow control and voltage regulation



#### 7.1.4.2. Celtic Interconnector

**Description:** Celtic Interconnector will be the first interconnection between Ireland and France. A survey of the route of the HVDC (VSC) link has been done from the southern coast of Ireland to La Martre (Finistère) in France.

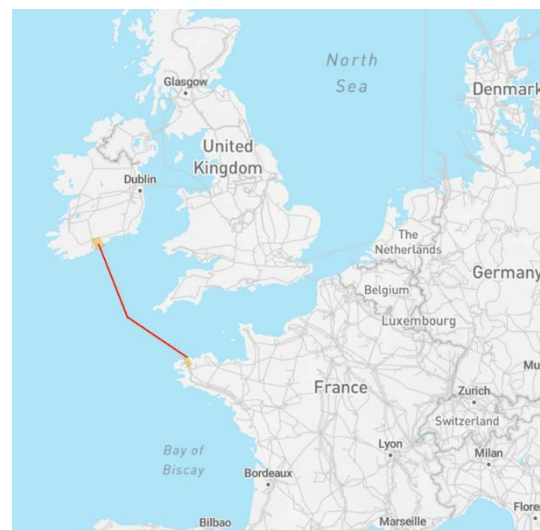
**Capacity:** 700 MW

**Commissioning year:** 2026

**Promotors:** EIRGRID & RTE

**Why is this a good case?**

- Frequency services by HVDC can be important for Ireland especially with RES penetration
- A good case for blackstart
- Grid forming might play an important role due to Ireland being an islanded system



### 7.1.4.3. Ultranet + A-North

**Description:** Ultranet together with A-North form a large-scale transmission link (so-called “Corridor A”) from the North Sea coast to Baden-Württemberg to channel wind energy from the north past the grid in the Rhineland and down to the south.

**Capacity:** 2000 MW

**Commissioning year:** 2024-2025

**Promotors:** AMPRION & TRANSNET BW

**Why is this a good case?**

- Combination of two embedded PtP projects: only embedded MTDC for 2030
- Probably a good use case to demonstrate the benefits of power flow control and voltage regulation by HVDC



### 7.1.4.4. EuroAsia Interconnector

**Description:** HVDC interconnector between Crete, Cyprus and Israel. It is also planned to form a four-terminal MTDC grid in the future with the HVDC link of the Ariadne HVDC connection between Attica and Crete.

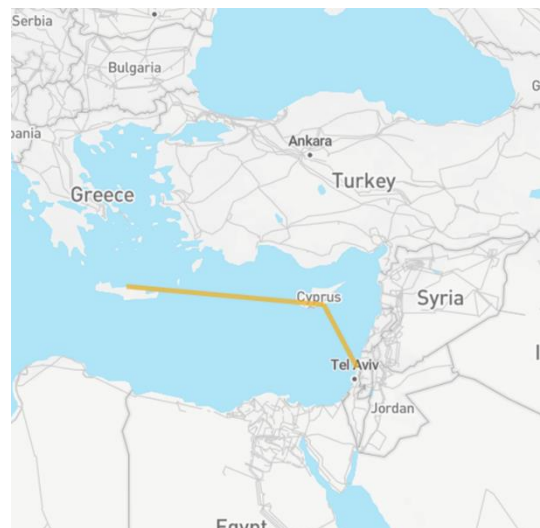
**Capacity:** 2000 MW

**Commissioning year:** 2026

**Promotors:** EuroAsia interconnector Ltd.

**Why is this a good case?**

- Includes external connection
- South-Eastern Europe (geographical indicator)
- Another good case for frequency regulation, grid forming and black-start considering that it involves the isolated island of Cyprus and the weakly connected island of Crete



### 7.1.4.5. MTDC multi-country backbone

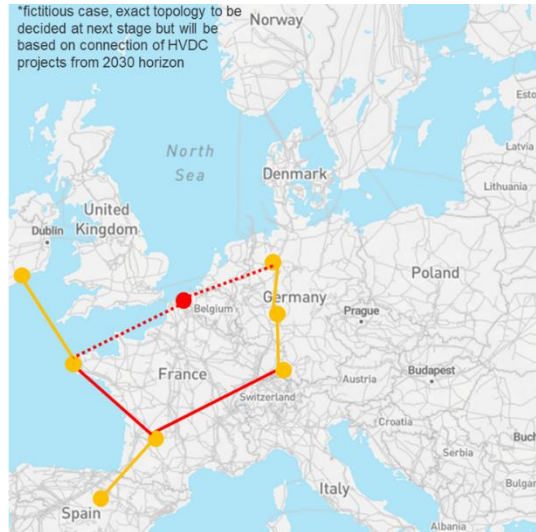
**Description:** Large meshed (asynchronous) HVDC grid connecting different member states. A stepwise approach could be taken in which the existing HVDC projects from the 2030 horizon are linked together to form a single meshed system.

**Capacity:** Not yet known

**Commissioning year:** Long-term horizon (2050)

**Why is this a good case?**

- Large MTDC connection among multiple countries
- Benefits for 2050 are expected to be significant since it connects multiple countries
- The number of connections can provide benefits with all kinds of services: grid forming, and power flow control can be significant



The subset of the use cases identified have been analysed to demonstrate the usefulness of the enhanced CBA methodology outlined throughout Chapter 5. The main objective of the following sections is to quantify benefits of HVDC technology with respect to system stability improvement and power flow controllability in a realistic setting. To that end, rather than determining all additional KPIs of the enhanced method on all use cases, certain use cases have been selected to demonstrate the relevant KPIs, as not all potential benefits of HVDC technology will have a significant effect on all types of networks. For instance, the stability improvement through HVDC technology is more relevant for asynchronously connected networks, whereas the benefits of power flow controllability are more relevant for uses cases with embedded HVDC links.

## 7.2. Navarra Landes

### 7.2.1. Assessment of techno-economic KPIs

#### 7.2.1.1. Overview of implementation, models and data used

This test case has been used to validate the NTC based zonal dispatch model, in order to investigate the sensitivities with respect to the capacity increase in RES generation as well as the increase in transmission capacity and how this is translated to socio-economic welfare and emission reduction benefits.

The Navarra Landes interconnector aims to increase the power transfer capacity between France and Spain by 1500 MW. The NTC based zonal economic dispatch model as introduced in section 6.2.1 is used to calculate the socio-economic KPIs. The calculations have been performed for the base case without the NTC increase between the French and the Spanish zone, and the case with the investment. As the NTC based model uses an aggregated capacity between both zones, in the case with the investment, the base case capacity is increased by 1500 MW, although the rating of the interconnector itself is 2000 MW.

The zonal TYNDP model consists of 64 market zones, where each market zone is representing 55 different types of generators, of which 53 are actual generators, 1 generator representing demand response, and one generator representing energy not served. The used generation cost data is provided in the appendix.

### 7.2.1.2. Simulations performed

The zonal model with and without interconnector is simulated for an entire year (8760 hours) for both GA2030 and GA2040 scenarios from the ENTSO-E TYNDP, for the climate year 2007 in both scenarios.

### 7.2.1.3. Comparisons of relevant KPIs without the project, with the project (CBA methodology) and with the project (proposed CBA)

Table 16 summarizes the KPIs for the zonal model when the Navarra – Landes interconnector is included in the European grid. The benefit in the socio-economic welfare obtained through the NTC based zonal dispatch model is 468 MEUR for the global ambition scenario (GA) 2030 and 532 MEUR for the GA2040 scenario. The difference between the two scenarios is mainly attributed to the installed renewable generation (solar PV, onshore and offshore wind) in Spain, which is 76.4 GW in 2030 and 114.95 GW in 2040, respectively. Figure 31 shows the interconnector flows for the GA2030 scenario.

Counterintuitively, the CO<sub>2</sub> emissions related to the French and Spanish zones do not have a similar decrease even though there is a higher RES integration. Although there is maximum export of renewable energy from Spain to France<sup>8</sup> as shown in Figure 31, the benefits of the CO<sub>2</sub> emission reduction do not increase to the same extend as the RES integration does. This is mainly attributed to the reduction of nuclear generation in France, where the installed capacity is 56.6 GW in 2030 and 37.2 GW in 2040, according to the scenario data.

A second effect that can be observed is that not all CO<sub>2</sub> emission benefits are achieved in Spain or France through the extension of the transfer capacities between both countries. The total emission CO<sub>2</sub> reduction across Europe is 495 kton / year through the capacity increase, where the emission reduction in Spain and France adds up to 264 kton / year as indicated in the table below. Thus the interconnector contributes to CO<sub>2</sub> reductions also in other market zones, owing it to the objective function where the generation cost (which is higher for non RES generation) is minimized over all market zones.

In Figure 31, we can see the interconnector flows in function of the total RES generation in both Spain and France. We observe that, for situations with the highest RES generation levels, the interconnector flows are from Spain to France as expected.

---

<sup>8</sup> Positive sign of the interconnector power flow indicates flows from France to Spain and vice versa

**Table 16 - Computed KPIs for the Navarra-Landes interconnector, zonal model, GA scenario for years 2030 and 2040, climate year 2007**

KPIs	GA2030, cy 2007			GA2040, cy 2007		
	No investment	Investment	Benefit	No investment	Investment	Benefit
B1 – Socio-economic welfare - all market zones	170.93 bn€	170.46 bn€	468 M€	186.12 bn€	185.58 bn€	532 M€
B2 – CO2 emissions [Mton/yr]	12.27	12.00	0.27	10.68	10.46	0.22
B3 – RES integration [TWh]	265.87	271.02	5.15	339.07	342.86	3.79
B4 – NOx emissions [kton/yr]	19.49	20.00	- 0.51	15.54	15.81	- 0.27
B4 – SOx emissions [ton/yr]	384.09	394.28	- 10.19	306.19	311.70	- 5.51
B6 – Adequacy, ENS [MWh/yr]	0	0	0	5.44	5.44	0

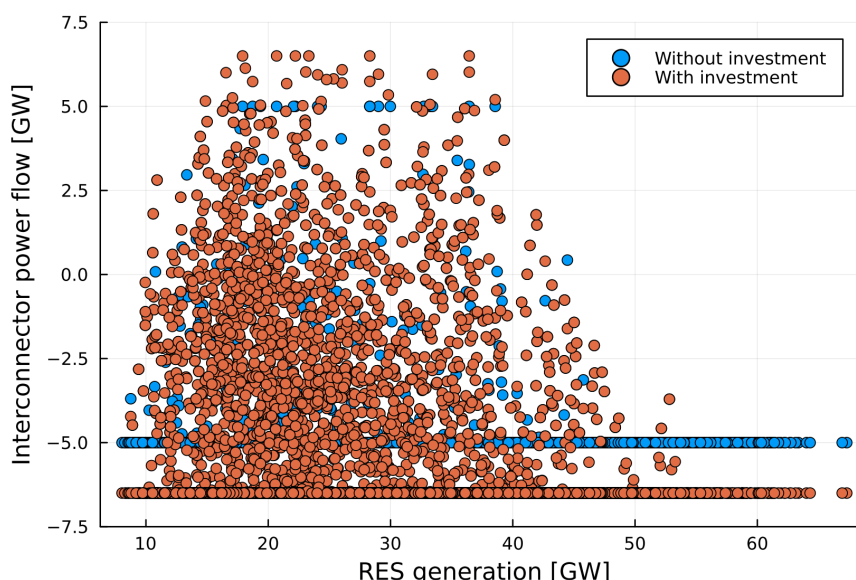


Figure 31-Comparison between the power flow between France and Spain with and without the Navarra-Landes interconnector for different RES generation levels, GA2030, climate year 2007

## 7.3. Celtic interconnector

### 7.3.1. Assessment of techno-economic KPIs

#### 7.3.1.1. Overview of implementation, models and data used

Using the Celtic interconnector, we want to demonstrate mainly two aspects. Firstly, the obtained socio-economic welfare benefits using an NTC based dispatch model versus using an optimal power flow (OPF) model can differ significantly, as the OPF model is capable of considering the internal congestion. Secondly, Ireland being an island, the effect of decreasing inertia due to RES integration will have more severe impact, and connected to that, the benefits provided through HVDC by means of inertia support are expected to be significant. In this use case, we make use of both the NTC based zonal and the nodal OPF models for the calculation of the social welfare benefits and quantify the effects of considering internal congestion. In the same way, we perform the zonal dispatch and nodal redispatch OPF models by introducing inertia constraints as outlined in section 6.2.3 to calculate the benefits through inertia provision through HVDC, with an approximate zonal approach and a detailed nodal approach.

For the zonal calculations we use the zonal TYNDP model consisting of 64 market zones, where each market zone is representing 55 different types of generators, of which 53 are actual generators, 1 generator representing demand response, and one generator representing energy not served. The used generation cost data is provided in Appendix III. This results in 3520 generators in total. The 64 market zones are connected by 119 interconnections. For the hourly dispatch calculations, the hourly demand time series from ENTSO-E and RES capacity factor time series from the European climate database are used. Both time series are given for a number of climate years, with an hourly resolution.

As for the nodal model, the ENTSO-E nodal grid model has been used. For the case of the Celtic interconnector, the French grid model consists of, 2764 nodes, 3680 branches (including transformers and breakers), 3556 generators and 8 HVDC links, whereas the Irish grid model consists of 2324 nodes, 2874 branches (including transformers and breakers), 672 generators and 2 HVDC links. In the next section further information is provided on the particular calculation methodologies, and the usage of the grid models within.

#### 7.3.1.2. Simulations performed

In order to compare the socio-economic welfare KPIs, first the NTC based zonal model is used without and with the Celtic interconnector and the KPIs have been calculated for each case separately. As it is computationally too expensive to perform the nodal model on the full scale European network, only the French and the Irish networks have been modelled in detail whereas their power exchanges with their respective neighbouring market zones are approximated using the outcome of the zonal dispatch model. To that end, the following approach has been used. First, the exchanges between the France and Ireland and their respective neighbouring countries have been assumed to be equal to the exchanges obtained through the zonal model. As in the nodal model, all interconnecting lines are modelled in detail, an additional constraint is implemented within the OPF model outlined in section 6.2.2, which states that the sum of all power flows on the interconnectors with a neighbouring market zone, need to be equal to the interconnector flow determined with the zonal model. This way we ensure the consistency between the two models.

Secondly, the nodal ENTSO-E model provides only one operational condition, e.g. one operating hour. To be able to consistently use the demand and RES time series of the

zonal model within the nodal model, a model disaggregation is performed. The aggregated total demand coming from the zonal model is distributed pro rata among the loads in the nodal model. In the same way, the total installed generation capacity, and capacity factors of RES generators are disaggregated pro rata, based on the generator ratings provided in the nodal model.

Figure 32 visualizes the calculation procedure for the zonal and nodal models and shows the model interactions.

To perform inertia constrained dispatch calculations, following approach is used as also described in Figure 33. First, using the zonal model including the Celtic interconnector, inertia constraints for the French and Irish networks are introduced using the methodology described in section 6.3, where the required inertia is determined based on the rate of change of frequency. This is done for two cases, namely for the case that the Celtic interconnector provides inertial/fast-frequency support and for the case that it does not. For both inertia constraints, the NTC based zonal *dispatch* model is extended by the inertia constraint as described 6.2.3 and the zonal calculations are performed. This way, the additional benefits of inertia provision through HVDC is determined. As the zonal model uses one aggregated generator for each type of generation per country, the inertia constraint in the zonal model is defined as

$$\sum_{g \in G} P_{g,z} \cdot H_g \cdot \alpha_g \geq H_z^{min} \quad \forall z \in Z$$

using the actual dispatch of each type of generator  $P_{g,z}$  as opposed to the installed capacity of the generator as described in section 6.2.3. Note that the objective of this optimisation model is the minimization of the generation dispatch cost as opposed to the nodal redispatch optimisation as described below.

Additionally, the inertia constrained *redispatch* OPF model is performed for the nodal model. The rationale therefore is that after performing the nodal OPF calculations, the generation dispatch is obtained per generating unit, and such, it is known which generators are online for any given operational hour. Thus, by performing the inertia constrained *redispatch* OPF, we can approximate the value of reserves that TSOs would have to commit to ensure frequency stability. In this case, as optimisation objective the *start-up costs of generators are minimized*, which can be one to two orders of magnitude higher than the fuel costs. Additionally, as the nodal redispatch OPF model is computationally expensive, this calculation has been performed for a selected number of operational points using the clustering approach described in section 5.5. As the nodal model can represent the power generation on the unit level, the original inertia constraint  $\sum_{g \in G} P_{g,z}^{rated} \cdot H_g \cdot \alpha_g \geq H_z^{min} \quad \forall z \in Z$  based on the rated power of online generators is enforced in the *redispatch* OPF.

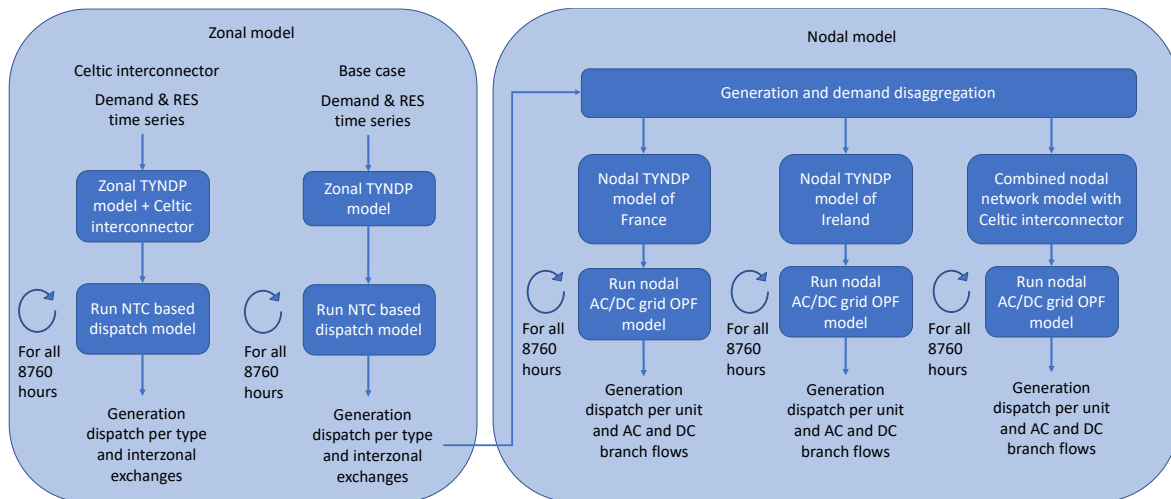


Figure 32 - Calculation procedure using zonal and nodal models and their interaction.

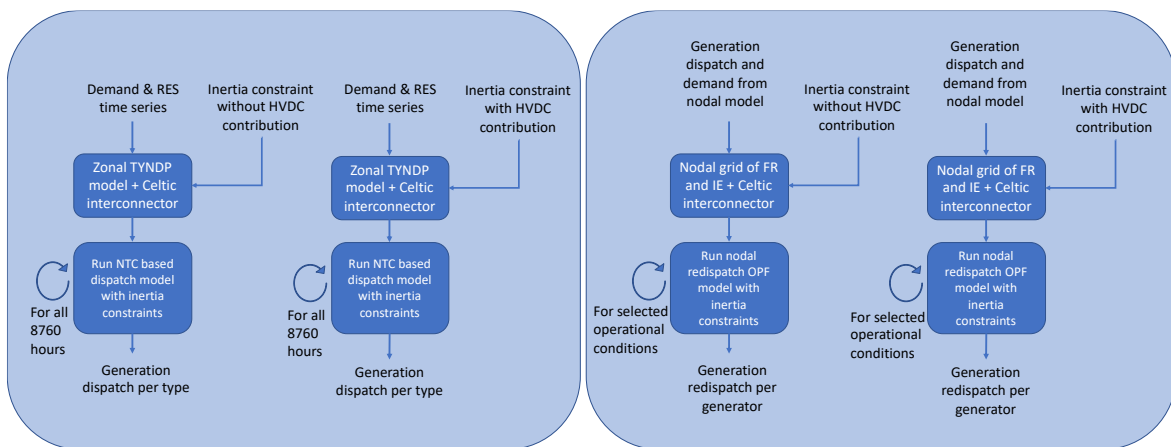


Figure 33 - Inertia constrained (re)dispatch calculations performed on zonal (left) and nodal (right) network models.

### 7.3.1.3. Comparisons of relevant KPIs without the project, with the project (standard CBA methodology) and with the project (proposed CBA)

Table 17 and Table 18 below show the computed KPIs for both the zonal and nodal model when the Celtic interconnector is included in the European power grid.

In the zonal model, the socio-economic welfare benefit brought by the investment increases over time. The social welfare obtained for the Global Ambition (GA) scenario for the planning year 2030 is 84.9 MEUR, and it is 114.7 MEUR for the GA2040 scenario. The results are comparable to the results in ENTSO-E's 2030 sustainable transition and distributed generation scenarios in 'Project 107 – Celtic interconnector' (<https://tyndp.entsoe.eu/tyndp2018/projects/projects/107>). The presence of the interconnector leads to an improvement in all KPIs, with all emissions (CO<sub>2</sub>, NOx and SOx) being reduced.

The nodal system, despite having higher computational requirements (roughly 24 hours for France and Ireland compared to 20 minutes for the whole European zonal grid), offers a deeper insight in the power grid. Aspects such as demand curtailment, demand reduction, physical congestions of the lines and grid stability can be investigated. In the nodal model, the improvement in the overall socio-economic welfare increases compared to the zonal one only for 2030. The main reason therefore is consideration of the internal

network congestion, which contains the integration of the cheaper RES resources, and leading to higher levels of demand reduction or curtailment than anticipated in the zonal model.

The nodal model indicates an increase in the CO<sub>2</sub> emissions and lower RES integration compared to the zonal one. This fact is related to the distributed nature of the RES generators. By not being aggregated in a single node, the power transmission constraints lead to an increased generation curtailment near the congested lines. Furthermore, Figure 34**Error! Reference source not found.** and Figure 35 show the relation between the RES generation in France and Ireland and respectively their demand reduction and demand curtailment for the scenario GA2030. The power exchange through the HVDC link reduces both in the intensity and frequency of demand reduction and demand curtailment events for the whole set of RES generation levels in the two countries. In fact, as shown by Figure 36, the Celtic interconnector is used at its full capacity of 700 MW for most of the hours independent of the RES generation in both directions alike.

**Table 17 - Computed KPIs for the Celtic interconnector, zonal model, GA scenario for years 2030 and 2040, climate year 2007**

KPIs	GA2030, cy 2007			GA2040, cy 2007		
	No investment	Investment	Benefit	No investment	Investment	Benefit
B1 – Socio-economic welfare – all market zones	170.93 bn€	170.85 bn€	84.92 M€	186.12 bn€	186.00 bn€	114.69 M€
B2 – CO <sub>2</sub> emissions [Mton/yr]	12.27	11.83	0.44	8.9	8.79	0.11
B3 – RES integration [TWh]	160.54	164.84	4.3	339.07	339.27	0.2
B4 – NOx emissions [kton/yr]	18.99	18.51	0.48	15.54	15.43	0.11
B4 – SOx emissions [ton/yr]	374.22	364.77	9.45	306.2	304.1	2.1
B6 – Adequacy, ENS [TWh/yr]	0	0	0	5.55	5.55	0

**Table 18 - Computed KPIs for the Celtic interconnector, nodal model, GA scenario for years 2030 and 2040, climate year 2007**

KPIs	GA2030, cy 2007				GA2040, cy 2007			
	FR	IE	FR_IE	Benefit	FR	IE	FR_IE	Benefit
B1 – Socio-economic welfare – FR and IE market zones	15.36 bn€	1.58 bn€	16.82 bn€	122.9 M€	16.16 bn€	15.0 bn€	17.56 bn€	105.9 M€
B2 – CO2 emissions [Mton/yr]	3.78	2.71	6.49	0	3.32	2.65	5.90	0.07
B3 – RES integration [MWh]	242.4	24.3	268.5	1.92	296.96	26.88	325.99	2.15
B4 – NOx emissions [kton/yr]	5778.1	3210.0	8972.3	15.8	5083.4	3151.5	8132.3	102.6
B4 – SOx emissions [ton/yr]	113.88	131.54	211.53	33.89	100.19	140.97	208.20	32.96
B5 – Grid losses [TWh]	13.92	2.02	16.21	- 0.27	15.49	2.29	18.44	- 0.66
B6 - Adequacy, ENS [GWh/yr]	0	0	0	0	0	0	0	0
Additional KPI – Demand curtailment [GWh]	0	206.90	27.96	178.94	0	55.30	2.32	52.98

Figure 34 provides another interesting insight. Considering that the objective of the optimal power flow calculation is to minimize the cost of generation, demand reduction and demand curtailment, we can observe that the demand reduction is being shifted from the Irish zone to the French system if both zones are interconnected, and thus the optimisation is performed on the interconnected system as a whole. The reason therefore is that the costs for demand reduction have been assumed to be the same in both networks, and as such on the system level no distinction between the countries are made. Looking at Figure 35, we can also observe that through the interconnection, the expected demand curtailment can be reduced by a significant amount (from 206.9 GWh to approximately 28 GWh as indicated in the above table), both in the Irish and the French grids. Again, there is a shift in demand curtailment from Ireland to France, owing it to the

price agnosticism of the model as through the interconnection the optimisation is performed on the combined network as a whole.

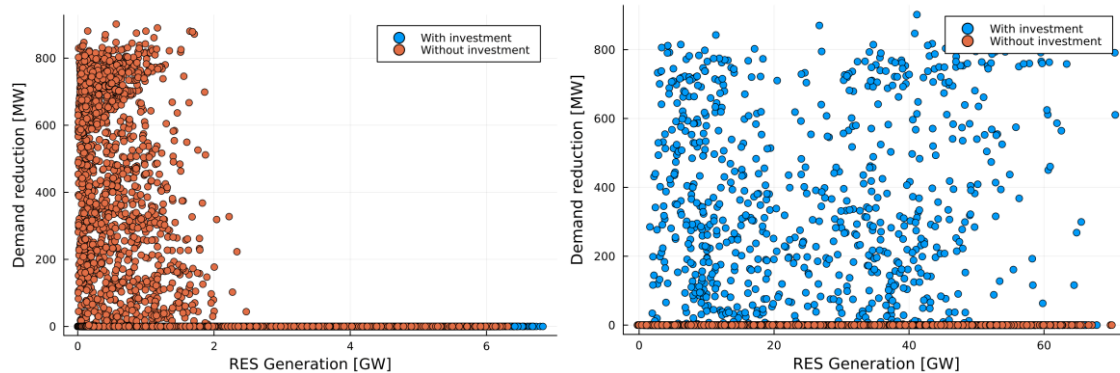


Figure 34 - Comparison between the demand reduction in Ireland (left) and France (right), with and without the Celtic interconnector for different RES generation levels, GA2030, climate year 2007.

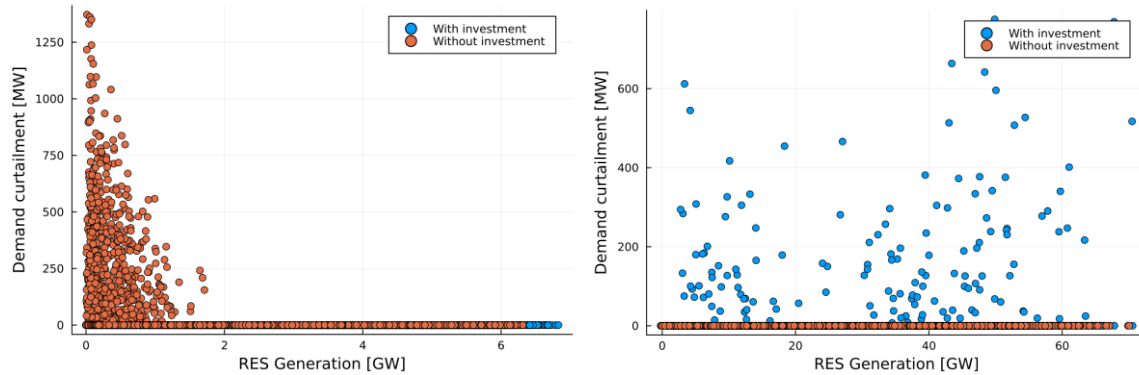


Figure 35- Comparison between the demand curtailment in Ireland (left) and France (right), with and without the Celtic interconnector for different RES generation levels, GA2030, climate year 2007.

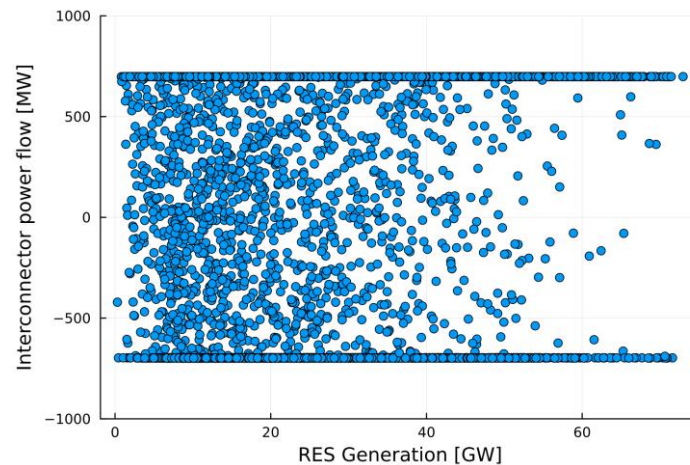


Figure 36 - Power flow through the Celtic interconnector for different RES generation levels, GA2030, climate year 2007.

The pattern seen for demand reduction and demand curtailment against RES generation in GA2030 is also observed in the GA2040 scenario, as shown in Figure 37 and Figure 38. The peak intensity of the demand reduction is higher for GA2040 though, with single instances reaching 1600 MW of demand reduction. Compared to the maximum value of 900 MW in GA2030, there is a 78% increase of the severity of the event. Demand reduction is as well more frequent in both cases with and without investment compared to

GA2030, owing it to the increased demand (~10% in total for France and Ireland), and the increase in RES generation.

In contrary, demand curtailment is greatly reduced in GA2040 compared to GA2030. The benefit through demand curtailment reduction is especially observed in situations with lower RES generation. In such cases, making use of the power exchanges through the interconnector, demand curtailment can be reduced to zero, which is not possible without the interconnector.

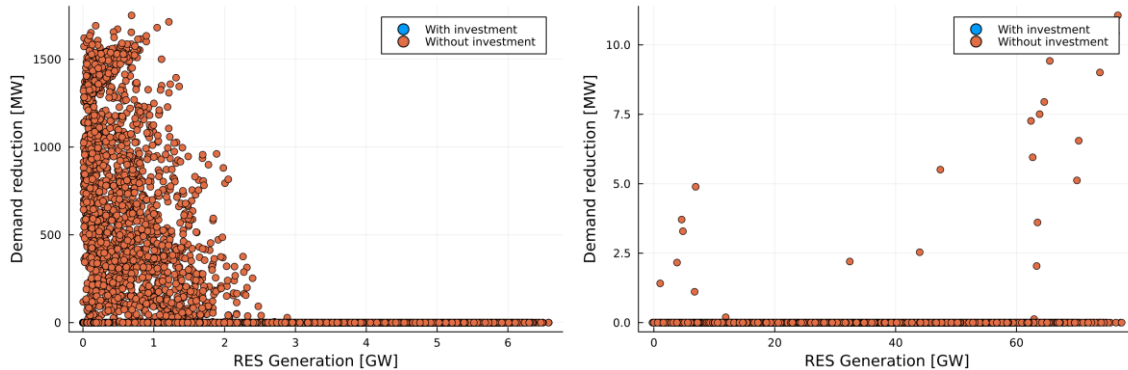


Figure 37 - Comparison between the demand reduction in Ireland (left) and France (right), with and without the Celtic interconnector for different RES generation levels, GA2040, climate year 2007

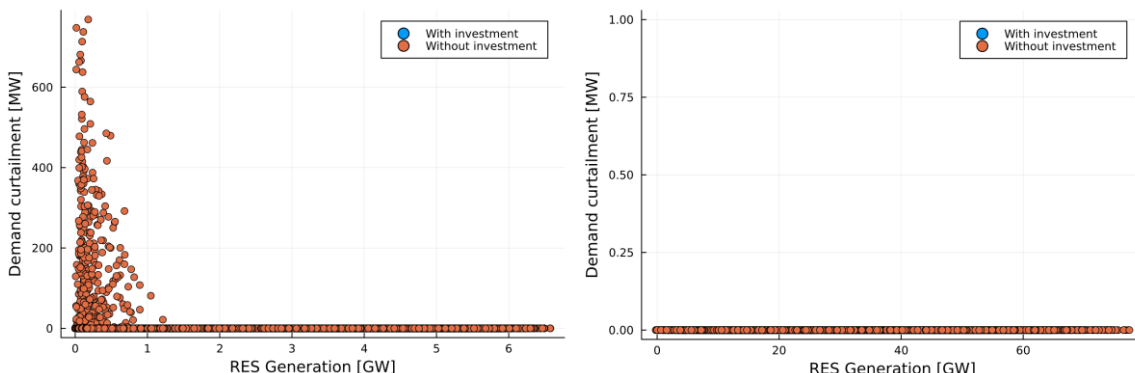


Figure 38 - Comparison between the demand curtailment in Ireland (left) and France (right), with and without the Celtic interconnector for different RES generation levels, GA2040, climate year 2007.

In the previous section 7.3.1.2 the use of the inertia constrained redispatch OPF model was described thoroughly. In this section, the effect of including inertia constraints is quantified.

The total costs for one year of operation of the three different OPF models are summarised in the following Table 19. As expected, the case without inertia constraints but with the Celtic interconnector installed is the cheapest with respect to generation costs compared to the other two cases including inertia constraints. We observe that the total generation costs increase with 62 MEuro and 113 MEuro, respectively if the HVDC link provides inertia or not. This means that the value of inertia provision through the HVDC equals to 51 MEUR, e.g., the difference of the cost increase of both inertia constrained cases.

The hours with low inertia can be seen in Figure 39, where the inertia values for Ireland are shown for different RES generation levels. The results suggest indeed that Ireland faces lack of inertia when there are no inertia constraints in the OPF problem and high RES generation is expected. When these constraints are included in the optimization problem, the minimum inertia is constrained by the inertia limits represented by the horizontal lines. The inertia limits obtained through the dynamic simulations are 8750

MWs (without frequency support from HVDC, assuming max. RoCoF of 2Hz/s) and 5625 MWs (with frequency support from HVDC (limited to 250MW) max. RoCoF of 2Hz/s). We can observe in Figure 39 that the system inertia remains above the imposed limits for the cases without (orange markers) and with (green markers) inertia support. For the case where no constraints are enforced (blue markers), the system inertia can be well below 5000 MWs.

**Table 19 – Total cost and comparison to the unconstrained zonal model with investment of the inertia-based OPF model with and without HVDC Celtic interconnector, GA2030, climate year 2007**

Case	Total cost [bn€]	Difference with respect to unconstrained model [M€]
Unconstrained model	170.85	-
Inertia constrained, no HVDC	170.96	113
Inertia constrained, with HVDC	170.91	62

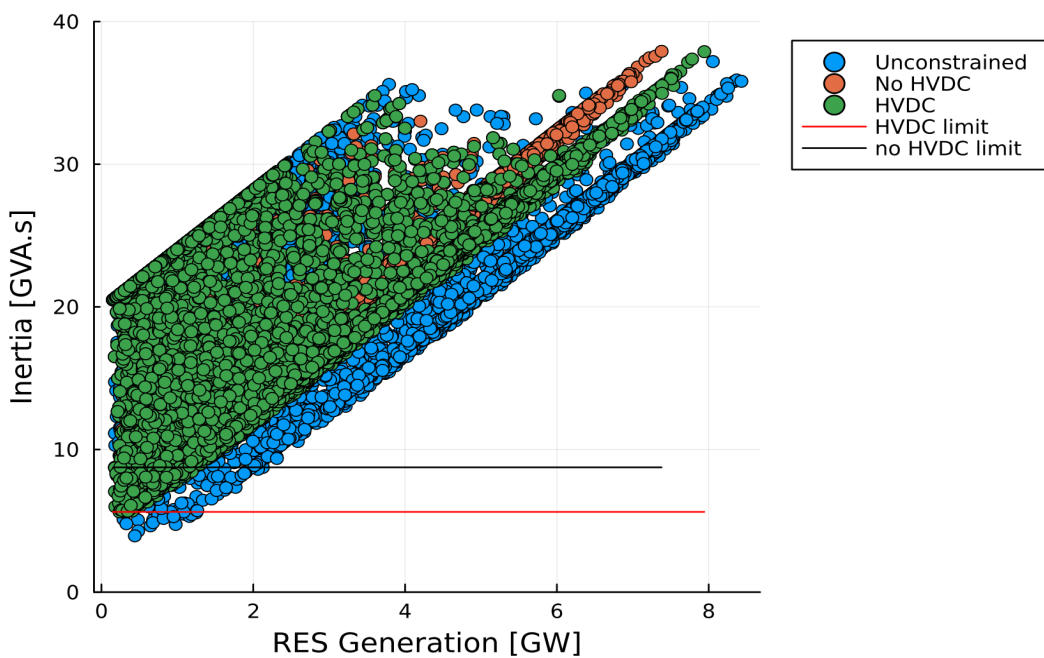


*Figure 39 – Inertia values for Ireland with different RES generation levels for the zonal model, unconstrained and inertia-based OPFs, with and without HVDC, GA2030, climate year 2007*

As already mentioned in the previous section, a redispatch calculation has been performed using the detailed nodal model of both networks where the generator start-up costs for conventional generators have been minimized for fulfilling the inertia constraints. This value can be seen as an upper bound on the costs needed to ensure the system inertia, as generator start-up costs are used in the objective. Table 20 provides the total annual generation start-up costs for the Irish network with both inertia constraints. These costs should be seen as an upper bound, as it assumes that in all low inertia hours generators would need to be started up as no unit commitment constraints are included in the optimisation model. However, we can assume that the effect of not having included such unit commitment constraints would affect both results to the same extend and thus can conclude that using the inertia contribution from the HVDC link can reduce the annual

generation start-up cost by roughly 50%, which is also in line with results provided in the zonal model.

**Table 20 - Total annual generation start-up costs for the Irish network to fulfill inertia constraints, for the scenario GA2030, climate year 2007.**

Case	Annual generation start-up costs [M€]
Inertia constrained, no HVDC	1073.6
Inertia constrained, with HVDC	544.6

### 7.3.2. Assessment of stability KPIs

#### 7.3.2.1. Converter driven stability

The first indicator that has been determined for the different clusters is the SCR. In order to obtain the SCR, a short-circuit analysis is firstly performed (according to standard IEC 60909) to obtain the short-circuit power at each connection point of the wind turbines in Ireland. Thereafter the SCR is calculated by taking the ratio of the short-circuit power (SCR) over the MVA rating of each wind unit. This analysis is performed using the operating points of the different clusters both for the case with the Celtic Interconnector and without.

As a first step, one could investigate the amount of hours where the converter-driven stability is at risk for each wind turbine or wind farm in the system. An example of such a duration curve (expressing the amount of time a certain SCR is exceeded) for a single turbine is presented in Figure 40. For this specific location approximately 28% of the year, production is at SCR<3, which can be considered critical for converter-driven stability. In this case, the duration curve with and without the Celtic interconnector looks very similar, but this may differ depending on the dispatch and location of the wind turbine.

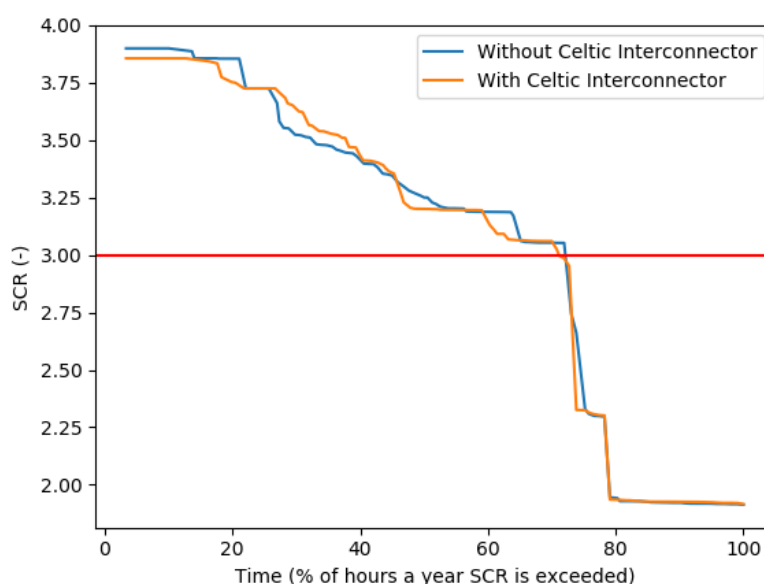


Figure 40 - Duration curve of SCR for a single WT in the Irish system

Next, the results of all wind turbines are aggregated and it is determined how much of the yearly total wind energy is produced at SCR levels below 3. As such an estimate of the yearly energy can be obtained at which converter-driven stability is at risk (see also KPI presented in Table 3). The outcome of this analysis is visualized in Figure 41 where the cumulative yearly wind energy is presented in function of increasing SCR. It is clearly shown in the figure that for the case with the interconnector more wind energy (2390 GWh) is produced at an SCR<3 compared to the case without the interconnector (1219 GWh). This can be explained by the fact that on the one hand more wind energy is produced with the interconnector but also that the change in dispatch leads to slightly lower SCR levels in the case of the interconnector.

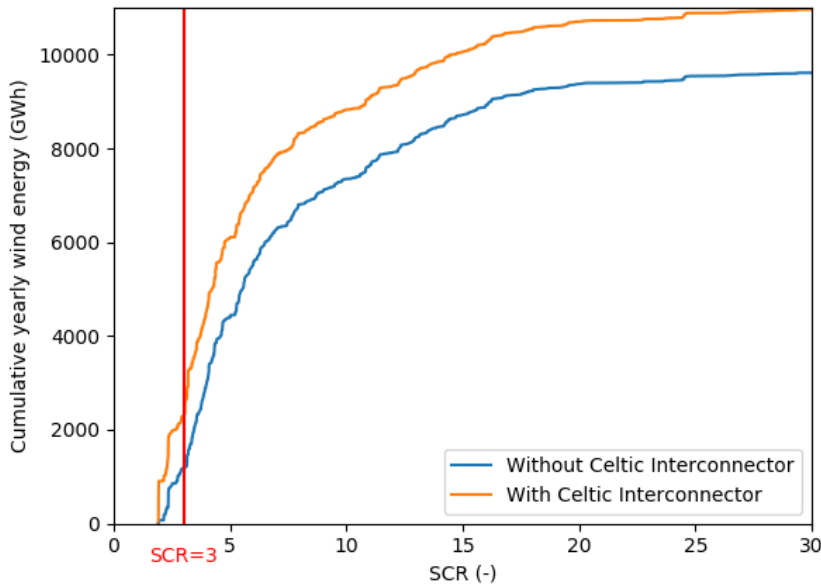


Figure 41 - Cumulative yearly wind energy in function of increasing SCR (results are only presented for SCR<30)

The second indicator that has been determined for the six considered operating conditions of the system (corresponding to the different clusters) is the IBR Critical Clearing Time (CCT). As introduced in section 6.3.2, this indicator is applied to assess the transient stability of IBR. We will focus in this report on the power system of Ireland.

To calculate the IBR-CCT, the operating points of the wind turbines in service (active and reactive power) as well as the voltage at their terminals are taken from the AC load flow results using the nodal data as input (to do so, an AC power flow calculation is performed which uses the active power set points of generators and HVDC links as provided by the nodal OPF calculations as input). The external system has been represented by its Thévenin equivalent using the short-circuit power at the wind turbine connection point. By applying the different analytical expressions as introduced in [33] (neglecting outer loop controller and current dynamics), the results as presented in Figure 42 are obtained (data with and without the Celtic Interconnector is merged). In this figure, the IBR-CCT is given in function of the loading of the wind turbines (active power output/rating of the machine) and the SCR. The results show the inversely proportional relationship between loading and IBR-CCT. The correlation between SCR and IBR-CCT is less clear, although for the operating points where the wind turbines are highly loaded (mainly out of cluster 1), lower SCR leads in general to a lower IBR-CCT.

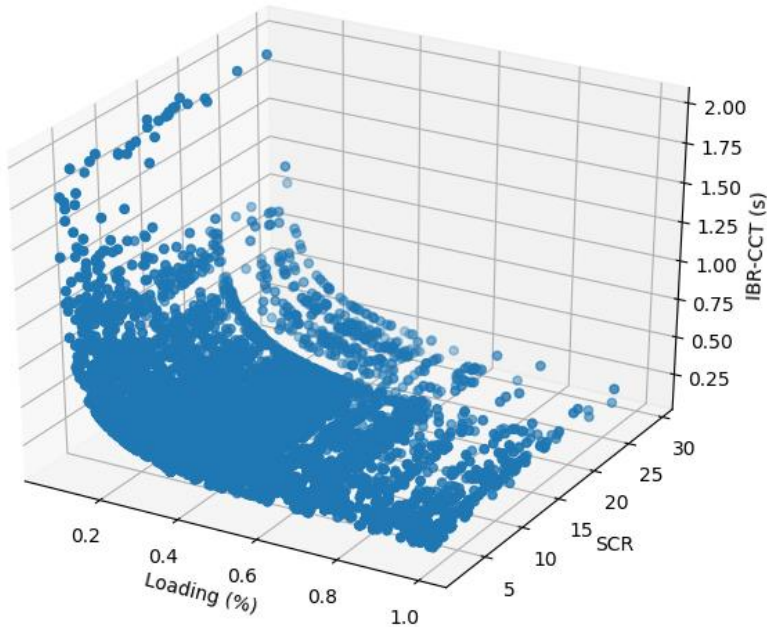


Figure 42- IBR-CCT for wind turbines within the 6 considered clusters (SCR<20)

### 7.3.2.2. Frequency stability

The frequency stability is investigated based on the simplified two-area system described in section 6.3. This model allows to assess the dynamic performance of the frequency regulation and whether the occurrence of the sizing incidence would lead to extreme ROCOF and frequency excursions. For illustrative purposes, the following simplifications/assumptions have been made:

- A threshold of 49 Hz has been considered, below which it is assumed that under-frequency load shedding would take place.
- The sizing incident would be the outage of the complete HVDC link when injecting power higher than 500 MW from France to Ireland. If power is exported through the Celtic interconnector, then the sizing incident would be either the outage of another HVDC link (Eastwest or Moyle) or the outage of a generator in Ireland. Since the zonal results do not include details about the actual unit dispatch, a 700 MW disturbance is considered in all cases. This is simulated by a sudden increase of the system load.
- The contribution of the Celtic interconnector to frequency regulation is modelled through a simple frequency droop that modifies its active power reference.
- The converter-based renewable units (wind and PV), as well as the run-of-river hydro units do not provide frequency support.

The benefits from HVDC frequency regulation depend on the capacity of the HVDC allocated for this purpose. Therefore, results are provided for four cases: 200 MW, 400 MW, 700 MW and 1400 MW (i.e., full range of VSC from maximum export to maximum import). In all cases, the maximum power of the HVDC is limited by the maximum current rating of 1.1 pu.

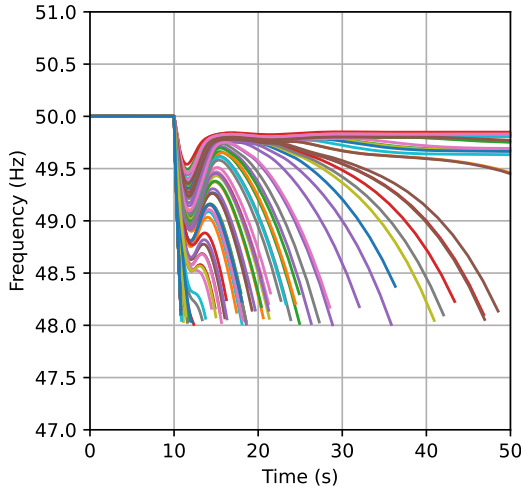


Figure 43 - Frequency of IE with maximum 200 MW of HVDC support.

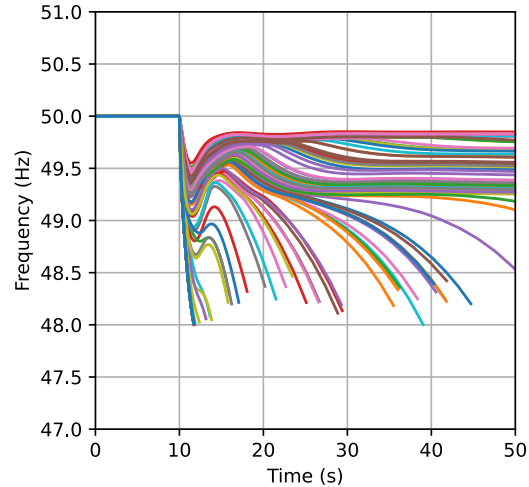


Figure 44 - Frequency of IE with maximum 400 MW of HVDC support

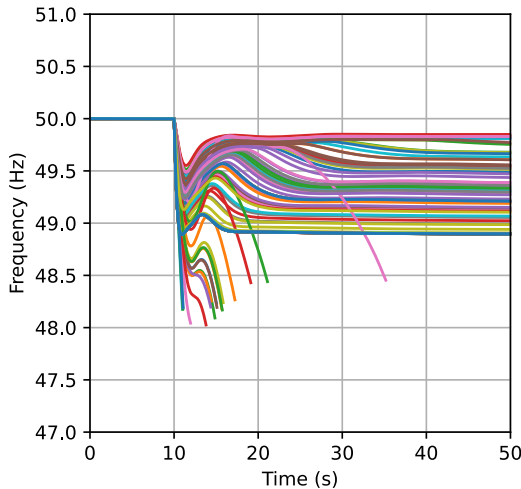


Figure 45 - Frequency of IE with maximum 700 MW of HVDC support

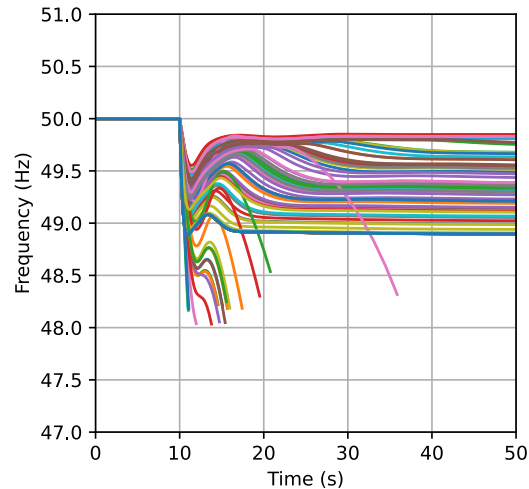


Figure 46 - Frequency of IE with maximum 1400 MW of HVDC support

As shown throughout Figure 43 and Figure 46, HVDC frequency support greatly improves the frequency stability of the Irish system. In particular, with 200 MW and 400 MW of support, several cases would lead to collapse of the system frequency and load shedding due to insufficient reserves. In practice, the operator would re-dispatch the generators of the system to have sufficient reserves. Obviously, this would decrease the penetration of renewable units by adding more conventional units to the mix (at partial power) and would limit the benefits obtained from the HVDC system.

When the HVDC link is operated near its maximum import before the disturbance, the obtained benefit is negligible since it cannot further increase its power. That is the reason why some of the cases could not be stabilized even with very high maximum contribution by the HVDC.

Figure 47 illustrates the benefit obtained by HVDC frequency support in reducing the risk of having under-frequency load shedding. When frequency regulation is not considered (e.g., as in the current version of the CBA), then KPIs such as the renewable integration tend to be overestimated and the redispatch costs (to allow for frequency reserves) tend to be underestimated. Frequency regulation by the HVDC decreases the risk associated with these parameters.

The total number of cases in Figure 47 is split into cases where the load shedding occurs before 5 s and after 5 s. This time duration is in the order of the typical response time of the governors of thermal power plants. It allows to have a clearer insight of the main reason for load shedding. In particular, in the cases where the load shedding occurs before 5s after the disturbance, it can be deduced that there is a lack of sufficient inertia in the system. In contrast, when the load shedding occurs after 5 s, there is a lack of sufficient primary frequency reserves. The contribution from the HVDC has a positive impact on both cases.

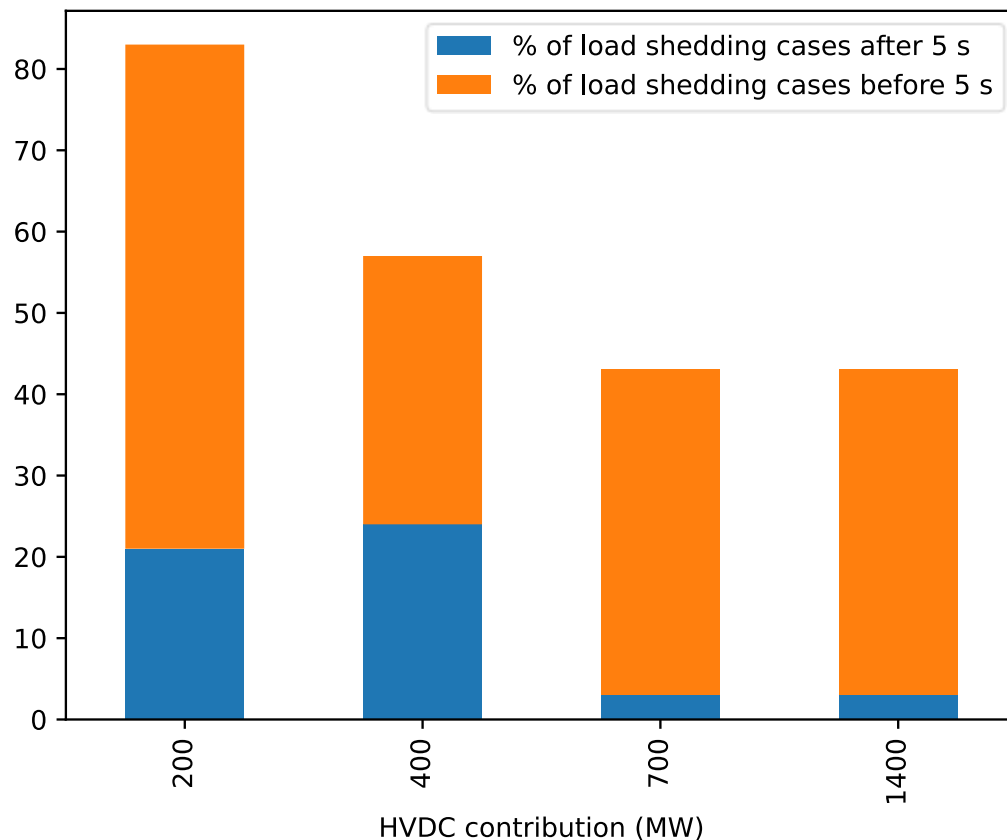


Figure 47 : Percentage of operating points with risk of under frequency load shedding

## 7.4. Ultranet + A-North

### 7.4.1. Assessment of techno-economic KPIs

#### 7.4.1.1. Overview of implementation, models and data used

This case is selected to demonstrate the additional benefits of power flow control capability of HVDC links, especially to minimize the redispatch costs in case of contingencies. To that end, the nodal ENTSO-E grid model of the German network is used. The network model consists of 2558 nodes, 3127 branches (including transformers and circuit breakers), 4954 generators and 8 HVDC links.

### 7.4.1.2. Simulations performed

As the aim is to demonstrate the benefits of power flow control through HVDC in cases of contingencies, first the generation dispatch is determined using the nodal grid model and applying AC/DC grid OPF model. By performing the calculations both with and without the planned investment, the socio-economic welfare indicators can be calculated (for validation), for which the results are shown in the next section. After having determined the generation dispatch, the redispatch optimisation can be performed as outlined in Figure 48.

Starting from the generation dispatch and the HVDC converter set points obtained from the nodal model, first a clustering of the operational hours has been performed using the k-means approach as described in section 6.3.3 using the RES generation and total demand as features for the clustering. The reason therefore is that the simulation of operational hours, e.g. 8760 hours is computationally too expensive. For the case at hand, 20 different clusters have been built as shown in Figure 49. As such, from each of the 20 clusters, 5 operating hours have been sampled, to sufficiently cover the entire range of operational conditions.

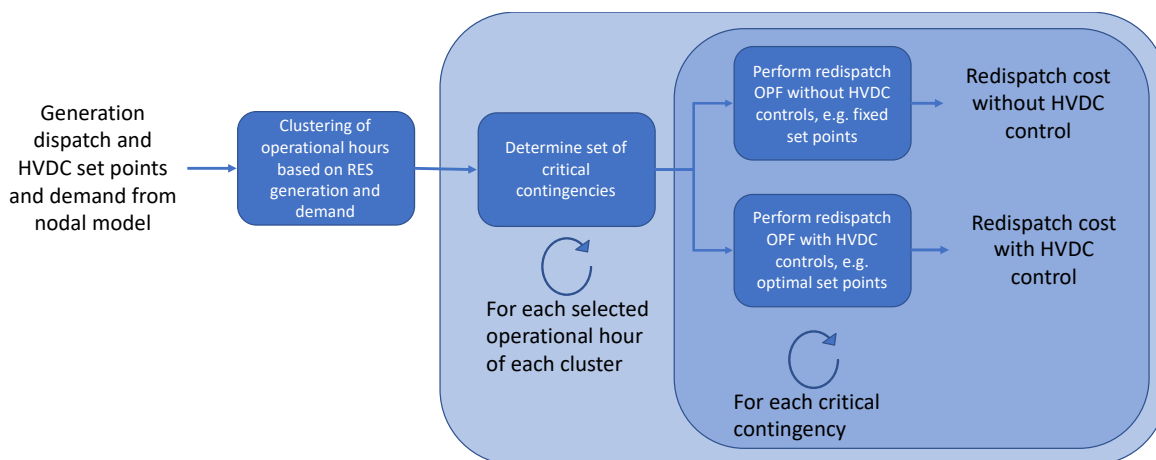


Figure 48 - Calculation procedure to determine the benefits of HVDC power flow control for contingencies

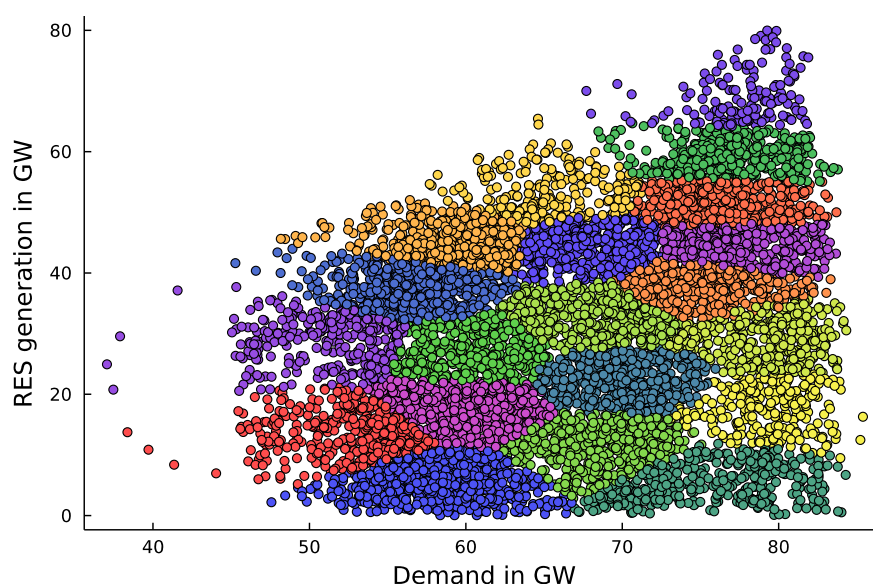


Figure 49 - RES generation / demand clusters for the German network, GA2030 scenario with climate year 2007

After performing the clustering, a sequential calculation routine is performed for each of the 5 operating hours of each of the 20 clusters selected. For each operational hour, first the set of critical contingencies is determined. To that end, all (AC and DC) lines exceeding a thermal rating of 1600 MVA (MW in case of DC lines) and a line loading above 70% are added to the set of critical contingencies. For the case at hand, depending on the selected operational hour, the number of critical contingencies varies between 70 and 100. Thereafter, for each critical contingency the optimal redispatch calculation is performed for two cases; first, where HVDC converter set-points are fixed to their pre-contingency values, and second, where the optimal HVDC converter set-points are optimized. This way, the redispatch costs both including and excluding HVDC control is determined, and by calculating their difference, the benefits through HVDC power flow control is determined. Eventually, the determined costs are extrapolated to a full year, both using the average benefits over all considered contingencies, as well as considering only the contingencies of each operating hour with the maximum benefits through HVDC control. These costs are illustrated in Table 22.

#### 7.4.1.3. Comparisons of relevant KPIs without the project, with the project (CBA methodology) and with the project (proposed CBA)

The following table shows the computed KPIs for the German nodal model with and without the UltraNet and A-North interconnectors. This use case highlights one limitation of the current ENTSO-E CBA, i.e., not being able to evaluate the benefits of such an investment within the zonal model, as this connection is entirely within Germany and as such, the determination of the increase of the NTCs with different market zones is not easy to determine a priori. Without the prior knowledge of the NTC increase, the KPIs cannot be computed if only one node per market zone is present in the model, as it happens with the current zonal simulations.

The project consists of a multi-terminal DC from the North to the South of Germany, enhancing the power flow controllability without having loop flows through the neighbouring countries. This aim reflects in the computed KPIs. The total costs are reduced by 113 M€ and 307 M€ respectively for GA2030 and GA2040 scenarios using the climate year 2007. Furthermore, the CO<sub>2</sub>, SOx and NOx emissions are reduced in both scenarios, as a result of the enhanced transmission power capacity.

**Table 21 - Benefits through HVDC power flow control for the UltraNet + A-North case**

KPIs	GA2030, cy 2007			GA2040, cy 2007		
	No investment	Investment	Benefit	No investment	Investment	Benefit
B1 – Socio-economic welfare – all market zones	17.47 bn€	17.35 bn€	113 M€	15.96 bn€	15.65 bn€	307 M€
B2 – CO <sub>2</sub> emissions [Mton/yr]	23.57	20.48	3.09	18.78	18.32	0.46
B3 – RES integration[TWh]	273.00	271.1	- 1.9	290.0	286.5	- 3.5

KPIs	GA2030, cy 2007			GA2040, cy 2007		
	No investment	Investment	Benefit	No investment	Investment	Benefit
B4 – Nox emissions [Mton/yr]	30.92	30.82	0.10	29.59	29.04	0.55
B4 – Sox emissions [ton/yr]	128.45	125.45	3.00	189.00	183.67	5.33
B5 – Grid losses [TWh]	2.76	2.77	- 0.01	2.86	2.86	0
B6 – Adequacy, ENS [GWh/yr]	0	0	0	0	0	0
Additional KPI – Demand curtailment [GWh]	132.64	132.64	0	303.60	303.60	0

Table 22 shows the benefits obtained through HVDC grid control in case of contingencies. The table provides two different values, namely the total annual benefits obtained by taking the *average value of the benefits* among all contingencies summed up over operating hours considered and extrapolated to a full year. The second column provides the total annual benefits obtained by taking the *maximum achieved benefits* among all considered contingencies summed up over all operating hours and extrapolated to a full year. We can observe that there exists a significant gap of one order of magnitude between the average value and the maximum value. Figure 50 illustrates the benefits of power flow control through HVDC for all clusters, chosen operating hours and contingencies. The figure clearly demonstrates that the maximum benefits are achieved for certain specific contingencies in a given operating hour or contingency indicated as outliers in the boxplots. In reality structural weaknesses network resulting in such high costs during contingencies would be solved with local reinforcements. As such, it can be expected that realistically the benefits through power flow control through HVDC will be closer to the average value provided in Table 22.

**Table 22 - Benefits through HVDC power flow control for the UltraNet + A-North case**

	Using average benefits of all contingencies [MEUR/year]	Using contingencies with maximum benefits [MEUR/year]
Annual benefits through power flow control through HVDC	33.5	473.2

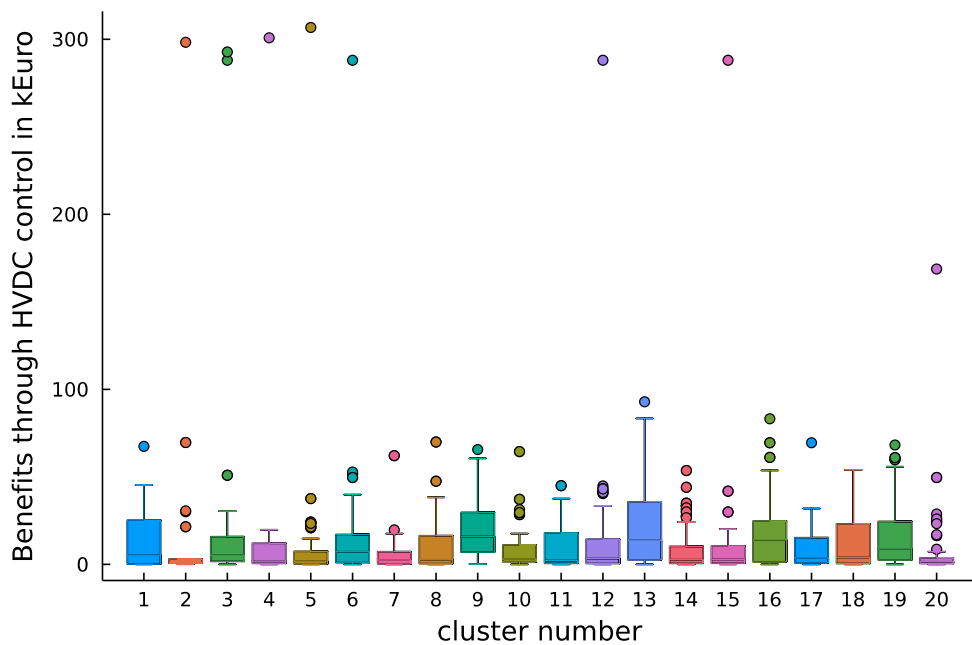


Figure 50 - Benefits of power flow control through HVDC for each RES-demand cluster, each operating hour per cluster and each contingency per operating hour.

## 7.5. EuroAsia

### 7.5.1. Assessment of techno-economic KPIs

#### 7.5.1.1. Overview of implementation, models and data used

The EuroAsia interconnector (<https://tyndp.entsoe.eu/tyndp2018/projects/projects/219>) aims to connect continental Greece (zone GR00), Crete (GR03), Cyprus (CY00) and Israel (IL00) with an HVDC interconnection. Even though the rated capacity of the cable is 2000 MW, only 1000 MW will be used for its preliminary stage. For this reason, the two cables being added to the zonal European grid have a rated capacity of 1000 MW. They interconnect Crete and Cyprus (GR03-CY00) and Cyprus and Israel (CY00-IL00). Since Israel is an islanded zone in the zonal model, its demand is assumed to follow the pattern of another Mediterranean market zone, ITSI. As the installed power plant capacities and peak demand for Israel are not provided within the zonal TYNDP model, the installed capacity is obtained from the website of International Trade Administration<sup>9</sup>. The peak demand assumed to be 13.8 GW<sup>10</sup>. As for the RES and demand time series, the same profiles as for the Southern Italian market zone are used.

This case study is chosen to demonstrate the added value of inertia provision through HVDC. Considering that power provided by the HVDC link will be higher than the current peak demand in Cyprus, as well as the envisaged RES penetration on the island, inertia provision through this HVDC link will be vital to maintain the stability of the system. As such, in this case study, we are using the same approach as in the case of the Celtic interconnector to determine the benefits through inertia provision using the zonal model of the system.

#### 7.5.1.2. Simulations performed

In order to validate the assumptions with respect to the assumed demand and generation mix in Israel, first the zonal NTC based economic dispatch model is used to calculate the socio-economic benefits for the cases, with and without the interconnector. We determine the socio-economic welfare KPIs and compare them to the benefits provided in the TYNDP for which the KPIs are provided in the next section for validation.

As in the case of the Celtic interconnector, subsequently, also the inertia constrained NTC based dispatch model is performed, for the cases where inertia contribution from HVDC is considered and omitted. This way the same comparison as in the case of the Celtic interconnector w.r.t the costs associated with stability constraints can be quantified, as well as the benefits achieved through inertia provision through HVDC control.

#### 7.5.1.3. Comparisons of relevant KPIs without the project, with the project (CBA methodology) and with the project (proposed CBA)

With the EuroAsia interconnector, all the KPIs improve for scenario GA2030, climate year 2007. In Table 23, the indicators computed with and without investments are compared to the values shown by ENTSO-E TNYDP in its 2030 Sustainable Transition scenario. As a

---

<sup>9</sup> See also <https://www.trade.gov/country-commercial-guides/israel-energy>

<sup>10</sup> See also <https://sympower.net/demand-peaks-in-israel/>

validation of our zonal model, the order of magnitude of all the KPIs falls in the range of values stated by ENTSO-E. The reason behind the difference for B1 (Socio-economic welfare) and B6 (Adequacy – ENS) resides probably in the assumptions made for the Israel zone IL00. Nevertheless, the difference is not substantial.

The benefits brought by the interconnector in terms of ENS reduction are shown in Figure 51 below, where the level of ENS for the whole RES generation spectrum is shown. When the EuroAsia interconnector is not included in the grid, there are loss of load events distributed for roughly all the generation levels. The frequency and magnitude of the ENS hours are brought to zero when the EuroAsia interconnector is added to the zonal dispatch.

In addition, Figure 52 displays the relation between the power flow through two parts of the EuroAsia interconnector and the RES generation levels in the area. The interconnectors are used at full capacity for a consistent number of hours. The link GR03 – CY00 sees a power flow to GR03 (Crete) for most of the time, highlighting how Crete is in constant need of power. Differently, the power flow for CY00 – IL00 is more distributed across the range of possible power flow values for the interconnector.

**Table 23 - Computed KPIs for EuroAsia interconnector, zonal model, scenario GA2030, climate year 2007**

KPIs	GA2030, cy 2007			ENTSO-E TYNDP data
	No investment	Investment	Benefit	Benefit
B1 – Socio-economic welfare – all market zones	175.91 bn€	176.16 bn€	246.25 M€	261 – 270 M€
B2 – CO2 emissions [Mton/yr]	15.31	15.76	0.45	0.76 - 2
B3 – RES integration [GWh]	464.92	477.11	12.19	0 - 22
B4 – NOx emissions [kton/yr]	19.51	18.81	0.70	-
B4 – SOx emissions [ton/yr]	901.67	370.74	530.93	-
B6 – Adequacy, ENS [GWh/yr]	8.855	0	8.855	0.78 – 2.96

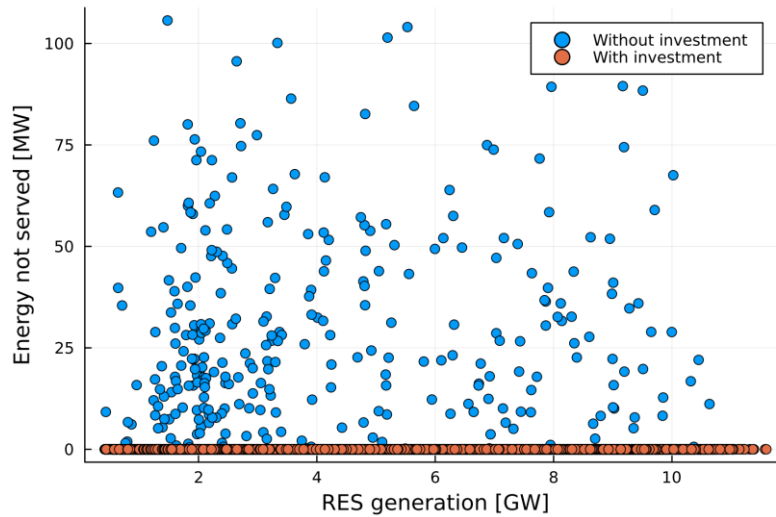


Figure 51 - Energy not served for different RES generation levels in the EuroAsia zonal model, GA2030, climate year 2007

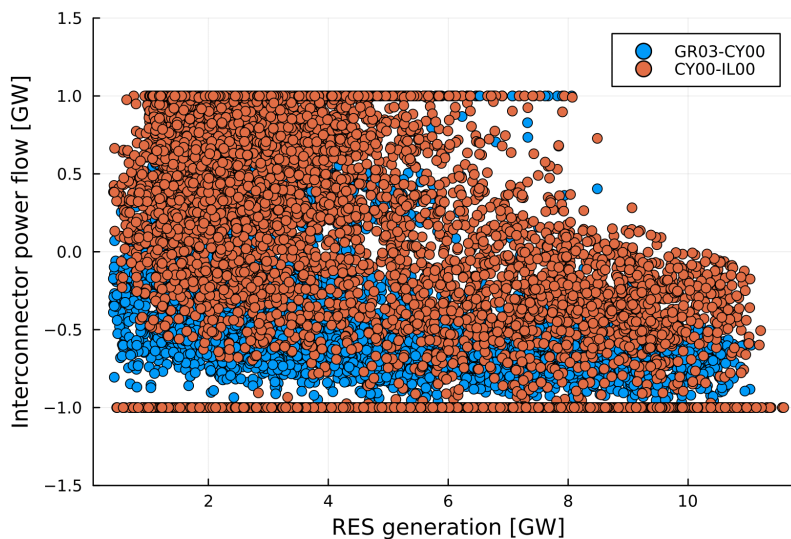


Figure 52 - Power flows through two parts of the EuroAsia interconnector for different RES generation levels in the EuroAsia zonal model, GA2030, climate year 2007

Table 24 shows the total system cost for the EuroAsia interconnector when the inertia constraints are enforced for Cyprus. As expected, the case without inertia constraints but with the EuroAsia interconnector installed is the cheapest with respect to generation costs compared to the other two cases including inertia constraints. We observe that the total generation costs increase with 16 and 104 and MEuro, respectively if the HVDC link provides inertia or not. This means that the value of inertia provision through the HVDC is 88 MEUR, e.g., the difference of the cost increase of both inertia constrained cases.

The hours with low inertia can be seen in Figure 53, where we see the inertia values for Cyprus over all operational hours. We can clearly observe that in many hours the system inertia can drop as low as to zero in the base case without inertia constraint (blue markers), where the entire demand is supplied by RES. This shows the importance of including inertia constraints in the optimal dispatch model, as such zero inertia cases would be infeasible in real life, if no counter measures such as synchronous condensers or grid forming HVDC links can be used.

When the inertia constraint is included in the optimization problem, the minimum inertia is constrained by the inertia limits represented by the horizontal lines. The inertia limits

obtained through the dynamic simulations are 6250 MWs (without frequency support from HVDC, assuming max. RoCoF of 2Hz/s) and 3125 MWs (with frequency support from HVDC (limited to 250MW) max. RoCoF of 2Hz/s). We can observe in Figure 53 that the system inertia remains above the imposed limits for the cases without (orange markers) and with (green markers) inertia support.

**Table 24 - Total cost and comparison to the unconstrained zonal model with investment of the inertia-based OPF model with and without HVDC EuroAsia interconnector, GA2030, climate year 2007**

Case	Total cost [bn€]	Difference with respect to unconstrained model [M€]
Unconstrained model	175.911	-
Inertia constrained, no HVDC	176.015	104
Inertia constrained, with HVDC	175.927	16

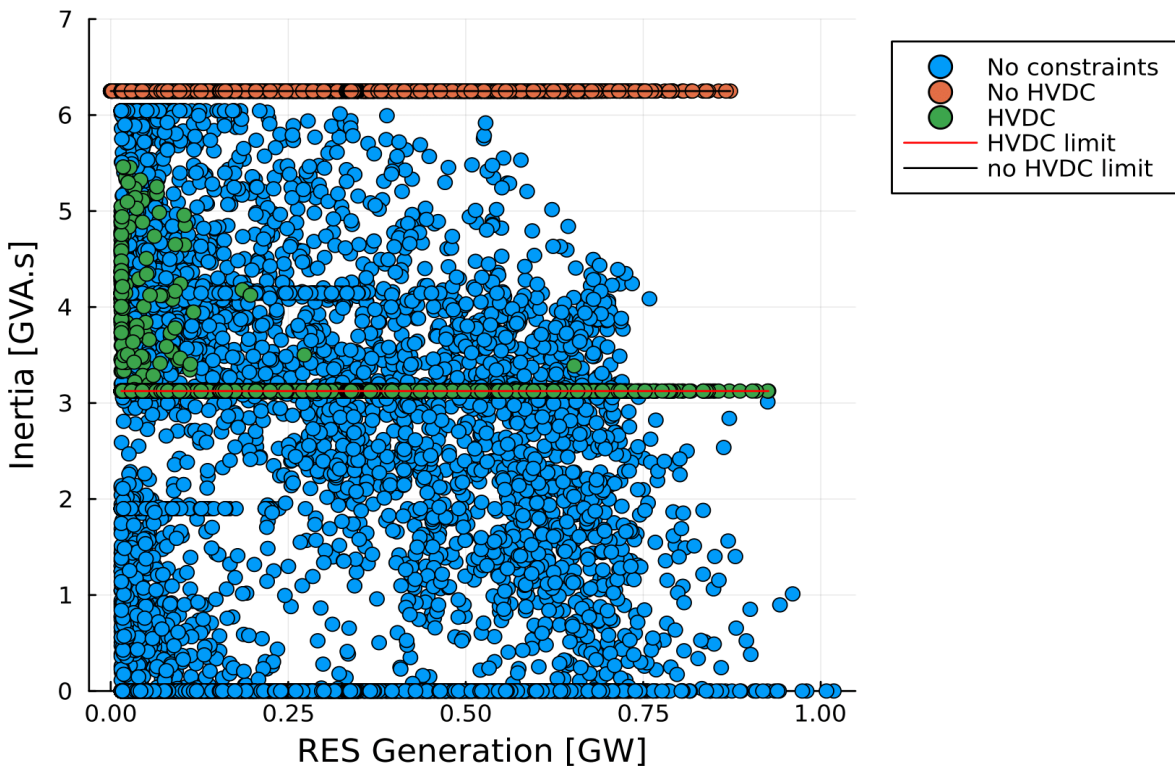


Figure 53 - Inertia values for Cyprus with different RES generation levels for the zonal model, unconstrained and inertia-based OPFs, with and without HVDC, GA2030, climate year 2007

#### 7.5.1.4. Frequency stability

As in the case of the Celtic Interconnector, the frequency stability is investigated based on the simplified two-area system described in section 6.3. For illustrative purposes, the following simplifications/assumptions have been made:

- A threshold of 49 Hz has been considered, below which it is assumed that under-frequency load shedding would take place.
- The sizing incident would be the outage of one pole of the HVDC link when injecting power to Cyprus. Compared to the case of Ireland though, here there is

only one HVDC connection to Cyprus, and the outage of 500 MW would be too constraining. In addition, it is expected that, in practice, the power of the HVDC injection to Cyprus would be limited below the maximum rating, namely, to allow to provide frequency reserves in case of the outage of one pole. For this reason, a sizing incident of 400 MW has been considered in this analysis.

- The converter-based renewable units (wind and PV), as well as the run-on-river hydro units do not provide frequency support.

Results are provided for four cases: 200 MW, 400 MW, 500 MW and 1000 MW (i.e., full range of one pole of the connection from maximum export to maximum import). They are shown in Figure 54 - Figure 58.

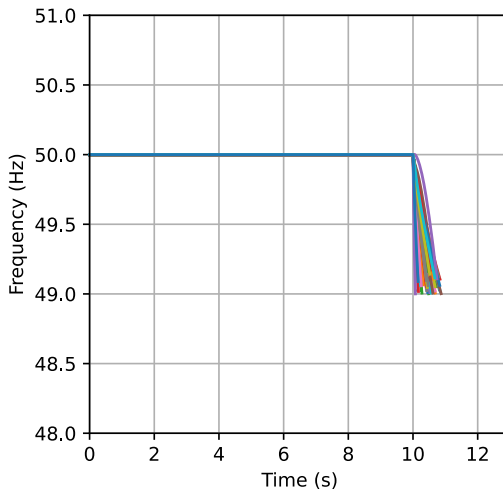


Figure 54 - Frequency of CY with maximum 200 MW of HVDC support

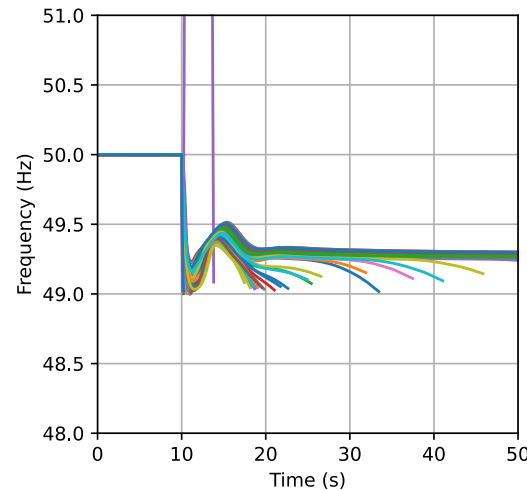


Figure 55 - Frequency of CY with maximum 400 MW of HVDC support

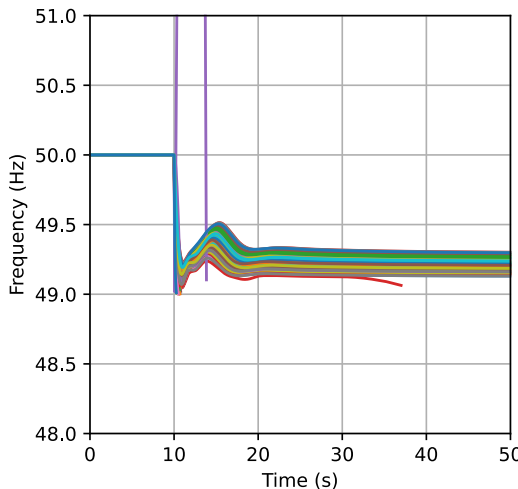


Figure 56 - frequency of CY with maximum 500 MW of HVDC support

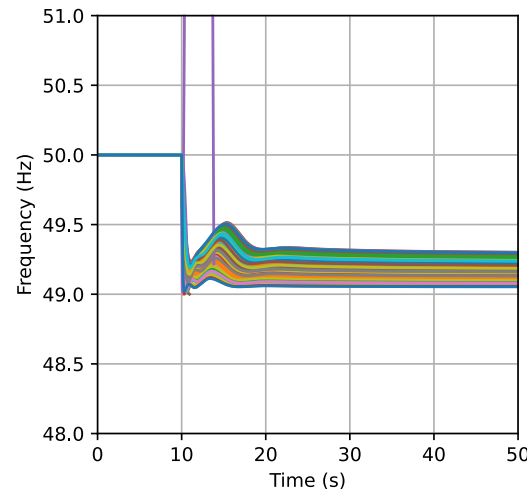


Figure 57 - frequency of CY with maximum 1000 MW of HVDC support

Similar conclusions are obtained as in the case of the Celtic Interconnector. Allowing more participation by the HVDC, results in more operating points without need for load shedding. As a result, the cost for redispatch to account for reserves is lower and the operating points with higher generation by renewable units can be achieved. It is interesting to note, that high renewable penetration is usually accompanied with export of power from the HVDC. Hence, in such cases:

- The outage of the HVDC is not the sizing incident (since its outage would result in over-frequency which is in general more easily managed)

- the actual range of the reserves that can be provided by the HVDC is higher (it could reach twice the rating of the VSC)

Figure 58 shows how the percentage of load shedding cases is improved with increasing contribution by the HVDC link. It is interesting to note that when increasing the HVDC contribution from 200 MW to 400 MW, the number of cases where load shedding occurs after 5 s is increased. This is because the fast response of the HVDC allows to delay the collapse of the system. Further increase of the contribution by the HVDC has a positive impact on the number of load shedding either due to insufficient reserves or due to low inertia.

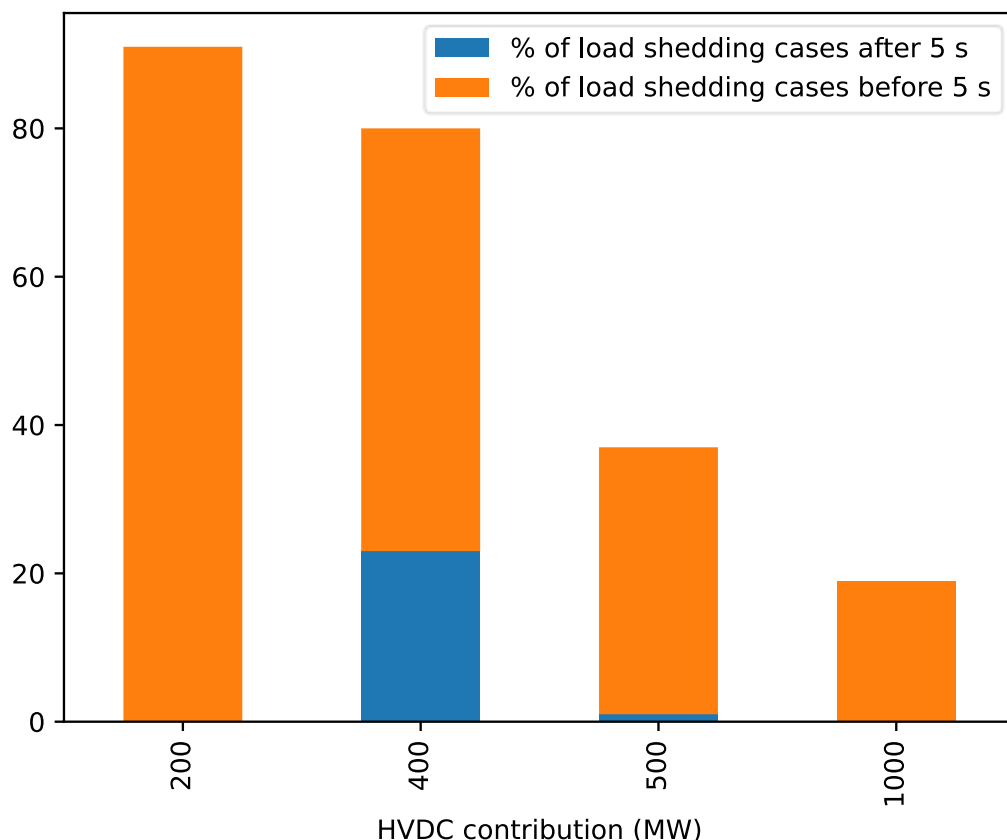


Figure 58 : Percentage of operating points with risk of under frequency load shedding

## 7.6. 2050 MTDC

The 2050 multi-terminal DC grid case was selected in order to illustrate extra benefits that could not be captured using the 2030 cases. However, based on the results of the four previous cases, we were able to show additional benefits for each study case. In fact, the combination of the four studied use cases covers the configuration of the 2050 MTDC case. When investigating the 2050 MTDC use case, it was identified that a pan-European use case brings additional complexities in terms of computation challenges, need for a harmonized dataset and also for adequate modelling of the different layers of control of the MTDC. However, it will not show additional benefits that were not covered in the previously studied cases.

In future work, the methodologies developed in this work could also be applied to the 2050 Multi-Terminal European backbone system, in order to better quantify the risks through IBR based generation and potential benefits through the use of HVDC technology.

However, harmonized power system models are needed both for the zonal as well as the nodal network models in order to obtain meaningful results.

Considering that such a backbone will have multiple terminals within some countries, the currently available zonal network model would need to be updated, also based on the outcome of the bidding zone review currently ongoing. Further, in the case of the backbone system, one could expect high benefits through power flow controllability considering the ring structure spanning over France, Belgium and Germany. This would require regional level redispatch calculations, for which again reliable and harmonised nodal network models are needed. Considering the computational intensity, also network reduction techniques would most likely need to be applied in this case.

## 7.7. Main challenges encountered during analysis of the use cases

The main challenges encountered during the implementation of the use cases have been related to the inconsistencies and/or incompatibilities of available data. Firstly, the translation/disaggregation of the zonal TYNDP model to the nodal high voltage grid model requires a number of assumptions, on the distribution of the demand and the renewable generation sources. Although the demand can be disaggregated linearly, as also done within this project, for the disaggregation of the generation, the type of generator needs to be known in the nodal model. However, for many of the provided detailed nodal models, the generator types are not directly visible, and heuristics based on the size of the generator, or the naming convention chosen by the TSOs need to be developed to extract generator types in the nodal model. Secondly, inconsistencies exist between the installed generation capacities in the zonal and nodal models. As such, the validation of the aforementioned use of heuristics to derive the generation types of the nodal model is needed. For the sake of validation of both models, in the future, it will be essential to ensure the consistency and compatibility of both models.

Another major challenge encountered w.r.t. data was inconsistencies of data within the nodal models. The aim of the nodal model is to provide a power flow solution to the non-linear AC power flow equations. However, to be able to use this model for optimal power flow type of calculations, the quality of the data should be improved. Inconsistencies of the data often result in infeasible solutions of the optimisation problem. The main sources of inconsistencies encountered were:

- Inconsistent power ratings in subsequent lines and circuit breakers
- Negative impedance values for branches
- Inconsistent bounds on generators, e.g.  $P_g^{min} \geq P_g^{max}$
- Non-unique node names
- Unrealistic generation and demand values, often from injections not modelled explicitly, e.g. from interconnectors or HVDC links
- Inconsistent modelling of HVDC links, e.g. modelling as equivalent generation versus modelling using actual converters
- Unrealistic line ratings, usually on lower voltage levels, or for antenna connections

## 8. Main findings and recommendations

### *Summary of the work and findings*

In order to try to answer to the following question “Are the existing methodologies, models and tools adequate to capture all risks and benefits when planning AC/DC hybrid grid?”, this work proposed some improvements to the current European CBA approach used by ENTSO-E. Therefore, the focus is at the planning stage when the evaluation of the costs and benefits of a project candidate takes place.

It was identified that commonly used CBA methods do not capture all the technical risks related to operations of a system with high-penetration of IBRs. Therefore, operating conditions might not be stable and would require additional investment or redispatch to be viable.

The proposed improvements were detailed in section 5 and can be summarized by the three following aspects:

- More detailed power system representation, towards a network model
- Integration of power flow control and stability constraints in the optimization problem
- Addition of qualitative KPIs regarding system stability (in particular for frequency and converter-driven stability)

These improvements are to be added to the existing ENTSO-E CBA approach which forms the basis of the proposed incremental approach (illustrated by the pyramid in Figure 8). These incremental levels of complexity are proposed to better quantify some KPIs and also risks in systems with high-penetration of Inverter-Based Resources. The main point is that the zonal approach may provide optimistic benefits, in the sense that some costs can be “hidden” when planning system with large penetration of inverter-based RES because of security and operational challenges. Therefore, it is highly recommended to perform a CBA using the static network model and considering stability metrics such as inertia and SCR. Both inertia and converter-driven stability metrics can be translated to KPIs by assessing how many operating conditions per year are at risk of frequency or converter-driven instability. These quantitative KPIs should be used as an indicator of the need for future investment or for operational measures. Regarding frequency stability, a cost is also evaluated based on redispatch methodology (similar to current B.10 KPI of ENTSO-E). Regarding the converter-driven stability KPI, it must be seen as a risk indicator, which can lead to more detailed simulations in the next stage of the project or even to additional investment.

Modelling requirements and guidelines for implementations of the proposed approach were detailed in section 6. In particular, modelling details focusing on the HVDC technology are summarized in section 6 and implementation details for the CBA approach could be found in section 6.2 and section 6.3.

It has been observed from the use case results that indeed the zonal CBA approach can lead to optimistic results in a system with high penetration of RES or when network thermal constraints are reached. It has also been identified that VSC HVDC technology can provide system stability services that would allow stable operation for a high number of operating conditions (in particular at higher penetration of IBRs). This was the case in particular for an HVDC link connecting two asynchronous areas and where one area had a significant share of IBR penetration. Also, it has been confirmed from the use case where the HVDC link is embedded to the AC grid that the power flow control abilities of HVDC provide additional benefits. In all studied cases, additional benefits of the HVDC technology could only be seen with the use of an inertia constraint and/or with the use of a nodal network model (even if there is an AC/DC interface between two zones).

Our methodology is valid for HVDC, but similar additional benefits can also be seen for devices participating to power flow control, frequency stability or with grid forming features.

The work performed can be summarized into the three following parts (which are more detailed in sections 5, 6 and 7).

## 1. Updated CBA methodology and implementation guidelines

The proposed CBA approach quantifies additional benefits and identifies potential risks for system stability. It is important to note that these additional benefits can only be seen when performing the CBA on a nodal model and/or with stability constraints (such as inertia).

Firstly, an existing open-source AC/DC grid optimal power flow (OPF) model has been used in order to determine the social welfare benefits considering internal congestion in the network, as opposed to using zonal models neglecting intrazonal constraints. Further, the OPF model has been modified to determine the additional benefits through power flow control provided by HVDC links during contingency situations. Using the modified OPF formulation, the redispatch costs are minimized for a number of selected critical contingencies. By performing two separate calculations with disabled and enabled power flow control, the additional benefits through power flow control are determined. The results show that security related redispatch costs can be significantly decreased by making use of such controllability.

Moreover, the developed OPF implementation allows to include additional constraints. An inertia constraint has been tested for two study cases and it was clearly observed that the HVDC technology could considerably reduce the minimum inertia constraint, which by consequence increase the number of stable operating conditions. This effect is also quantified by means of redispatch cost reduction as a proxy of required reserves to ensure frequency stability. Further, it has been demonstrated that such inertia constraints can be included in detailed nodal optimal power flow models, and either inertia constrained dispatch or re-dispatch simulations can be performed.

An extremely important aspect is power system stability in a system with high penetration of IBR. The main initial idea was to perform RMS (or EMT) simulation in order to capture instabilities of grid-following assets in weak grids (e.g. PLL control). However, while it is generally agreed that EMT simulations are needed in order to assess stability in a weak grid, models with the required level of details and accuracy of the control parameters are typically not available for the considered planning horizon. For this reason, it is recommended to evaluate risk of instabilities (at specific locations of the grid and/or at specific operating conditions) via calculation of simplified indicators. A simple indicator is the short-circuit ratio (SCR) but other indicators considering some control loop parameters of IBRs and their dispatch provide a more accurate view of the stability risk. The common philosophy of these indicators is to try to catch the relationship between a variation of the (grid following) converter output and the variation of voltage at the point of connection. If the sensitivity is high, then the risk of instability is higher. These stability indicators are translated to a clear quantitative KPI which is the number of hours per year of having a risk of instability.

## 2. Technical aspects and modelling requirements

One part of the work (summarized in section 6.1) specifically focuses on the modelling requirements for the HVDC technology. A comprehensive review of the type of models and level of details adequate for each phenomenon was presented. For each functionality/technical aspects of HVDC systems, the modelling was specified.

Section 6.2 and section 6.3 detail the modelling requirements for implementing the proposed CBA approach, and outline how additional CBA KPIs can be implemented within

steady-state optimisation models, and how steady-state and dynamic simulations can be combined to analyse risks of IBR based generation, as well as additional benefits of HVDC technology. These sections provide to the interested reader all the required information for implementing the proposed approach.

### 3. Illustration on realistic use cases

The use cases provided us not only with quantitative results but also with a return of experience on the proposed implementation. The zonal approach has been easily implemented, however it is clear that the nodal approach has led to significant challenges, mainly attributed to available data. It has been shown that our approach could be implemented on multi-country systems with several thousands of nodes, lines and generators. An important outcome is also that, while highly recommended with an accurate dataset, conclusions from time-domain power system simulations should be analysed with care in systems with high penetration of RES and with uncertainties on the control loops. It is therefore recommended to start with indicators based on the “static” network model in order to identify stability risks.

#### *Main findings and recommendations for future improvements*

##### (i) Main Findings

- (1) **Use of nodal network model is necessary:** Although zonal models can determine the socio-economic benefits of new interconnectors in a computationally efficient manner, they tend to underestimate these benefits as the internal congestion in the network is not considered. The reason therefore is the zonal approach underestimates the curtailment of renewable energy due to internal network congestion in high RES scenarios, where the added value of interconnection is even more significant. **Our study shows that more complex nodal models can be feasibly used within of CBA methodologies** despite higher computational complexity (24 hours vs. 30 min for yearlong calculations) and higher data requirements.
- (2) **Power flow control provides significant benefits:** **The study shows that HVDC technology provides significant benefits through power flow control in case of contingencies by reducing the required redispatch cost.** Especially embedded HVDC links can reduce redispatch costs in the order of several tens of millions of Euros per year in case of severe contingencies in the system. To analyse such benefits, the use of nodal models is unavoidable.
- (3) **Stability constraints are necessary:** It is essential to consider stability / inertia constraints in long term planning models to estimate the additional risk of deteriorating system inertia for determining the best mitigation options. Further, our study shows that **inertia provision through HVDC decreases the necessary cost for ensuring system stability** in the order of several ten million Euros per year.
- (4) **Stability indicator can be used to identify operational risks:** **Our study shows that simplified models with stability and inertia constraints can provide acceptable high-level results for CBA analysis.** In terms of dynamic data and control parameters, it is clear that the most accurate data allow to be more confident in the results of advanced tools. **However, with currently available models and data sets, it is not adequate to perform intensive detailed simulations for long-term planning studies.** We conclude that detailed dynamic simulations should only be used in cases where detailed network and equipment models are available which can represent different control loops and where control parameters are known. As such, potential risks and de-

risking actions have to be identified but can be done later in the planning process when detailed models are available.

- (5) **Harmonized models are needed:** Our study shows the need to harmonize the network models used in the context of CBAs. Especially, to quantify the effects of congestion and benefits through power flow control as well as to better approximate dynamic stability constraints, harmonized models are essential.

## ***(ii) Recommendations for future improvements***

- (1) **Dataset Improvement:** As the network data are mandatory in our proposed approach, it is extremely important to have a reliable European network model (static). To that end, different data sets used for long term generation and transmission expansion planning versus detailed grid models used to perform power flow studies should be harmonized in order to obtain accurate results capturing all benefits. The modelling section provides clear requirements in terms of the tools and model details for studying each phenomenon. It has been shown in this study (and also in the literature) that control parameters have a huge influence on IBR stability. Therefore, in the near future it is extremely important to have a European grid model with representative control parameters for existing IBRs. This will allow to perform a better screening of the instabilities that might occur
- (2) **Need for high-performance computer infrastructure:** Although detailed nodal models are computationally more expensive, parallelization of calculations, application of artificial intelligence methods for contingency filtering, improved clustering techniques for selecting a subset of representative operating points (both for steady state and dynamic analysis) and the use of dedicated high-performance computer infrastructure can allow the implementation of the demonstrated mathematical models within state-of-the art tools. Further, the development of dedicated open-source tools can help to provide transparent results in the context of the CBA.
- (3) **Defining power system stability in the future grid:** Our study shows a particular approach for including stability indicators within CBA methodologies. However, there are a variety of stability indicators, which all can be quantified using different types of optimisation / simulation models. As such, in the long run it will be important to define stability indicators in a harmonized way. Especially, in the context of grid forming and black start capabilities, clear definitions are needed based on which, indicators can be defined, and subsequently models can be developed to quantify these indicators. We believe that fundamental research and a broad stakeholder involvement are necessary to achieve this goal.

## 9. Appendix I: stakeholder interaction

During this project, two presentations with external stakeholders were done.

First a virtual stakeholder workshop took place on 31<sup>st</sup> March 2022, for which approximately 75 people registered and covered OEM, TSOs, Consulting, developers, research centre and academia. Secondly, a virtual was performed an IEEE Working Group Meeting on “Studies for Planning of HVDC”.

Later this year, it is also expected to present this work in a panel session “Infrastructure for the bulk energy transmission in high RES systems” at the 2022 IEEE Power & Energy Society General Meeting. While not in the scope of the initial offer, the Consortium would be open to additional virtual stakeholder interactions if requested by the European Commission.

In addition to these above-mentioned stakeholder meetings, punctual interactions with ENTSO-E are expected, in particular on the data available and technical details on the modelling.

### 9.1. Stakeholder feedback on use case selection

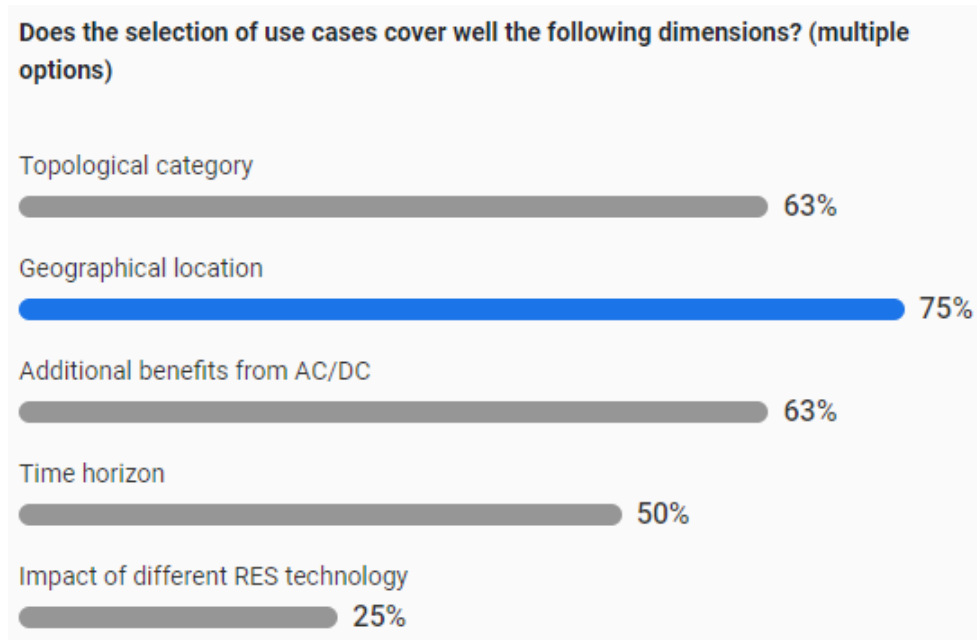


Figure 59 - Stakeholder feedback on use case selection

### 9.2. Modelling requirements and cost-benefit analysis

As shown in Figure 60, it has been confirmed during the workshop that benefits of HVDC are not well evaluated in the existing CBA. Also, the first functionality identified as most relevant is power flow control, which is a very important part of our work. Care should be taken when generalizing responses from a single workshop. However, these answers confirm the important of this project for stakeholders. The second ranked functionality is on black start capabilities, closely followed by grid forming functionality. Therefore, these points have to be analysed in detail in this project, keeping in mind that our work focuses at the planning stage (which is performed usually without knowing detail design and operational procedures). Participants also asked whether benefits such as permitting, public acceptable, environmental impact and total footprint of an HVDC project should not

also be quantified. It is however believed that these aspects are project specific and therefore very difficult to quantify and generalize.

**Are some benefits of HVDC underestimated in the classical planning exercise? If yes, What would be the most important features/particularities of HVDC converters to include in a CBA calculation? Please rank the answer from most relevant to less relevant.**

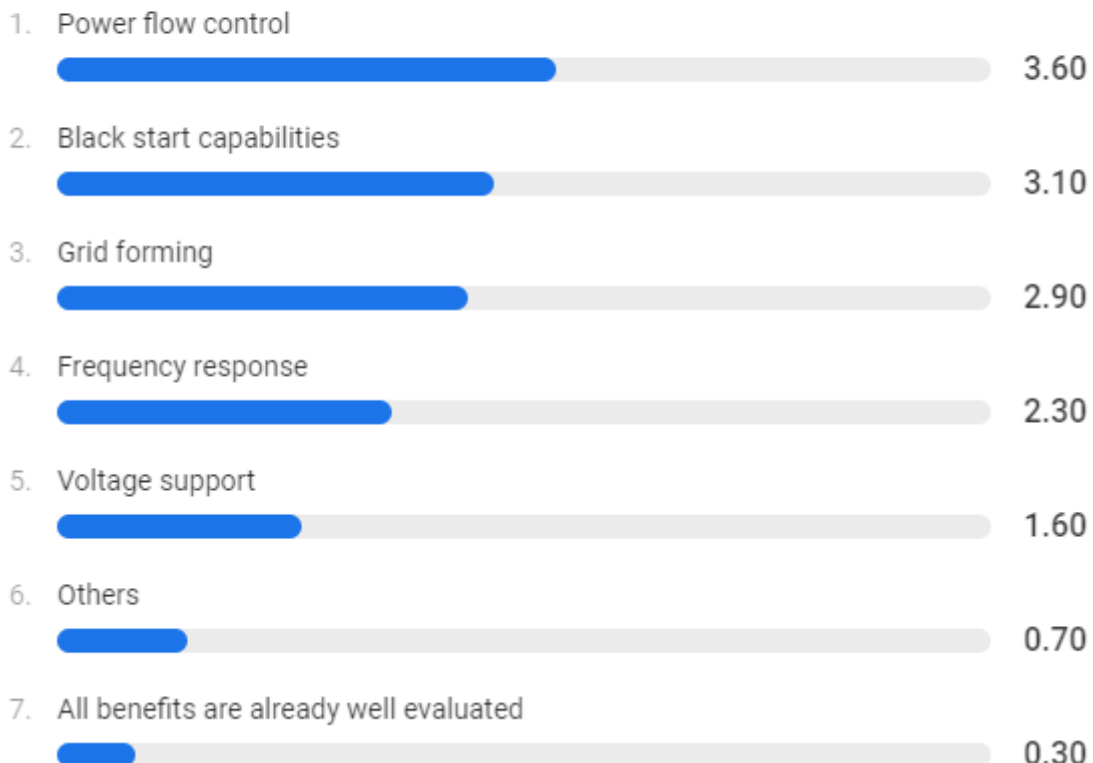


Figure 60 - Workshop question on benefits of HVDC in classical planning approach

In terms of simulations, modelling and methodology, a meeting took place with ENTSO-E on 14<sup>th</sup> March 2022. Some important remarks were formulated, including the practical constraints that ENTSO-E face during the TYNDP process. Therefore, it is important to extend the existing methodology step by step. For example, the use of simplified stability KPIs allowing to perform a screening of potential problem is seen as a very promising way forward. It will allow to clearly define for which operating conditions and at which locations, additional detailed simulations need to be performed.

Another important question was asked regarding further extension of HVDC links (as shown in Figure 61). While most of the persons responded that HVDCs should be “extendible” (via anticipation and standardization) and that MTDC grid should not be considered as a single project, it is important to outline that this is technically complex and will most likely lead to extra-cost (with the current technology and design). Therefore, an extra cost-margin will be considered in this project to allow for future extension. This extra-margin can include assets (DCCB, measurement devices, DC switchgear, etc.), software/control upgrade, or simply spare space.

Existing multi-terminal HVDC grids have been planned knowing the final configuration. Therefore, planning HVDC grid is less “modular” than an AC grid. From your point of view, which of the following statements are correct? (multiple options)

A (cross-border) MTDC grid should be considered as a single project

 17%

When planning a point-to-point HVDC (or an MTDC), standardization should be foreseen to anticipate future expansion

 50%

When planning a point-to-point HVDC (or an MTDC), extra functionalities (or equipment) should be foreseen to anticipate future expansion

 75%

Potential interoperability issues (and cost of mitigation measures, e.g. replicas) should be included in the cost-benefit analysis

 42%

*Figure 61 - Workshop question on HVDC extendibility*

## 10. Appendix II: use case selection

**Table 25 - Assessment of to the long list of use cases considering the economic indicators as defined in section 7.1.3.2**

Use case	Voltage regulation	Frequency regulation	Grid forming	Power flow control	Black start	Sum
1. Slovenia-Italy link	4	0	2	3	1	10
2. HVDC SuedOstLink	4	0	2	3	1	10
3. Navarra-Landes Link	4	0	2	3	2	11
4. MONITA project	4	0	2	3	1	10
5. Celtic interconnector	2	3	3	2	3	13
6. TUN.ITA.	2	3	2	2	3	12
7. Viking DKW-GB	2	3	2	2	3	12
8. TuNur	2	2	1	1	2	8
9. Ultranet + A-North	5	0	2	4	2	13
10. EuroAsia interconnector	2	5	3	2	5	17
11. MaresConnect	2	3	3	2	4	14
12. LaSGo Link	2	3	3	3	5	16
13. Nautilus	2	3	2	3	3	13
14. MTDC multi-country backbone	5	5	4	5	5	24
15. North Sea Wind Power Hub (NSWP)	5	5	4	5	5	24

## 11. Appendix III: Data sources for the zonal economic dispatch model

The installed generation capacities for each market zone, planning year, scenario and considered climate year can be found under: <https://2020.entsos-tyndp-scenarios.eu/wp-content/uploads/2020/06/TYNDP-2020-Scenario-Datafile.xlsx.zip>

Further, the NTCs between the market zones can be found under: <https://www.entsoe.eu/Documents/TYNDP%20documents/TYNDP2020/Reference%20Grid%202025%20-%20TYNDP%202020.xlsx>

The demand time series for the different climate years for the different climate years, scenarios and planning years can be found under: <https://tyndp.entsoe.eu/maps-data>

The hourly capacity factor time series for offshore wind, onshore wind, and solar PV generation for 35 climate years can be found under: <https://zenodo.org/record/3702418#.YnOn7C8Rp-X>

The detailed ENTSO-E network model for all European countries can be requested under confidentiality agreement under: <https://www.entsoe.eu/publications/statistics-and-data/#entso-e-on-line-application-portal-for-network-datasets>

The generation cost data have been obtained from the TYNDP 2020: [https://2020.entsos-tyndp-scenarios.eu/wp-content/uploads/2020/06/Charts-and-Figures\\_Underlying-Data-for-TYNDP-2020.xlsx.zip](https://2020.entsos-tyndp-scenarios.eu/wp-content/uploads/2020/06/Charts-and-Figures_Underlying-Data-for-TYNDP-2020.xlsx.zip). Approximate costs based on the above information have been assigned to generator types that are not presented in the above data. An overview of these costs is presented below (all values are given in Euro / MWh):

```
"DSR" => 119, # demand side response
"Other non-RES" => 120,
"Offshore Wind" => 59,
"Onshore Wind" => 25,
"Solar PV" => 18,
"Solar Thermal" => 89,
"Gas CCGT new" => 89,
"Gas CCGT old 1" => 89,
"Gas CCGT old 2" => 89,
"Gas CCGT present 1" => 89,
"Gas CCGT present 2" => 89,
"Reservoir" => 18,
"Run-of-River" => 18,
"Gas conventional old 1" => 120,
"Gas conventional old 2" => 120,
"PS Closed" => 120,
"PS Open" => 120,
```

```
"Lignite new" => 120,  
"Lignite old 1" => 120,  
"Lignite old 2" => 120,  
"Hard coal new" => 120,  
"Hard coal old 1" => 120,  
"Hard coal old 2" => 120,  
"Gas CCGT old 2 Bio" => 120,  
"Gas conventional old 2 Bio" => 120,  
"Hard coal new Bio" => 120,  
"Hard coal old 1 Bio" => 120,  
"Hard coal old 2 Bio" => 120,  
"Heavy oil old 1 Bio" => 120,  
"Lignite old 1 Bio" => 120,  
"Oil shale new Bio" => 120,  
"Gas OCGT new" => 89,  
"Gas OCGT old" => 120,  
"Heavy oil old 1" => 150,  
"Heavy oil old 2" => 120,  
"Nuclear" => 110,  
"Light oil" => 140,  
"Oil shale new" => 150,  
"P2G" => 120,  
"Other non-RES DE00 P" => 120,  
"Other non-RES DKE1 P" => 120,  
"Other non-RES DKW1 P" => 120,  
"Other non-RES FI00 P" => 120,  
"Other non-RES FR00 P" => 120,  
"Other non-RES MT00 P" => 120,  
"Other non-RES UK00 P" => 120,  
"Other RES" => 60,  
"Gas CCGT new CCS" => 89,  
"Gas CCGT present 1 CCS" => 60,  
"Gas CCGT present 2 CCS" => 60,  
"Battery" => 119,  
"Lignite old 2 Bio" => 120,  
"Oil shale old" => 150,  
"Gas CCGT CCS" => 89,  
"VOLL" => 10000, # value of lost load
```

## 12. References

- [1] European Commission, "Stepping up Europe's 2030 climate ambition," COM(2020) 562 final, Brussels, 2020.
- [2] European Commission, "An EU Strategy to harness the potential of offshore renewable energy for a climate," COM(2020) 741 final, Brussels, 2020.
- [3] ENTSO-E, "3rd Guideline for Cost-Benefit Analysis of Grid Development Projects (draft)," 2019. [Online]. Available: [https://consultations.entsoe.eu/system-development/cba-methodology-3-0/supporting\\_documents/191023\\_CBA3\\_Draft%20for%20consultation.pdf](https://consultations.entsoe.eu/system-development/cba-methodology-3-0/supporting_documents/191023_CBA3_Draft%20for%20consultation.pdf).
- [4] WP 4.7, PROMOTIoN Project Deliverable, "Preparation of cost-benefit analysis from a protection point of view," 2020. [Online]. Available: [https://www.promotion-offshore.net/fileadmin/PDFs/D4.7\\_Preparation\\_of\\_cost-benefit\\_analysis\\_from\\_a\\_protection\\_point\\_of\\_view.pdf](https://www.promotion-offshore.net/fileadmin/PDFs/D4.7_Preparation_of_cost-benefit_analysis_from_a_protection_point_of_view.pdf).
- [5] ENTSO-E, "System Needs Study - System dynamic and operational challenges," July 2022. [Online]. Available: <https://eepublicdownloads.blob.core.windows.net/public-cdn-container/tyndp-documents/TYNDP2022/public/syst-dynamic-operational-challenges.pdf>.
- [6] W. Baker, D. Ramasubramanian, M. Val Escudero, E. Farantatos and A. Gaikwad, "Application of advanced short circuit strength metric to evaluate Ireland's high renewable penetration scenarios," in *The 9th Renewable Power Generation Conference (RPG Dublin Online 2021)*, Dublin, 2021.
- [7] CIGRE WG C4.56 TB881, "Electromagnetic transient simulation models for large-scale system impact studies in power systems having a high penetration of inverter-connected generation," CIGRE C4, 2022.
- [8] N. Hatziargyriou et al., "Definition and Classification of Power System Stability – Revisited & Extended," *IEEE Transactions on Power Systems*, vol. 36, no. 4, pp. 3271-3281, 2021.
- [9] T. V. Cutsem, *Classification of power system stability*, University of Liege.
- [10] ENTSO-E, "TYNDP 2020," [Online]. Available: [https://eepublicdownloads.blob.core.windows.net/public-cdn-container/tyndp-documents/TYNDP2020/Forconsultation/TYNDP2020\\_Report\\_forconsultation.pdf](https://eepublicdownloads.blob.core.windows.net/public-cdn-container/tyndp-documents/TYNDP2020/Forconsultation/TYNDP2020_Report_forconsultation.pdf).
- [11] L. Papangelis, "Local and centralized control of multi-terminal DC grids," ULiege, 2018.
- [12] European Commission, COMMISSION REGULATION (EU) 2017/2196, Official Journal of the European Union, 2017.
- [13] Jiang-Hafner, Ying et al., "HVDC with voltage source converters-a powerful standby black start facility," in *IEEE/PES T&D Conf. and Expo.*, 2008.
- [14] Midtsund, T., et al., "A live black-start capability test of a voltage source HVDC converter," in *CIGRE Canada Conference*, 2015.
- [15] The National HVDC Centre, "Maximising HVDC Support for GB Black Start and System Restoration," 2019.

- [16] CIGRE WG B4.70, *TB 832:Guide for electromagnetic transient studies involving VSC converters*, 2021.
- [17] ELIA – National Control Center & Market Development, “Study on the Review of the Black Start Ancillary Services,” 2018.
- [18] ENTSO-E - WGAS, “Survey on Ancillary Services Procurement, Balancing Market Design 2017,” 2018.
- [19] ENTSO-E, *High Penetration of Power Electronic Interfaced Power Sources and the Potential Contribution of Grid Forming Sources*, 2017.
- [20] Z., Emin et al., “System Strength,” *Cigre Science and Engineering*, no. CSE 020, 2021.
- [21] OSMOSE Project WP3, “D3.2: Overall Specifications of the Demonstrations,” 2019.
- [22] M. Paolone, T. Gaunt, X. Guillaud, M. Liserre, S. Meliopoulos, A. Monti, T. Van Cutsem, V. Vittal and C. Vournas, “Fundamentals of power systems modelling in the presence of converter-interfaced generation,” *Electric Power Systems Research*, 2020.
- [23] C. Schöll and H. Lens, “Design-and simulation-based comparison of grid-forming converter control concepts,” in *20th International Workshop on Large-Scale Integration of Wind Power into Power Systems as well as on Transmission Networks for Offshore Wind Power Plants*, 2021.
- [24] P. Unruh, M. Nuschke, P. Strauß and F. Welck, “Overview on grid-forming inverter control methods,” *Energies*, 2020.
- [25] ESIG Task Force on High Share of Inverter-Based Generation, “Grid-Forming Technology in Energy Systems Integration,” 2022.
- [26] R. Rosso, X. Wang, M. Liserre, X. Lu and S. Engelken, “Grid-forming converters: control approaches, grid-synchronization, and future trends-A review,” *IEEE Open Journal of Industry Applications*, 2021.
- [27] Power System Dynamic Performance Committee, “Stability definitions and characterization of dynamic behavior in systems with high penetration of power electronic interfaced technologies,” IEEE, 2020.
- [28] ENTSO-E, “Inertia and Rate of Change of Frequency (RoCoF) - Version 17,” 2020.
- [29] EirGrid, Soni, “Shaping our Electricity Future - Technical Report,” 2021.
- [30] Transpower System Operator, “RMT\_Specification\_V9,” 2022. [Online]. Available: [https://www.transpower.co.nz/sites/default/files/bulk-upload/documents/RMT\\_Specification\\_V9\\_issue.pdf](https://www.transpower.co.nz/sites/default/files/bulk-upload/documents/RMT_Specification_V9_issue.pdf).
- [31] NERC, “Odessa Disturbance - Texas Events: May 9, 2021 and June 26, 2021 Joint NERC and Texas RE Staff Report,” 2021.
- [32] AEMO, *System strength in the NEM explained*, 2020.
- [33] W. Wenzong, M. H. Garng, R. Deepak and F. Evangelos, “Transient stability analysis and stability margin evaluation of phase-locked loop synchronised converter-based generators,” *IET Generation, Transmission & Distribution*, vol. 14, no. 22, 2020.

- [34] ENTSO-E, ““One Vision 2030” Roadmap towards PE-Dominated Power Systems (incl. HVDC”).
- [35] D. Ramasubramanian et al., “Positive sequence voltage source converter,” *IET Generation, Transmission & Distribution*, vol. 14, no. 1, pp. 87-97, 2020.
- [36] P. Borowski, “Zonal and Nodal Models of Energy Market in European Union,” *Energies*, vol. 13, no. 10.3390/en13164182, p. 4182, 2020.
- [37] ENTSO-E, “System dynamic and operational challenges - Final version after ACER opinion,” August 2021. [Online]. Available: [https://eepublicdownloads.blob.core.windows.net/public-cdn-container/tyndp-documents/TYNDP2020/FINAL/entso-e\\_TYNDP2020\\_IoSN\\_Systemdynamicandoperationalchallenges\\_2108.pdf](https://eepublicdownloads.blob.core.windows.net/public-cdn-container/tyndp-documents/TYNDP2020/FINAL/entso-e_TYNDP2020_IoSN_Systemdynamicandoperationalchallenges_2108.pdf).
- [38] B. Badrzadeh, Z. Emin, S. Goyal, S. Grogan, A. Haddadi, A. Halley, A. Louis, T. Lund, J. Matevosyan, T. Morton, D. Premm, S. Sproul, “System strength,” 2021.
- [39] A. Hoke, V. Gevorgian, S. Shah, P. Koralewicz, R. Kenyon and B. Kroposki, “Island power systems with high levels of inverter-based resources: Stability and reliability challenges,” *IEEE Electrification Magazine*, 2021.
- [40] ENTSO-E, *Overview: Operational Limits and Conditions for Frequency Coupling*, 2018.
- [41] ENTSO-E, “Research, Development and Innovation Roadmap 2020-2030,” 2022. [Online]. Available: [https://eepublicdownloads.azureedge.net/clean-documents/Publications/RDC%20publications/entso-e-rdi\\_roadmap-2020-2030.pdf](https://eepublicdownloads.azureedge.net/clean-documents/Publications/RDC%20publications/entso-e-rdi_roadmap-2020-2030.pdf).
- [42] ENTSO-E, “Grid-Forming Capabilities: Towards System Level Integration,” 31 March 2021. [Online]. Available: [https://eepublicdownloads.entsoe.eu/clean-documents/RDC%20documents/210331\\_Grid%20Forming%20Capabilities.pdf](https://eepublicdownloads.entsoe.eu/clean-documents/RDC%20documents/210331_Grid%20Forming%20Capabilities.pdf).
- [43] ENTSO-E, “System Needs Study - Opportunities for a more efficient European power system in 2030 and 2040,” July 2022. [Online]. Available: <https://eepublicdownloads.blob.core.windows.net/public-cdn-container/tyndp-documents/TYNDP2022/public/system-needs-report.pdf>.

## **GETTING IN TOUCH WITH THE EU**

### **In person**

All over the European Union there are hundreds of Europe Direct information centres. You can find the address of the centre nearest you at: [https://europa.eu/european-union/contact\\_en](https://europa.eu/european-union/contact_en)

### **On the phone or by email**

Europe Direct is a service that answers your questions about the European Union. You can contact this service:

- by freephone: 00 800 6 7 8 9 10 11 (certain operators may charge for these calls),
- at the following standard number: +32 22999696, or
- by email via: [https://europa.eu/european-union/contact\\_en](https://europa.eu/european-union/contact_en)

## **FINDING INFORMATION ABOUT THE EU**

### **Online**

Information about the European Union in all the official languages of the EU is available on the Europa website at: [https://europa.eu/european-union/index\\_en](https://europa.eu/european-union/index_en)

### **EU publications**

You can download or order free and priced EU publications from: <https://op.europa.eu/en/publications>. Multiple copies of free publications may be obtained by contacting Europe Direct or your local information centre (see [https://europa.eu/european-union/contact\\_en](https://europa.eu/european-union/contact_en)).

### **EU law and related documents**

For access to legal information from the EU, including all EU law since 1952 in all the official language versions, go to EUR-Lex at: <http://eur-lex.europa.eu>

### **Open data from the EU**

The EU Open Data Portal (<http://data.europa.eu/euodp/en>) provides access to datasets from the EU. Data can be downloaded and reused for free, for both commercial and non-commercial purposes.



Publications Office  
of the European Union

ISBN 978-92-76-60277-4